AFCRL-69-0412 Technical Report 2183-3

AD699228

ASYMPTOTIC SERIES DESCRIBING THE DIFFRACTION OF A PLANE WAVE BY A WEDGE

David L. Hutchins and Robert G. Kouyoumjian

The Ohio State University

ElectroScience Laboratory

(formerly Antenna Laboratory)

Department of Electrical Engineering

Columbus, Ohio 43212

Scientific Report No. 3

Contract Number AF19(628)-5929

Project No. 5635

Task No. 563502

Work Unit No. 56350201

15 December 1969

Contract Monitor: John K. Schindler

Microwave Physics Laboratory

Prepared for

Air Force Cambridge Research Laboratories

Office of Aerospace Research

United States Air Force

Bedford, Massachusetts 01730

57

NOTICES

Qualified requestors may obtain additional copies from the Defense Documentation Center. All others should apply to the Clearinghouse for Federal Scientific and Technical Information.

AFCRL-69-0412 Technical Report 2183-3

ASYMPTOTIC SERIES DESCRIBING THE DIFFRACTION OF A PLANE WAVE BY A WEDGE

David L. Hutchins and Robert G. Kouyoumjian

Scientific Report No. 3

Contract Number AF19(628)-5929
Project No. 5635
Task No. 563502
Work Unit No. 56350201

15 December 1969

Contract Monitor: John K. Schindler
Microwave Physics Laboratory

Prepared for
Air Force Cambridge Research Laboratories
Office of Aerospace Research
United States Air Force
Bedford, Massachusetts 01730

FOREWORD

This report, OSURF Report Number 2183-3, was prepared by The ElectroScience Laboratory, Department of Electrical Engineering, The Ohio State University at Columbus, Ohio. Research was conducted under Contract AF 19(628)-5929. Dr. John K. Schindler, CRDG of the Air Force Cambridge Research Laboratories at Bedford, Massachusetts was the Program Monitor for this research.

ABSTRACT

The Pauli and the Oberhettinger asymptotic expansions for the diffracted field produced by the scattering of a plane wave by a wedge are compared analytically and numerically, and their range of application is extended.

The Pauli-Clemmow method of steepest descents is used to evaluate Sommerfeld's complex integral expression for the total field produced by the scattering of a plane electromagnetic wave by a perfectly conducting wedge. This method is applied in a manner somewhat different from that employed by Pauli and yields an asymptotic expansion which is simpler in form and of wider applicability than Pauli's original expression. This generalized form of Pauli's expansion can, for example, be applied to the computation of the fields diffracted by wedges which have exterior angles less than 180 degrees. It is shown that simply by rearranging the terms in this generalized Pauli expansion a generalized form of Oberhettinger's asymptotic expansion can be produced. This generalized expansion is applicable to problems involving wedges having exterior angles less than 180 degrees, and it is comparable with Oberhettinger's original series when the wedge angle is greater than this value.

Several examples of the scattering of a plane wave by a wedge are studied numerically. The superiority of the generalized Pauli asymptotic expression over previously derived asymptotic expressions is demonstrated in these numerical examples.

These asymptotic expressions are used to obtain scalar diffraction coefficients which are valid in the transition regions at the shadow and reflection boundaries.

CONTENTS

CHAPTER I

INTRODUCTION

This chapter contains a statement of the problem considered in the report, the motivation for considering the problem, a summary of the contents, and a brief survey of the literature on wedge diffraction.

The Problem

Let a plane time-harmonic electromagnetic wave of arbitrary polarization be incident on a perfectly conducting, infinite, two-dimensional wedge; the situation is depicted in Figure 1. The field is propagating in free space, and its propagation vector $\bar{k}$ is perpendicular to the edge of the wedge. When this wave strikes the wedge, it is scattered. The sum of the incident field and scattered field is called the total field. This total field can be broken down into two linearly polarized fields, one having its electric vector parallel to the edge of the wedge and the other having its magnetic vector parallel to this edge. These two polarization components can be studied individually.

An exact mathematical expression, called G_p in this work, has been developed to describe these polarization

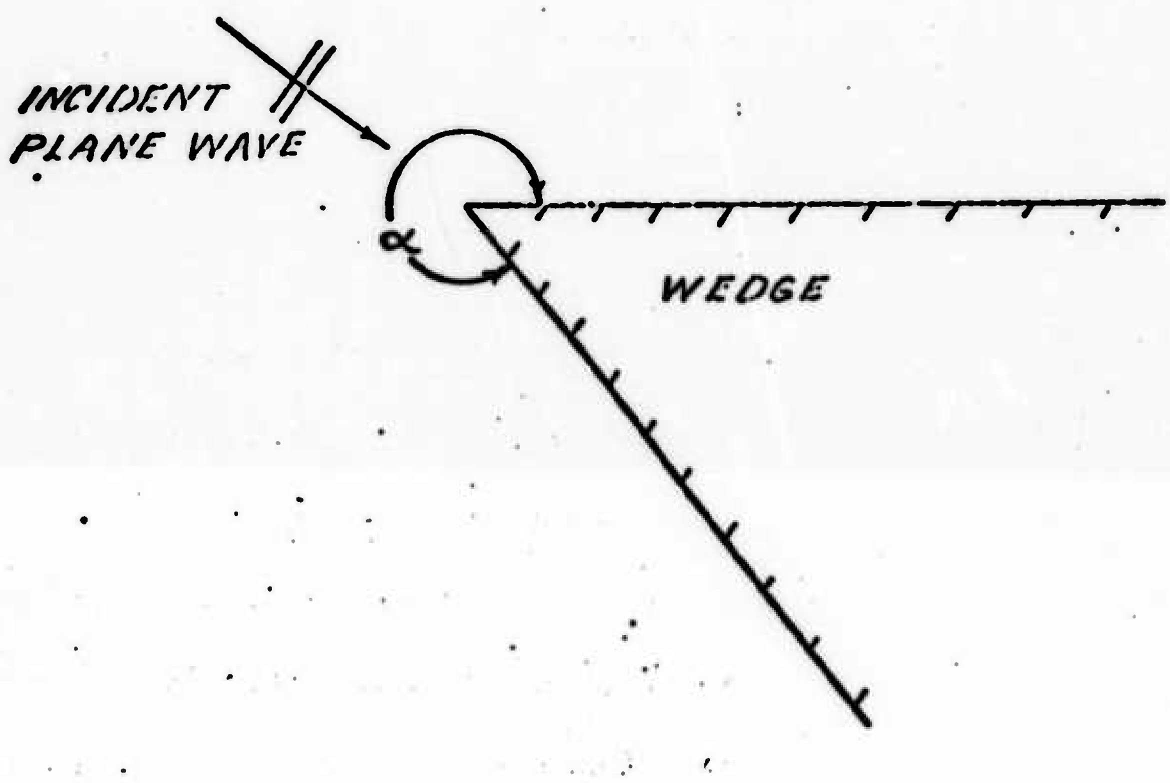

Figure 1. A plane electromagnetic wave incident on a perfectly conducting wedge of exterior wedge angle α.

components, and this can be written in a variety of forms. Possibly the most familiar of these is the infinite eigenfunction series of products of Bessel and trigonometric functions. If G_p is to be evaluated at points which are a large number of wavelengths from the edge of the wedge, then it is convenient and, in fact, necessary to write it in the form of an asymptotic expression in the variable kr, where k is the propagation constant and r is the perpendicular distance from the edge to the field point.

There are two such asymptotic expressions which are commonly used to compute G_p in such cases. One of these was derived by Pauli;[1] the other, by Oberhettinger.[2] Pauli's expression is written as a Fresnel integral plus an infinite series of confluent hypergeometric functions. Oberhettinger's expression contains a Fresnel integral and an infinite series of terms of the form

$$(kr)^{\frac{-N}{2}},$$

where N is an integer. One purpose of this work is to investigate the relation between these two series. Are they, for instance, actually the same series written in different forms? Another purpose is to determine which of these series is superior for computational purposes.

Each of these series suffers from certain inadequacies. Some of these are listed below.

a) Both series are restricted to applications where the exterior wedge angle α is greater than 180 degrees.

b) The Pauli series cannot be applied to all situations even when α is greater than 180 degrees. For example, if α is close to but greater than 180 degrees and the propagation vector $\bar{k}$ is nearly parallel to one of the faces of the wedge, the Pauli series will not describe G_p accurately in the vicinity of the other face.

c) The Pauli series is written in terms of the relatively unfamiliar confluent hypergeometric functions.

In this work, these series are re-examined, and these inadequacies are in part removed.

The Motivation

The geometrical theory of diffraction[3] provides a simple method for calculating the fields produced by the scattering of high frequency electromagnetic waves by perfectly conducting bodies of quite general shape. This theory is particularly useful for describing the scattering by edges of bodies, such as the curved edge of a circular disk,[4] the curved edge of a parabolic antenna,[5] the straight edge of a horn antenna,[6] or the straight edge of a polygonal cylinder.[7]

In the geometrical theory of diffraction, the description of diffraction from edges is treated in the following way. As in the theory of geometrical optics, the field incident on the edge is assumed to propagate along ray paths. Upon striking an edge, the incident ray is scattered, giving rise to a family of diffracted rays. The direction of propagation of these diffracted rays is determined by the generalized Fermat's principal. The distribution of the incident energy among these diffracted rays is described by a diffraction coefficient. The diffraction of the incident rays is a local phenomenon, so the diffraction coefficient depends on the geometry of the edge in the region surrounding the point of diffraction and on the local polarization state of the incident field.

The exact form of the diffraction coefficient must be derived from the rigorous solution of a "canonical" problem. The canonical problem, which yields the diffraction coefficient for an edge, is the diffraction of a linearly polarized plane wave by a two-dimensional, infinite wedge. The diffraction coefficient is found from Sommerfeld's[8] asymptotic, high frequency solution to this problem.

This edge diffraction coefficient adequately describes the diffracted field at points well removed from the point of diffraction and transition regions, that is, shadow and reflection boundaries. In these transition regions, however, the diffraction coefficient fails to describe the field and, the geometrical theory must be supplemented by a more sophisticated equation. The equations normally employed are the asymptotic expansions of the wedge diffracted field given by Pauli and by Oberhettinger.

When applying these formulas to practical geometrical theory of diffraction computations a number of questions naturally arise. Which formula is superior from the computational point of view, or which asymptotic expansion will provide the best description of the field in the transition region with the minimum amount of computational effort? What is the smallest value of kr for which these formulas are useful? Since the expressions are asymptotic series, what is the effect of higher order terms? This study was motivated by practical computational questions of this nature as well as by the desire to extend the useful range of Pauli and Oberhettinger asymptotic expressions and to determine the relation between them.

Summary

The starting point of this work is the eigenfunction series form of the Green's function for a line source radiating in the vicinity of an infinite, two-dimensional wedge. After a brief discussion of this expression, it is assumed that the line source recedes to infinity, and this solution is reduced to that for the scattering of a plane wave. The resulting infinite series is then summed in closed form and written as a complex contour integral. This integral is identical with the ansatz first deduced by Sommerfeld.[8] This complex, integral expression for G_p is then rewritten in a slightly different but more convenient form, and distribution of the saddle points and poles of the integrand of the resulting expression is studied. The integral expression is then evaluated by the ordinary method of steepest descents, and then by a modification of this method. This modified method of steepest descents was first used by Pauli in the derivation of his asymptotic series for G_p. The method is used here in a somewhat different manner to yield an expression for G_p which is both simpler and more general than Pauli's expression. The expression derived in this work consists of an infinite series of functions. Each function is the sum of a Fresnel integral and a finite number of terms of the form

$$(kr)^{-\frac{N}{2}} .$$

It is next demonstrated that for certain cases the expression for G_p developed in this work can be reduced to the one derived by Pauli. The cases for which this reduction is not possible are just those to which the Pauli expression does not apply.

The relation between the expression for G_p developed in this work and that developed by Oberhettinger is investigated. It is shown that for cases where α is greater than 180 degrees they are the same series written in a different form. In Chapter IV several examples of scattering of a plane wave by a wedge are studied numerically, and some conclusions regarding the relative merit of the various solutions presented in Chapter III are drawn from the results. In Chapter V the asymptotic solutions are used to obtain expressions for the diffraction coefficients.

Literature Survey

The problem of diffraction of electromagnetic waves by a wedge has been the subject of numerous theoretical and experimental studies. An extensive list of many of the papers is given in the bibliography. Sommerfeld[9] was the first to develop a rigorous solution for the diffraction of a plane wave by a perfectly conducting half-plane. He used an extension of image theory to deduce an integral solution for this problem and showed that his solution reduced to the Fresnel integral. A similar solution was derived by Carslaw,[10] who used image theory, and by

Poincaré,[11] who reduced the diffraction problem to one of solving an integral equation. Macdonald,[12, 13] using the classical methods of separation of variables, was the first to obtain the complete solution to the problem of diffraction of plane, cylindrical, and spherical waves by a perfectly conducting wedge of arbitrary angle. Macdonald's solution is in the form of an infinite series but has been written in integral form by means of an integral transformation relating the ordinary and modified Bessel functions. Sommerfeld[8] employed his extension of the method of images to derive an integral expression for the diffraction of a plane wave by a perfectly conducting wedge of arbitrary angle. Carslaw[14] and Bromwich[15] also constructed solutions to this problem using the method of images. Oberhettinger[16] used an integral transform method to derive another integral expression for the diffraction of plane, cylindrical, and spherical waves by a perfectly conducting wedge of arbitrary angle. Kontorovich and Lebedev[17] and Karp[18] have developed the solution for a half-plane using transform methods.

The Wiener-Hopf method has been applied to this problem by Harrington,[19] Copson,[20] and Magnus.[21] Recently Nomura,[22] Senior,[23] and Heins[24] have studied the diffraction of a dipole field by a perfectly conducting half-plane. The solution for the diffraction of pulses by wedges has been examined by Oberhettinger,[25] Freidlander,[26] and others.[27, 41]

The problems of diffraction by imperfectly conducting wedges, dielectric wedges, and wedges having mixed boundary conditions have been treated in recent years.[42, 93] Senior has developed an exact solution for the imperfectly conducting half-plane[42] and right-angled wedge.[43] Approximate solutions to this problem have been found by Jones and Pidduck,[44] Felsen,[45] Williams,[46, 47] and Malyuzinec.[48] Diffraction from unidirectional conducting half-planes has been studied by Radlow,[50] Hurd,[51] and Seshadri,[52, 53] and the problems of diffraction by wedges immersed in conducting and anisotropic media have been investigated by Dmitriev,[54, 57] Jull,[55] Williams,[56] and Seshadri.[57] The diffraction of surface waves by right-angled wedges was treated by Karp and Karal,[58-63] Chu and Kouyoumjian,[64-67] and others.[68-70] Diffraction of waves by wedges with various kinds of exotic boundary impedances have been examined by Karp,[71-75] Felsen,[76-79] and others.[80-90]

The results of some of the theoretical investigations of wedge diffraction have been applied to the calculation of horn and surface wave antenna patterns,[91, 92] to studies of scattering from terrain features,[93] and objects possessing edges,[7, 94, 95] and to the problems of diffraction from thick screens,[96] irregular edges,[97-98] and various double wedge configurations.[99, 100] A number of experimental studies have been made to verify the predictions of wedge diffraction theory.[101-106]

Asymptotic forms of the solution for the diffraction of a plane wave by a perfectly conducting wedge have been derived and studied by Sommerfeld,[9] Pauli,[1] Clemmow,[107] Van der Waerden,[108] and Oberhettinger.[2] Sommerfeld[9] attempted to derive an asymptotic expression for his integral solution of this problem. However, his result failed to predict the correct value for the field near the shadow and reflection boundaries. This failure was due to the fact that he used the conventional method of steepest descents developed by Debye.[109] This method is not applicable to cases in which a pole lies near the saddle point over which the integration is taken, a situation which occurs when the diffracted field is evaluated near a shadow or reflection boundary. Pauli[1] modified the method of steepest descents and derived a suitable asymptotic solution for the problem. Ott[110] examined Pauli's method and simplified it. Clemmow[107] studied Pauli's method in detail and found it yields a partial asymptotic expansion. Clemmow suggested that such an expansion can always be rearranged in the form of an asymptotic expansion in inverse powers of an appropriate variable. Oberhettinger[2] applied Watson's lemma to his integral expression for the diffraction of a plane wave by a wedge to produce a new asymptotic expansion. Van der Waerden[108] and Oberhettinger[111] showed that Oberhettinger's expansion could be derived by an application of Van der Waerden's modified method of steepest descents.

CHAPTER II

SERIES AND INTEGRAL FORMS OF THE SOLUTION

In this chapter the infinite-series form of the Green's function for the diffraction problem of a line source radiating in the presence of a two-dimensional wedge of arbitrary angle is introduced, and the infinite-series form of the solution for the diffraction of a plane wave by a wedge is derived from this. This series is then transformed to a complex integral representation.

Series Form of the Solution

Consider a two-dimensional wedge and a line source to be situated in space as shown in Figure 2. The faces of the wedge are formed by two semi-infinite planes intersecting on the z-axis of the cylindrical coordinate system. One plane is located at $\phi = 0$; the other, at $\phi = \alpha$. The infinitely-long line source is parallel to the edge of the wedge, and its position is described by the coordinates (r', ϕ'). The typical field point is denoted by (r, ϕ). The line source is assumed to have unit strength and time dependence of the form $e^{j\omega t}$.

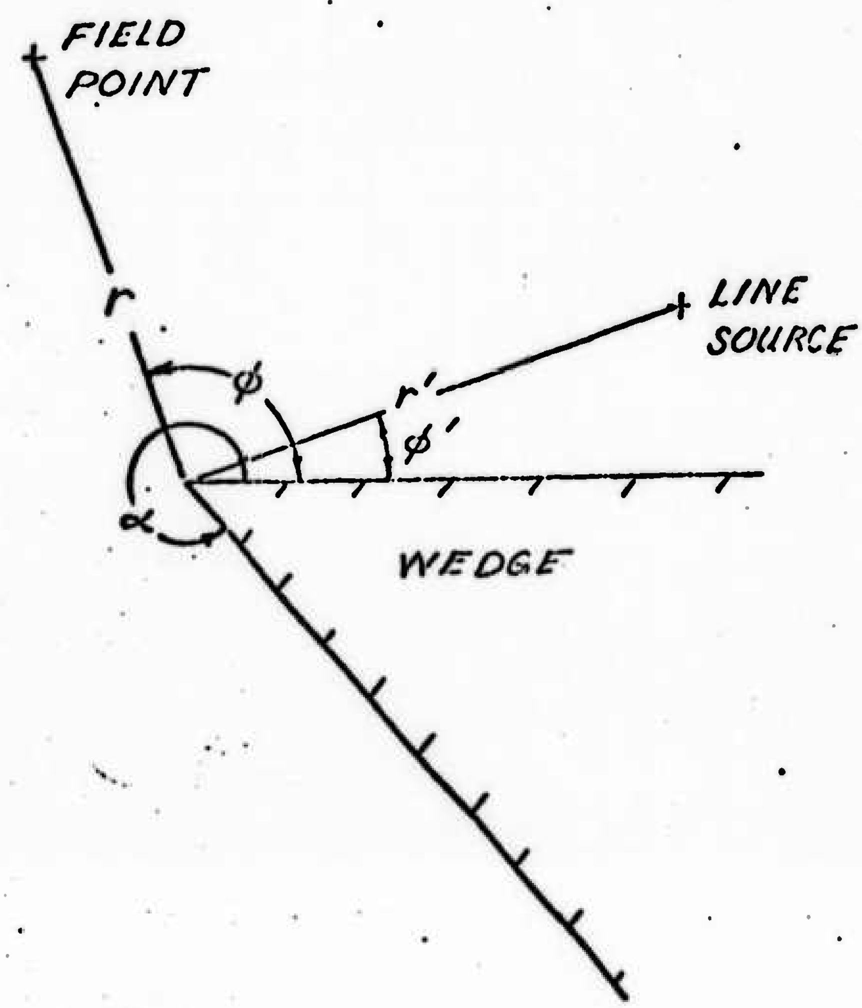

Figure 2. A line source and diffracting wedge.

The Green's function for this radiating system can be written[16]

$$G = \frac{1}{n} \sum_{m=0}^{\infty} \epsilon_m J_{\frac{m}{n}}(kr') H^{(2)}_{\frac{m}{n}}(kr) \left[\cos\left\{ \frac{m}{n}(\phi - \phi') \right\} \pm \cos\left\{ \frac{m}{n}(\phi + \phi') \right\} \right] \tag{1}$$

if $r > r'$. For the case $r' < r$, r and r' are interchanged. In this expression ϵ_m is the Neumann number which is equal to one if m is zero; otherwise it is equal to two. $J_{\frac{m}{n}}(kr)$ and $H^{(2)}_{\frac{m}{n}}(kr)$ represent Bessel and Hankel functions respectively. The variable n describes the wedge angle and is related to α by the following equation:

$$\alpha = n\pi . \tag{2}$$

k is the propagation constant. The plus sign is used between the two cosine terms if the boundary condition is of the homogeneous Neumann type ($\frac{\partial G}{\partial \phi} = 0$ on both faces of the wedge). For the homogeneous Dirichlet boundary condition ($G = 0$ on both faces of the wedge), the minus sign is used.

This convergent series is an exact solution to the time-harmonic, inhomogeneous wave equation for the problem of a radiating line source and wedge embedded in a linear, isotropic, homogeneous, lossless medium. It satisfies the homogeneous Neumann or Dirichlet boundary conditions, the radiation condition[114] and the Meixner edge condition.[115-120] This series converges for all values of r, r', ϕ, and ϕ', and is valid for all values of n.

The expression describes the total radiation field created by the direct radiation from the line source and that scattered from the wedge. If the line source is an electric current of strength I, then G represents the electric field vector, that is, $E_z = -j\omega\mu IG$; and the boundary condition $G = 0$ applies. If the line source is a magnetic current of strength M, then G represents the magnetic field vector, that is, $H_z = -j\omega\epsilon MG$; and the boundary condition $\frac{\partial G}{\partial \phi} = 0$ applies.

In many cases it is necessary to determine the total radiation field when the field point is far removed from the vertex of the wedge. In such cases Equation 1 can be simplified by replacing the Hankel functions by the first term of their asymptotic expansion, that is, by the relation

$$H^{(2)}_{\frac{m}{n}}(kr) \sim \left[\frac{2}{\pi kr}\right]^{\frac{1}{2}} e^{-j\left(kr - \frac{\pi}{4} - \frac{m}{n}\frac{\pi}{2}\right)} \qquad (3)$$

This substitution reduces G to the form

$$G = \left[\frac{2}{\pi kr}\right]^{\frac{1}{2}} e^{-j(kr - \frac{\pi}{4})} \frac{1}{n} \sum_{m=0}^{\infty} \epsilon_m J_{\frac{m}{n}}(kr') e^{j\frac{m}{n}\frac{\pi}{2}}$$

$$\left[\cos\left\{\frac{m}{n}(\phi - \phi')\right\} \pm \cos\left\{\frac{m}{n}(\phi + \phi')\right\}\right] \qquad (4)$$

This substitution is strictly valid only for those terms of the series for which kr is large compared to the order of the Hankel function. Therefore, when making this substitution an additional assumption is required. This is that kr' is small enough compared to kr so that the terms of the series which do not satisfy the requirement $kr > \frac{m}{n}$ are negligibly small and, for practical purposes, contribute nothing to G.

If the line source rather than the field point is far removed from the vertex of the wedge, G can be written

$$G = \left[\frac{2}{\pi kr'}\right]^{\frac{1}{2}} e^{-j(kr' - \frac{\pi}{4})} G_p \ , \qquad (5)$$

where

$$G_p = \frac{1}{n} \sum_{m=0}^{\infty} \epsilon_m J_{\frac{m}{n}}(kr) e^{j\frac{m}{n}\frac{\pi}{2}} \left[\cos\left\{\frac{m}{n}(\phi - \phi')\right\} \pm \cos\left\{\frac{m}{n}(\phi + \phi')\right\}\right] \qquad (6)$$

G_p is the series form of the Green's function describing the total field created by the scattering of a plane wave by a wedge. It is an exact solution to this problem in the sense described on pages 15 and 16. The remainder of this work concerns the evaluation of G_p.

Equation 6 converges rapidly for small values of kr. If kr is less than 1.0, less than 15 terms of the series are required to compute a value of G_p which is accurate to 5 significant figures. When kr is large, the series still converges but very slowly. If kr = 10, 40 terms are required to achieve 5 significant figure accuracy in G_p. In view of this slow convergence for large values of kr the expression for G_p must be cast in another form if it is to be useful for computational purposes. An asymptotic expansion of G_p in inverse powers of kr is such a useful form. In order to derive an asymptotic expression for G_p by the standard method of steepest descents it must first be transformed into an integral or integrals of the type

$$\int_c F(z) e^{krf(z)} dz \tag{7}$$

In the next section a method for making this transformation is described.

Integral Form of the Solution

Sommerfeld deduced, by an extension of the method of images, a complex integral form for G_p and derived the eigenfunction series given by Equation 6 from this integral.

In this section the inverse derivation is presented. This procedure is more systematic since one is not required to start with a solution arrived at by intuition. First one writes the Bessel functions of Equation 6 in integral form. Next the order of integration and summation is interchanged, and, finally, the resulting sums are written in closed form.

G_p will first be written as the sum of two terms as shown below:

$$G_p = I(kr, \phi - \phi', n) \pm I(kr, \phi + \phi', n) , \tag{8}$$

where

$$I(kr, \phi \pm \phi', n) = \frac{1}{n} \sum_{m=0}^{\infty} \epsilon_m J_{\frac{m}{n}}(kr) e^{j \frac{m}{n} \frac{\pi}{2}} \cos \frac{m}{n} (\phi \pm \phi') \tag{9}$$

In the analysis to follow both of these terms will be denoted by $I(kr, \beta, n)$, where $\beta = \phi \pm \phi'$.

If $\cos \frac{m}{n} \beta$ is expressed in complex form, Equation 9 can be written

$$I(kr, \beta, n) = \frac{1}{n} \sum_{m=1}^{\infty} e^{j \frac{m}{n} \frac{\pi}{2}} e^{j \frac{m}{n} \beta} J_{\frac{m}{n}}(kr) +$$

$$+ \frac{1}{n} \sum_{m=0}^{\infty} e^{j \frac{m}{n} \frac{\pi}{2}} e^{-j \frac{m}{n} \beta} J_{\frac{m}{n}}(kr) \tag{10}$$

The Bessel functions in this expression can be expressed in terms of contour integrals in the complex z-plane as follows:

$$J_{\frac{m}{n}}(kr) = \frac{1}{2\pi}\int_{c} e^{jkr\cos z + j\frac{m}{n}(z - \frac{\pi}{2})}\,dz \tag{11}$$

or

$$J_{\frac{m}{n}}(kr) = \frac{1}{2\pi}\int_{c'} e^{jkr\cos z - j\frac{m}{n}(z + \frac{\pi}{2})}\,dz \tag{12}$$

The contours c and c' are pictured in Figure 3. The cross-hatched strips in the figure represent the regions in which the integrands vanish when $|\mathrm{Im}z| \to \infty$. Now, if the integral over c is substituted into the first summation in Equation 10, the integral over c' is substituted into the second, and if the order of integration and summation is interchanged in each term, the following results:

$$I(kr, \beta, n) = \frac{1}{2\pi n}\int_{c} e^{jkr\cos z}\sum_{m=1}^{\infty} e^{j\frac{m}{n}(\beta + z)}\,dz +$$

$$+ \frac{1}{2\pi n}\int_{c'} e^{jkr\cos z}\sum_{m=0}^{\infty} e^{-j\frac{m}{n}(\beta + z)}\,dz \tag{13}$$

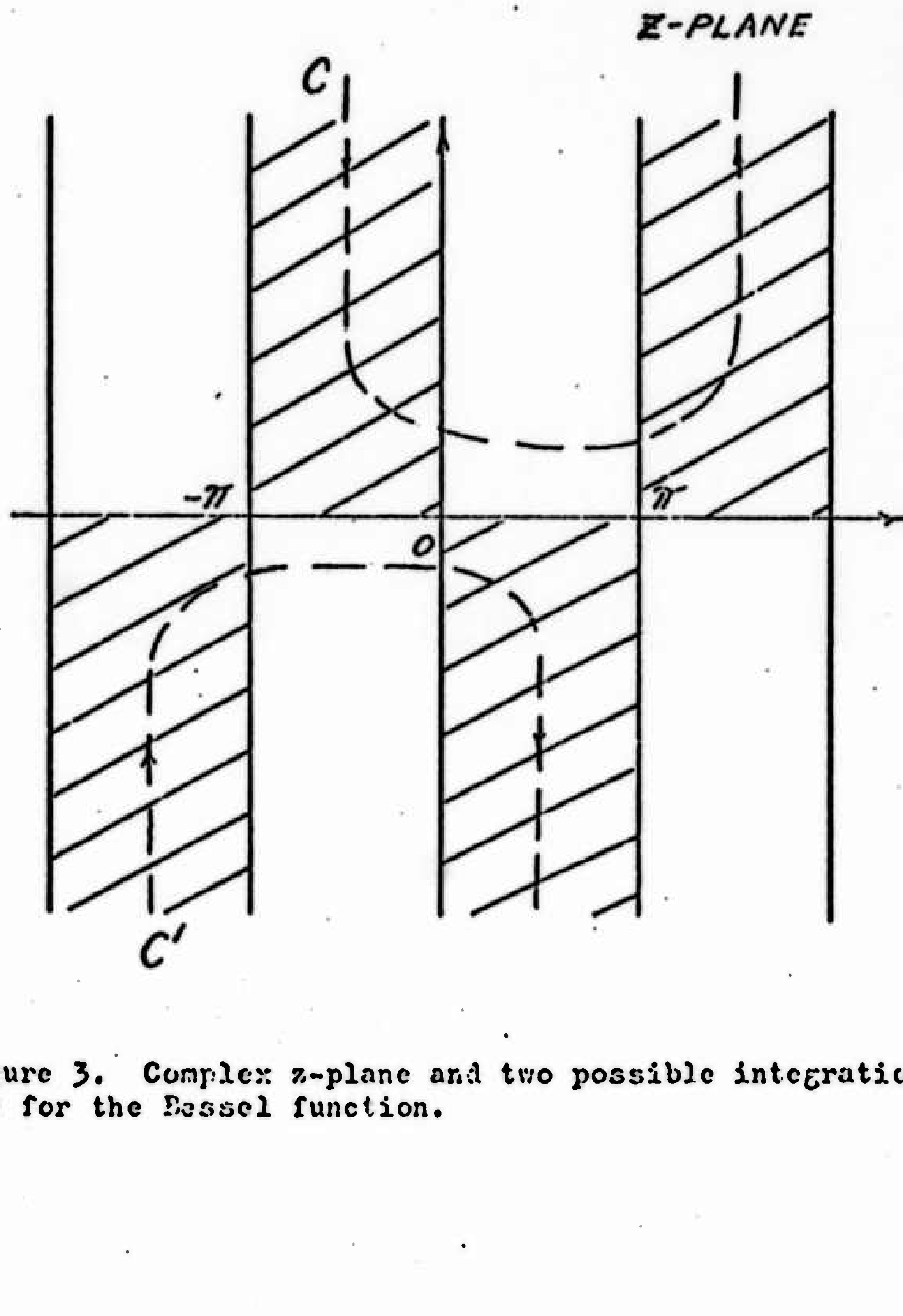

Figure 3. Complex z-plane and two possible integration contours for the Bessel function.

The two summations can be reduced to the closed forms

$$\sum_{m=1}^{\infty} e^{j \frac{m}{n}(\beta + z)} = \frac{-1}{1 - e^{-j \frac{\beta + z}{n}}} \tag{14}$$

and

$$\sum_{m=0}^{\infty} e^{-j \frac{m}{n}(\beta + z)} = \frac{1}{1 - e^{-j \frac{\beta + z}{n}}} , \tag{15}$$

Equation 13 can, therefore, be written

$$I(kr, \beta, n) = \frac{1}{2\pi n} \int_{(c' - c)} \frac{1}{1 - e^{-j \frac{\beta + z}{n}}} e^{jkr \cos z} dz \tag{16}$$

The negative sign before the c indicates that this integration contour is to be traversed in the direction opposite to that indicated in Figure 3. Substitution of Equation 16 into 8 yields

$$0_p = \frac{1}{2\pi n} \int_{(c' - c)} \frac{e^{j \frac{z}{n}}}{e^{j \frac{z}{n}} - e^{-j \frac{\phi - \phi'}{n}}} e^{jkr \cos z} dz \pm$$

$$\pm \frac{1}{2\pi n} \int_{(c' - c)} \frac{e^{j \frac{z}{n}}}{e^{j \frac{z}{n}} - e^{-j \frac{\phi + \phi'}{n}}} e^{jkr \cos z} dz \tag{17}$$

This is the expression deduced by Sommerfeld.

Equation 16 can be put in a form more convenient for later use by noting that

$$\frac{1}{1 - e^{-j\frac{\beta + z}{n}}} = \frac{e^{j\frac{\beta + z}{2n}}}{e^{j\frac{\beta + z}{2n}} - e^{-j\frac{\beta + z}{2n}}}$$

$$= \frac{1}{2j} \cot\left(\frac{\beta + z}{2n}\right) + \frac{1}{2} \qquad (18)$$

Substituting this into Equation 16 and making use of the fact that

$$\frac{1}{2} \int_{(c' - c)} e^{jkr \cos z} dz = \frac{1}{2} J_o(kr) - \frac{1}{2} J_o(kr) = 0 \ , \qquad (19)$$

yields

$$I(kr, \beta, n) = \frac{1}{4n\sqrt{j}} \int_{(c' - c)} \cot\left(\frac{\beta + z}{2n}\right) e^{jkr \cos z} dz \qquad (20)$$

G_p is now expressed in the integral form specified by Equation 7. In the next chapter two modifications of the method of steepest descents will be utilized to evaluate this integral asymptotically.

CHAPTER III

ASYMPTOTIC EVALUATION OF THE INTEGRAL FORM OF THE SOLUTION

In the previous chapter the eigenfunction series solution for the diffraction of a plane wave by a wedge of arbitrary angle was expressed as the sum of two integrals, each of the form

$$I(kr, \beta, n) = \frac{1}{4n\pi j} \int_{(c' - c)} F(z) e^{krf(z)} dz \tag{21}$$

where

$$f(z) = j \cos z \tag{22}$$

and

$$F(z) = \cot\left(\frac{\beta + z}{2n}\right) \tag{23}$$

In this chapter these integrals are evaluated for the case of large kr by means of the method of steepest descents and the Pauli-Clemmow modification of this method. In the first section the saddle points of f(z) are located, and the integration contour c - c' is closed by means of steepest descent paths through two of these saddles. Next, the poles of $F(z)$ are located, their contribution to G_p is determined, and their behavior for various values of β and n is described. In the next section the integrals which remain in $I(kr, \beta, n)$ are transformed from the z-plane representation to a u-plane representation. In this new representation the integration contour coincides with the real axis of the u-plane. In the third section the u-plane integrals are evaluated by the common method of steepest descents. The resulting series is shown to be of limited value. In the next section these integrals are evaluated by a modification of the method of steepest descents developed by Pauli. The resulting asymptotic series is compared with the Pauli series and some of its advantages over that series are pointed out. It is then demonstrated that this series can be rearranged and put in the form of the Oberhettinger series. In the final section the equations presented in this chapter are summarized.

The Saddle Points and Poles of the Integrand

The saddle points of $f(z)$ are found by solving for the roots of the equation

$$\frac{d}{dz} f(z) = -j \sin z = 0 \tag{24}$$

These roots are $z_s = N\pi$, where N is zero or a positive or negative integer. $f(z)$, therefore, possesses an infinite number of saddle points, equally spaced along the real axis of the z-plane. In view of the locations of the saddle points and the behavior of $\exp[krf(z)]$ for large values of Imz, it is appropriate to create a closed path of integration C_T consisting of $c' - c$, $SDP_{-\pi}$, and SDP_{π}. This path is shown in Figure 4. $SDP_{-\pi}$ and SDP_{π} represent the steepest descent paths through the saddle points at $z = -\pi$ and $z = \pi$, respectively.

It follows from the Cauchy residue theorem that

$$I(kr, \beta, n) = \frac{1}{4n\pi j}\left[-\int_{SDP_{-\pi}} F(z)e^{krf(z)}\,dz - \int_{SDP_{\pi}} F(z)e^{krf(z)}\,dz + \right.$$

$$\left. + 2\pi j \sum(\text{Residues of poles enclosed by } C_T)\right] \qquad (25)$$

$F(z)$ has poles at the points

$$z = -\beta + 2n\pi N \quad , \qquad (26)$$

where N is zero or a positive or negative integer. These poles lie on the real axis of the z-plane, and their positions on this axis are determined by the values of n, ϕ, and ϕ'.

When $-\pi \leq (-\beta + 2n\pi N) \leq \pi$, the pole is enclosed by C_T and its residue must be included in the evaluation of $I(kr, \beta, n)$ as is indicated in Equation 25. This residue can be found by first writing the integrand of Equation 21

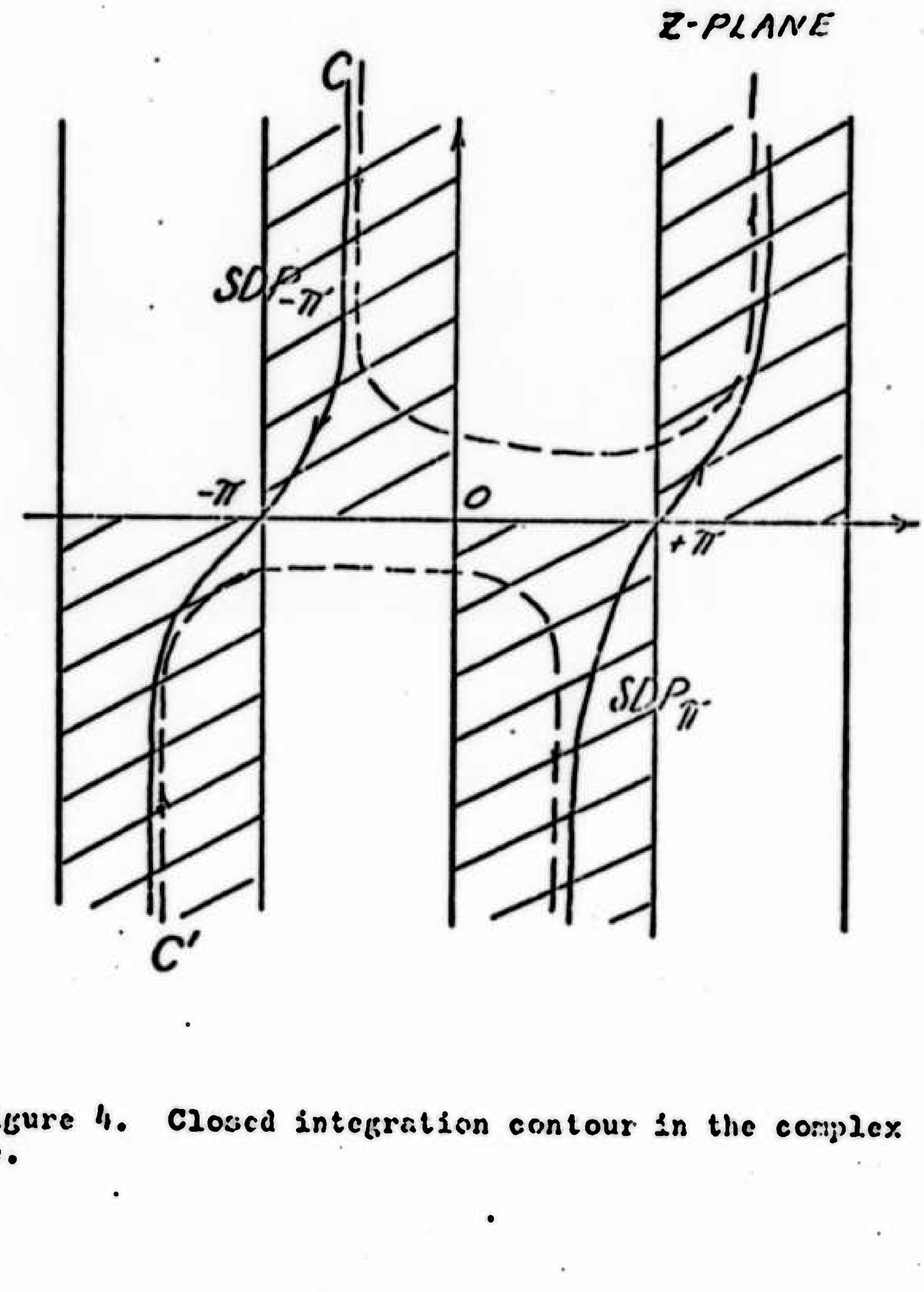

Figure 4. Closed integration contour in the complex z-plane.

as the ratio $p(z)/q(z)$, where

$$p(z) = \cos\left(\frac{z+\beta}{2n}\right) e^{jkr\cos z} \quad . \tag{27}$$

and

$$q(z) = 4\pi jn \sin\left(\frac{z+\beta}{2n}\right) \tag{28}$$

Since $p(z)$ and $q(z)$ are analytic, R, the residue of their ratio at $z = -\beta + 2n\pi N$, is

$$R = \left.\frac{p(z)}{q'(z)}\right|_{z = -\beta + 2n\pi N} \tag{29}$$

or

$$R = \frac{1}{2\pi j} e^{jkr\cos(-\beta + 2\pi nN)} \tag{30}$$

The residue contribution to G_p from the pole at $z = -\beta + 2n\pi N$ is, therefore,

$$e^{jkr\cos(-\beta + 2n\pi N)}\, U\left[\pi - \left|-\beta + 2n\pi N\right|\right] ,$$

where U represents the unit step function.

$$U(t) = \begin{cases} 0 \text{ if } t < 0 \\ 1 \text{ if } t > 0 \\ \frac{1}{2} \text{ if } t = 0 \end{cases} \tag{31}$$

The last requirement in the above definition of U(t) accounts for the fact that the residue of the pole has the Cauchy principal value when the pole lies on the integration contour.

The above contribution to G_p describes a plane wave propagation in a restricted region of space. If N = 0 and $\beta = \phi - \phi'$ the residue contribution to G_p has the form

$$e^{jkr\cos(\phi-\phi')}\,U(\pi - |\phi - \phi'|).$$

This term describes the plane wave field incident on the wedge. The angular space illuminated by this wave depends on the angle of incidence ϕ'. The illuminated region is described by $\pi - |\phi - \phi'| > 0$. The transition between the illuminated region and dark region, that is, the shadow boundary, is defined by $\pi - |\phi - \phi'| = 0$. If $\alpha - \pi < \phi' < \pi$, or if $\alpha < \pi$, no shadow boundary can occur. When a field point falls on the shadow boundary the pole associated with the incident field falls on a saddle point. If $\phi' < \alpha - \pi$ the pole coincides with the saddle at $z = -\pi$, while if $\phi' > \pi$ it coincides with the saddle at $z = +\pi$.

All of the other residue contributions to G_p describe reflected plane wave components. The angular regions of space illuminated by these reflected fields are described by $\pi - |2n\pi N - (\phi \pm \phi')| > 0$, and the boundaries of these fields by $\pi - |2n\pi N - (\phi \pm \phi')| = 0$, except when N = 0 and $(\phi \pm \phi') = \phi - \phi'$. Clearly, when the field point falls on a reflection boundary the pole associated with that field component coincides with a saddle point.

The poles of $F(z)$ play two roles in the determination of the asymptotic expression for G_p. First, they determine the plane wave components of the field through the residue contributions discussed in the previous paragraphs. Second, they strongly influence the form of the asymptotic expression for the integrals in Equation 25. For these reasons, it is important to have a complete description of the pole configurations of $F(z)$. In particular, the index N of the pole nearest the saddle points of the integrals in Equation 25 must be known.

Figures 5 and 6 illustrate a method for describing the possible pole configurations which can occur as ϕ and ϕ' are varied; α is assumed to be fixed at 100 degrees in this example. Figure 5 illustrates the possible pole configurations for $\beta = \phi - \phi'$; Figure 6 is drawn for $\beta = \phi + \phi'$. The rectangles denote the range of Rez over which the poles move as ϕ, the angle of observation, varies. The right-hand side of each rectangle coresponds to $\phi = 0$, and the left to $\phi = \alpha$. Each rectangle corresponds to a fixed value of N, the pole index, and ϕ', the angle of incidence.

The angular regions illuminated by the incident and reflected fields can easily be determined from this diagram as can the locations of the field boundaries.

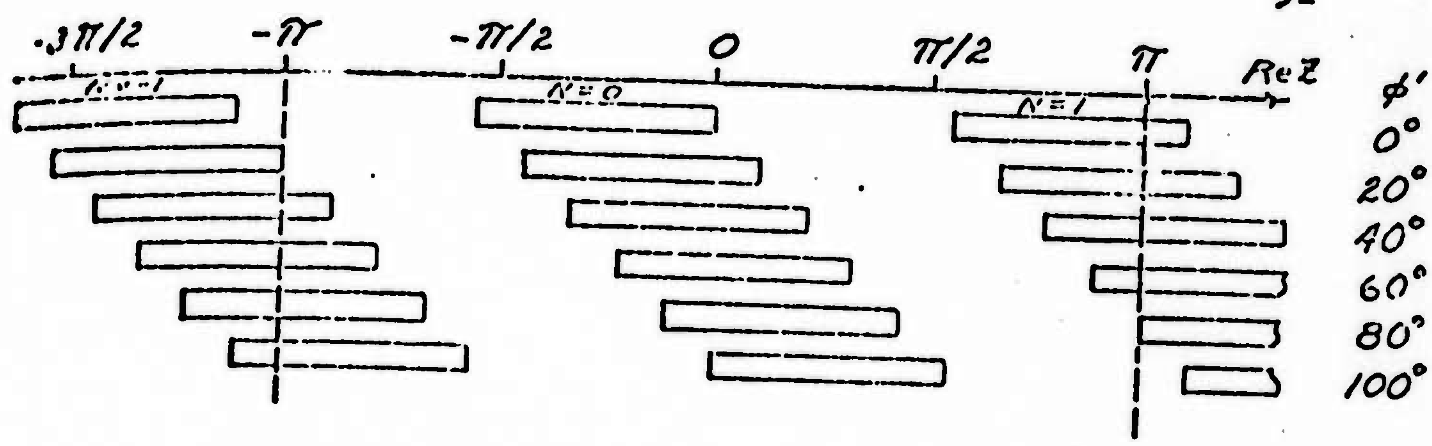

Figure 5. The allowed ranges for the poles of $F(z)$ for various values of ϕ'. $\beta = \phi - \phi'$ and $\alpha = 100^\circ$.

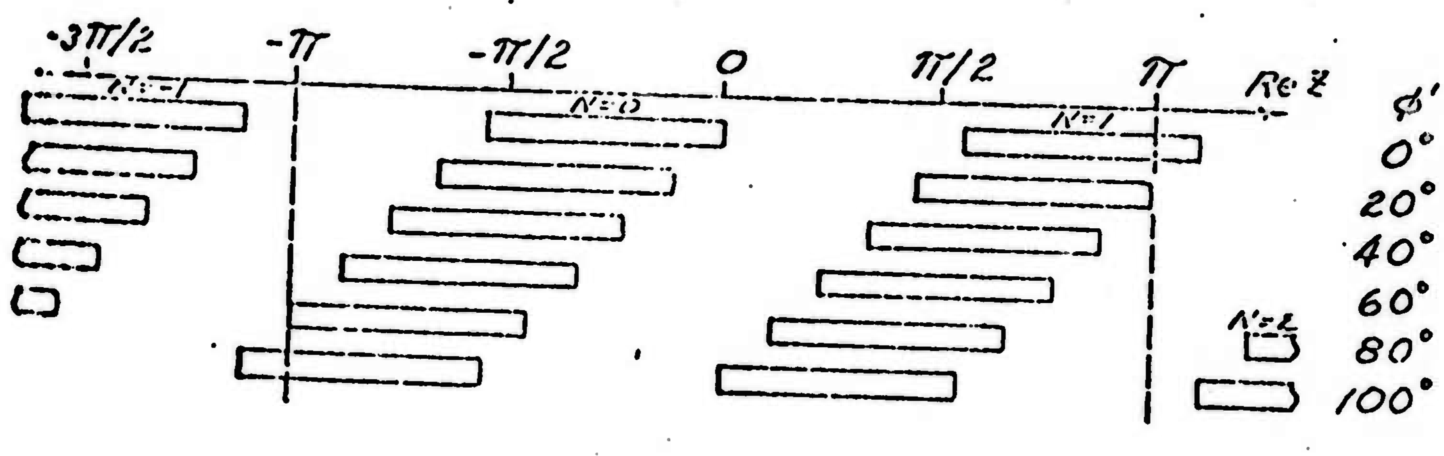

Figure 6. The allowed ranges for the poles of $F(z)$ for various values of ϕ'. $\beta = \phi + \phi'$ and $\alpha = 100^\circ$.

The illuminated regions are defined by the values of ϕ, ϕ', and N for which the poles lie between the vertical lines at $z = \pm\pi$. The field boundaries occur for the values of ϕ, ϕ', and N at which the poles coincide with these lines.

It is important to observe that various poles can lie near the saddle points at $z = \pm\pi$, depending on the value of ϕ and ϕ'. In Figure 6, for example, if $\phi' = 100$ degrees and $\phi = 100$ degrees, the pole $N = 0$ falls near the saddle at $z = -\pi$, and the pole $N = 2$ lies near $z = +\pi$. On the other hand, if $\phi' = 0$ and $\phi = 0$, the pole $N = -1$ is near $z = -\pi$ while the pole $N = +1$ is near $z = +\pi$.

Figures 7 and 8 picture the possible pole configurations for a 40 degree wedge. This example illustrates that as n decreases toward zero an increasing number of poles will fall within the region $-\pi \leq \mathrm{Re}\, z \leq \pi$, and that higher order poles, that is, poles described by larger values of N, will lie near the saddle points.

Later in the analysis it will be important to recognize that the pole nearest the saddle point at

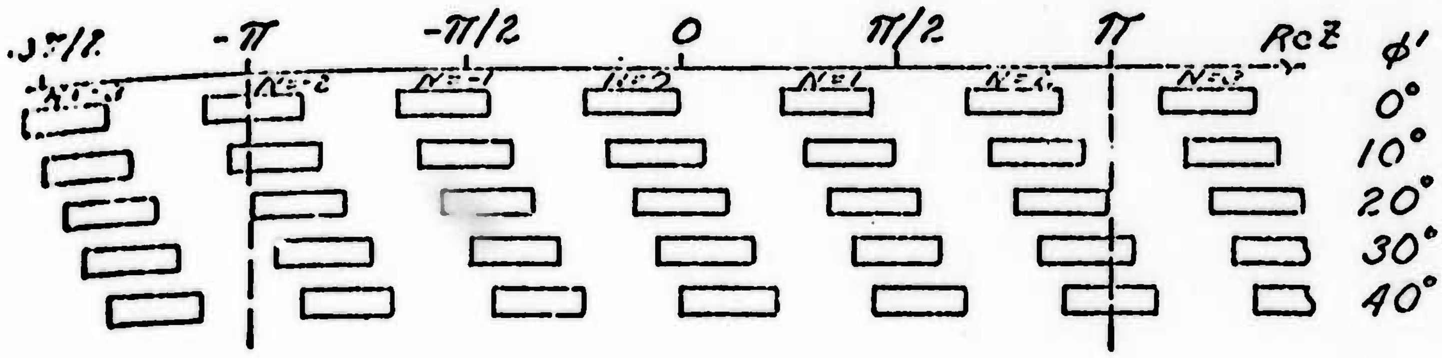

Figure 7. The allowed ranges for the poles of $F(z)$ for various values of ϕ'. $\beta = \phi - \phi'$ and $\alpha = 40^{\circ}$.

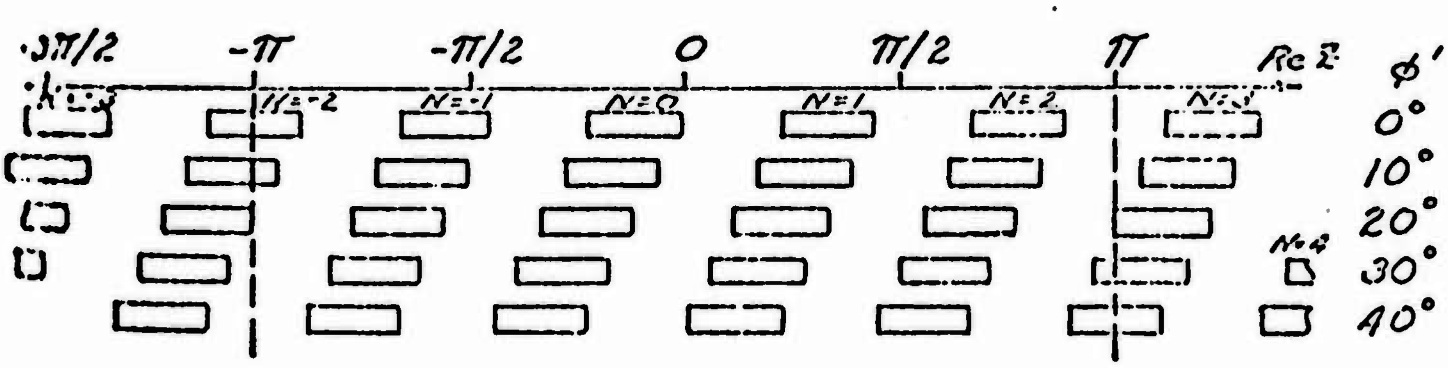

Figure 8. The allowed ranges for the poles of $F(z)$ for various values of ϕ'. $\beta = \phi + \phi'$ and $\alpha = 40^{\circ}$.

$z = \pm \pi$ is described by the N which most nearly satisfies the equation

$$2n\pi N - (\phi \pm \phi') = \pm \pi . \tag{32}$$

The next step required in the derivation of the asymptotic expression for G_p is the evaluation of the two integrals in Equation 25, that is, the asymptotic evaluation of

$$I_{-\pi}(kr, \beta, n) = \frac{-1}{4n\pi j} \int_{SDP_{-\pi}} \cot\left(\frac{\beta + z}{2n}\right) e^{jkr \cos z} \, dz \tag{33}$$

and

$$I_{+\pi}(kr, \beta, n) = \frac{-1}{4n\pi j} \int_{SDP_{\pi}} \cot\left(\frac{\beta + z}{2n}\right) e^{jkr \cos z} \, dz \tag{34}$$

Transformation to a New Complex Plane

In order to evaluate these integrals, it is most convenient to transform variables to a complex plane in which $SDP_{\pm\pi}$ coincides with the real axis. This new complex plane will be called the u-plane. The transformation equation relating the z- and u-planes is found in the following way. For values of z on $SDP_{\pm\pi}$

$$\mathrm{Re}f(z) \lessgtr \mathrm{Re}f(\pm\pi) \tag{35}$$

and

$$\mathrm{Im}f(z) = \mathrm{Im}f(\pm\pi) \quad . \tag{36}$$

Therefore, on $SDP_{\pm\pi}$, f(z) can be written

$$f(z) = f(\pm\pi) - u^2 \quad , \tag{37}$$

when u is real. Substituting Equation 22 into 37 yields the transformation

$$j \cos z = -j - u^2 \tag{38}$$

or

$$u = \pm e^{-j\frac{\pi}{4}}\sqrt{2}\cos\frac{z}{2} \tag{39}$$

The choice of sign must now be made. The equation for the steepest descent path SDP_{π} is

$$\cos x \quad \cosh y = -1 \tag{40}$$

In the vicinity of $z = \pi$, this reduces to

$$x - \pi = y \quad , \tag{41}$$

a straight line making an angle of 45° with the x-axis. In this vicinity z can, therefore, be expressed as

$$z = \pi + se^{j\frac{\pi}{4}} \quad , \tag{42}$$

where s is the distance measured along the path. The value of s is zero at $z = \pi$, positive for $\mathrm{Im}z > 0$, and negative for $\mathrm{Im}z < 0$. It follows from Equations 39 and 42 that for z in the vicinity of

$$u = \pm \left(\frac{-s}{2} \right) \tag{43}$$

When $z > 0$, u must be positive if integration along SDP is to correspond to integration from $-\infty$ to $+\infty$ along the real u-axis. The minus sign should, therefore, be used in Equation 39. The transformation which maps SDP_{π} onto the real axis of the u-plane is, therefore,

$$u = -e^{-j\frac{\pi}{4}} \sqrt{2} \cos \frac{z}{2} \tag{44}$$

It can be shown in a similar manner that this transformation also maps $SDP_{-\pi}$ onto the real axis of the u-plane.

Figure 9 pictures the strip of the z-plane defined by $0 \leq \mathrm{Re}\, z \leq 2\pi$. SDP_{π} is also shown here. Figure 10 shows how the various regions of this strip map onto the u-plane. Other strips of the z-plane map onto other Riemann sheets of the complex u representation. The strip defined by $-2\pi < \mathrm{Re}\, z < 0$ maps onto a sheet adjacent to the one pictured in this figure. The small, lettered circles on these figures illustrate the manner in which the poles of $F(z)$ map onto the u-plane. Notice that the poles in the u-plane move to the origin [illegible] their counterparts in the z-plane move toward the saddle [illegible] $z = \pi$.

Applying the transformatio[illegible] defined by Equation 44 to Equations 33 and 34 yields

$$I_{\pm\pi}(kr, \beta, n) = -\frac{e^{-jkr}}{4\pi n j} \int_{-\infty}^{\infty} g(u)\, \frac{dz}{du}\, e^{-kru^2}\, du \;, \tag{45}$$

where

$$g(u) = \cot\left(\frac{\beta + z(u)}{2n}\right) \tag{46}$$

and

$$\frac{dz}{du} = \frac{e^{j\frac{\pi}{4}}\sqrt{2}}{\sin \frac{z(u)}{2}} \,. \tag{47}$$

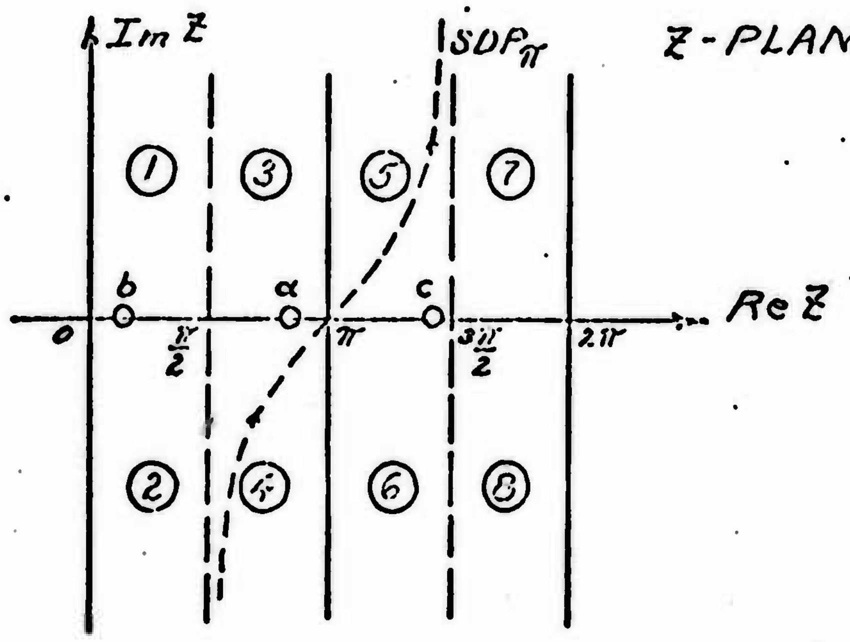

Figure 9. A portion of the strip of the complex z-plane defined by $0 \leq \mathrm{Re}\, z \leq 2\pi$. The dotted line denotes SDP_π and the small circles represent poles of F(z).

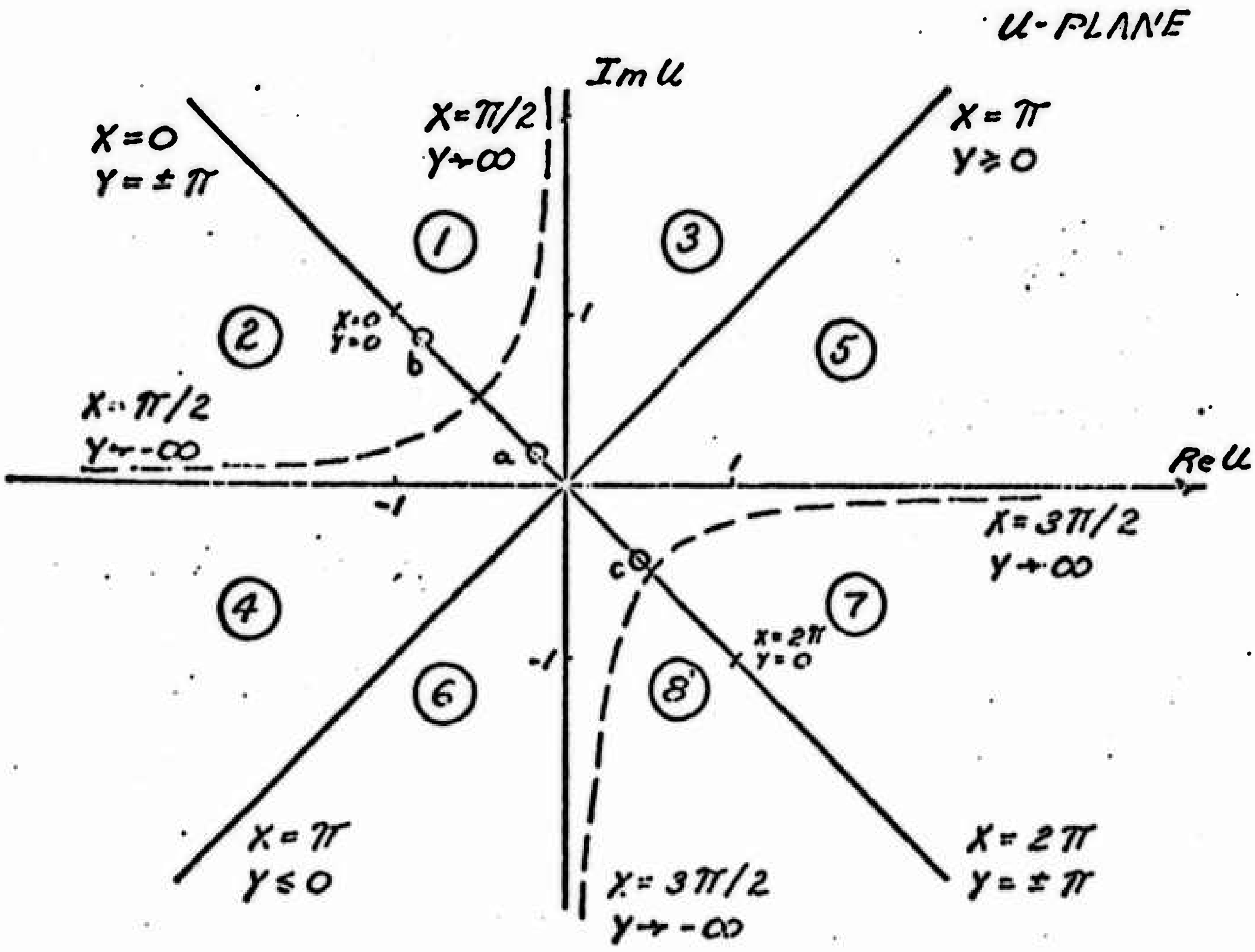

Figure 10. The portion of the complex u-plane corresponding to the portion of the z-plane shown in Figure 9. Several of the z-plane boundary lines are indicated. The circled numbers indicate corresponding regions in the two planes. SDP_π coincides with the real u-axis.

Thus Equation 45 can be written

$$I_{\pm\pi}(kr, \beta, n) = -\frac{e^{-j(kr + \frac{\pi}{4})}}{\pi 2\sqrt{2}\, n} \int_{-\infty}^{\infty} \frac{\cot \frac{\beta + z(u)}{2n}}{\sin \frac{z(u)}{2}} e^{-kru^2} du \qquad (48)$$

or

$$I_{\pm\pi}(kr, \beta, n) = -\frac{e^{-j(kr + \frac{\pi}{4})}}{\pi 2\sqrt{2}\, n} \int_{-\infty}^{\infty} G(u) e^{-kru^2}\, du \qquad (49)$$

with

$$G(u) = \frac{\cot \frac{\beta + z(u)}{2n}}{\sin \frac{z(u)}{2}} \qquad (50)$$

This completes the transformation of $I_{\pm\pi}(kr, \beta, n)$ from the z-plane to the u-plane representation. In the remaining sections of this chapter, this integral will be evaluated by the method of steepest descents and the Pauli-Clemmow modification of this method.

Evaluation of $I_{\pm\pi}(kr, \beta, n)$ by the Method of Steepest Descents

In this section Equation 49 is evaluated by the ordinary method of steepest descents.[112] In this evaluation it is assumed that none of the poles of F(u) lie near the origin of the u-plane. This is equivalent to assuming that none of the poles of F(z) lie near $z = \pm\pi$. Physically this assumption imples that the diffracted components of the field are being evaluated at points well removed from shadow and reflection boundaries.

If $G(u)$ has no poles near $u = 0$, it can be expanded in a Maclaurin series having a radius of convergence extending from the origin to the first pole. If this expansion is made, and the result substituted into Equation 49, $I_{\pm\pi}(kr, \beta, n)$ takes the form

$$I_{\pm\pi}(kr, \beta, n) \sim -\frac{e^{-j(kr + \frac{\pi}{4})}}{\pi 2\sqrt{2}\, n} \sum_{m=0}^{\infty} C_m^{\pm} (\beta, n) \cdot$$

$$\cdot \int_{-\infty}^{\infty} u^m e^{-kru^2} du \quad , \tag{51}$$

where

$$C_m^{\pm} (\beta, n) = \frac{1}{m!} \frac{d^{(m)}}{du^{(m)}} G(u) \Bigg|_{\substack{u = 0 \\ (z = \pm\pi)}} \tag{52}$$

The positive superscript on the coefficients of the Maclaurin series indicates that the derivative of $G(u)$ is to be evaluated at $u = 0$ on the Riemann sheet corresponding to the z-plane strip $0 \leq Re z \leq 2\pi$. The minus sign denotes that the evaluation is to be made on the u-plane Riemann sheet corresponding to the strip $-2\pi < \mathrm{Re}\,z < 0$.

The odd terms of Equation 51 integrate to zero so it can be written

$$I_{\pm\pi}(kr, \beta, n) \sim - \frac{e^{-j(kr + \frac{\pi}{4})}}{\pi 2\sqrt{2}\, n} \sum_{m=0}^{\infty} C_{2m}^{\pm}(\beta, n) \cdot$$

$$\cdot \int_{-\infty}^{\infty} u^{2m} e^{-kru^2} du \tag{53}$$

Integration of this series reduces it to the following form

$$I_{\pm\pi}(kr, \beta, n) \sim - \frac{e^{-j(kr + \frac{\pi}{4})}}{\pi 2\sqrt{2}\, n} \Bigg[C_0^{\pm}(\beta, n) \frac{1}{\sqrt{kr}} +$$

$$+ \sum_{m=1}^{\infty} C_{2m}^{\pm}(\beta, n) \frac{1\cdot 3\cdot 5 \cdots (2m-1)}{2^m} \cdot$$

$$\cdot \frac{1}{(kr)^{m+\frac{1}{2}}} \Bigg] \tag{54}$$

or, in more compact notation,

$$I_{\pm\pi}(kr, \beta, n) \sim - \frac{e^{-j(kr + \frac{\pi}{4})}}{\pi 2\sqrt{2}\, n} \sum_{m=0}^{\infty} C_{2m}^{\pm}(\beta, n) \frac{\Gamma(m + \frac{1}{2})}{(kr)^{m+\frac{1}{2}}} \tag{55}$$

The coefficients of Equation 55 are found by the simple but tedious evaluation of Equation 52. The first three of these coefficients are listed below.

$$C_0^{\pm}(\beta, n) = \pm \cot \frac{\beta \pm \pi}{2n} \tag{56}$$

$$C_2^{\pm}(\beta, n) = jC_0^{\pm}(\beta, n)\left[\frac{1}{4} + \frac{1}{2n^2}\csc^2 \frac{\beta \pm \pi}{2n}\right] \tag{57}$$

$$C_4^{\pm}(\beta, n) = -\frac{1}{4}C_0^{\pm}(\beta, n)\left[\frac{3}{8} + \frac{1}{n^4}\csc^4 \frac{\beta \pm \pi}{2n} + \right.$$
$$\left. + \left\{\frac{5}{6n^2} - \frac{1}{3n^4}\right\}\csc^2 \frac{\beta \pm \pi}{2n}\right] \tag{58}$$

When Equations 8, 25, 33, and 34 are combined, G_p takes the form

$$G_p = I_{-\pi}(kr, \beta = \phi - \phi', n) + I_{+\pi}(kr, \beta = \phi - \phi', n) \pm$$
$$\pm I_{-\pi}(kr, \beta = \phi + \phi', n) \pm$$
$$\pm I_{+\pi}(kr, \beta = \phi + \phi', n) +$$
$$+ e^{jkr\cos(\phi - \phi')}U(\pi - |\phi - \phi'|) +$$
$$+ \text{plane wave terms corresponding to reflected field components.} \tag{59}$$

It follows from the derivation presented in this section that so long as the field point at which G_p is being evaluated does not lie on or near a shadow or reflection boundary G_p can be written as follows:

$$G_p \sim - \frac{e^{-j(kr + \frac{\pi}{4})}}{\pi 2\sqrt{2}\, n} \Bigg[\sum_{m=0}^{\infty} \left[C_{2m}^{-}(\phi - \phi', n) + C_{2m}^{+}(\phi - \phi', n) \right] \cdot$$

$$\cdot \frac{\Gamma(m + \frac{1}{2})}{(kr)^{m + \frac{1}{2}}} \pm \sum_{m=0}^{\infty} \left[C_{2m}^{-}(\phi + \phi', n) + C_{2m}^{+}(\phi + \phi', n) \right] \cdot$$

$$\cdot \frac{\Gamma(m + \frac{1}{2})}{(kr)^{m + \frac{1}{2}}} \Bigg] + e^{jkr \cos(\phi - \phi')} U(\pi - |\phi - \phi'|) +$$

+ plane wave terms corresponding to reflected field components. (60)

This equation is identical to the asymptotic expression for G_p developed by Oberhettinger for the case in which the field point is well-removed from shadow and reflection boundaries. If only the first term is retained in each of the summations in this equation it reduces to the familiar form for G_p used in the geometrical theory of diffraction, that is,

$$G_p = \frac{e^{-jkr}}{\sqrt{r}} \left(D(n, \phi - \phi') \pm D(n, \phi + \phi') \right) +$$

$$+ e^{jkr \cos(\phi - \phi')} \, u(\pi - |\phi - \phi'|) +$$

+ plane wave terms corresponding to reflected field components, (61)

where

$$D(n, \phi \pm \phi') = \frac{e^{-j\frac{\pi}{4}} \sin\frac{\pi}{n}}{n\sqrt{2k\pi}\left(\cos\frac{\pi}{n} - \cos\frac{\phi \pm \phi'}{n}\right)}$$

is the edge diffraction coefficient.

It was pointed out in the examples on pages 29 through 34 that when ϕ, the angular coordinate describing the field point, approaches a shadow or reflection boundary a pole approaches at least one of the saddles at $z = \pm\pi$. In such a situation the corresponding u-plane pole will move toward $u = 0$. This will cause the radius of convergence of the Maclaurin series used in the evaluation of Equation 49 to shrink to zero, and the coefficients of that series to grow without bound. This renders invalid the asymptotic series expression for at least one of the first four terms of Equation 59. A method must, therefore, be developed for evaluating Equations 33 and 34 for the case in which a pole of $F(z)$ lies near the saddle point. One such method is discussed in the next section.

Evaluation of $I_{\pm\pi}(kr, \beta, n)$ by the Pauli-Clemmow Modified Method of Steepest Descents

In this section Equations 33 and 34 are evaluated for the case in which a single pole lies near $z = -\pi$ or $z = +\pi$. This evaluation utilizes the basic ideas employed by Pauli but yields a more general result. The approach is somewhat easier to follow than Pauli's, and the result is in a more convenient and useful form since the confluent hypergeometric functions are not introduced.

The essential steps in this evaluation are the following:

a) The integrand of the equations is first written as the product of two functions. One of these describes the pole near the saddle; the other is analytic at the origin and at the pole in question.

b) The integral is then transformed to the u-plane representation. The analytic portion of the integrand is expanded in a Maclaurin series, and the order of summation and integration is interchanged.

c) The resulting series is then integrated term by term.

This process is described in detail for the evaluation of $I_{-\pi}(kr, \beta, n)$ for the case in which the pole of $F(z)$ at $z = -\beta$ is near the saddle point at $z = -\pi$. The results are then presented for the evaluation of $I_{+\pi}(kr, \beta, n)$ for a pole near $z = +\pi$. The technique used in this section fails for small values of n.

It is convenient to begin our discussion with Equation 33. The integrand of this equation has poles at $z = -\beta + 2n\pi N$. So long as n is somewhat greater than 1 only the pole at $z = -\beta$ can lie near the saddle point at $z = -\pi$. A technique for evaluating $I_{-\pi}(kr, \beta, n)$ for this case will now be described. If the integrand of Equation 33 is multiplied and divided by $(\cos z - \cos\beta)$, then it can be written

$$\cot\left(\frac{z+\beta}{2n}\right) e^{jkr\cos z} = H(z)\frac{1}{\cos z - \cos\beta} e^{jkr\cos z} \tag{62}$$

where

$$H(z) = \cot\left(\frac{\beta+z}{2n}\right)(\cos z - \cos\beta) \quad . \tag{63}$$

$H(z)$ is analytic at and near $z = -\beta$, and $H(-\beta) = 2n\sin\beta$. The information concerning the pole at $z = -\beta$ is contained now in the function $(\cos z - \cos\beta)^{-1}$. If $I_{-\pi}(kr, \beta, n)$ is now transformed to the u-plane representation it takes the form

$$I_{-\pi}(kr, \beta, n) = -\frac{e^{-j(kr + \frac{\pi}{4})}}{j2\sqrt{2}\pi n}\int_{-\infty}^{\infty}\frac{H(u)e^{-kru^2}}{u^2 + ja}\,du \tag{64}$$

where

$$H(u) = \frac{\cot \frac{z(u) + \beta}{2n}}{\sin \frac{z(u)}{2}} (\cos z(u) - \cos\beta) \quad , \tag{65}$$

$$a = 1 + \cos\beta \tag{66}$$

and

$$j(u^2 + ja) = \cos z(u) - \cos\beta \quad . \tag{67}$$

$H(u)$ is analytic in the vicinity of the origin so long as only the pole at $z = -\beta$ is near $z = -\pi$, and can be expanded in a Maclaurin series. Therefore, Equation 64 can be written

$$I_{-\pi}(kr, \beta, n) \sim - \frac{e^{-j(kr + \frac{\pi}{4})}}{j2\sqrt{2}\pi n} \sum_{m=0}^{\infty} B_m^-(\beta, n) \cdot \int_{-\infty}^{\infty} \frac{u^m}{u^2 + ja} e^{-kru^2} du \quad , \tag{68}$$

where

$$B_m^-(\beta, n) = \frac{1}{m!} \frac{d^m}{du^m} H(u) \Bigg|_{\substack{u = 0 \\ (z = -\pi)}} \tag{69}$$

All of the odd terms of this series vanish. The remaining terms can be expressed as combinations of well-known functions, namely the Fresnel integrals and inverse powers of kr.

The evaluation of this series is now described. The integrals are treated first, then the coefficients are discussed. The integral in the first term of Equation 68 is

$$I_o(\lambda) = \int_{-\infty}^{\infty} \frac{e^{-\lambda u^2}}{u^2 + ja} \, du \quad , \tag{70}$$

where $\lambda = kr$. This can be evaluated by first differentiating with respect to λ, integrating on u, then λ, and finally again on u. The details of this procedure are as follows. Consider

$$I_o(\lambda) e^{-j\lambda a} = \int_{-\infty}^{\infty} \frac{e^{-\lambda(u^2 + ja)}}{(u^2 + ja)} \, du \quad . \tag{71}$$

Differentiation with respect to λ followed by integration on u yields

$$\frac{d}{d\lambda}\left[I_o(\lambda) e^{-j\lambda a}\right] = - e^{-j\lambda a} \int_{-\infty}^{\infty} e^{-\lambda u^2} \, du = -\sqrt{\frac{\pi}{\lambda}} \, e^{-j\lambda a} \tag{72}$$

Integrating now on λ results in

$$I_o(\lambda)e^{-j\lambda a} = \int_{-\infty}^{\infty} \frac{du}{u^2 + ja} - \sqrt{\pi}\int_0^{\lambda} \frac{e^{-ja\lambda'}}{\sqrt{\lambda'}}\, d\lambda' \quad . \tag{73}$$

The first integral in this equation can be evaluated by integrating over the closed path C shown in Figure 11.

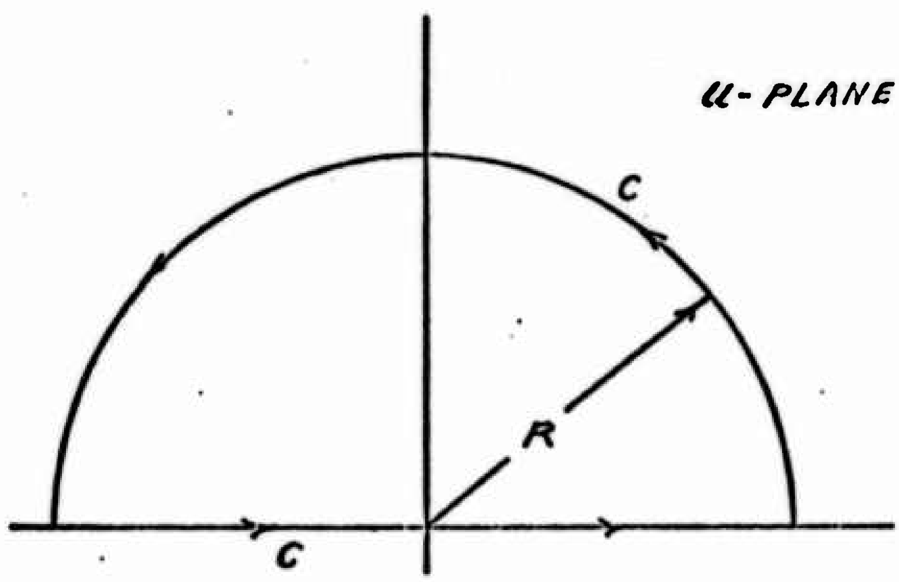

Figure 11. A contour for evaluating $\int_{-\infty}^{\infty} \frac{du}{u^2 + ja}$.

Since the integral over the semicircular part of C vanishes as R approaches infinity,

$$\int_{-\infty}^{\infty} \frac{du}{u^2 + ja} = \oint_C \frac{du}{(u + e^{-j\frac{\pi}{4}}\sqrt{a})(u - e^{-j\frac{\pi}{4}}\sqrt{a})} \tag{74}$$

$$= 2\pi j \left\{ \text{Residues of poles enclosed by } C \right\}.$$

The residue of the pole at

$$u = -e^{-j\frac{\pi}{4}}\sqrt{a}$$

is

$$(-2\sqrt{a}\, e^{-j\frac{\pi}{4}})^{-1}$$

and, therefore,

$$\int_{-\infty}^{\infty} \frac{du}{u^2 + ja} = \frac{-\pi j e^{j\frac{\pi}{4}}}{\sqrt{a}} \tag{75}$$

Substituting this result into Equation 73 yields

$$I_0(kr) = -\sqrt{\pi}\, e^{jkra} \int_0^{kr} \frac{e^{-ja\lambda'}}{\sqrt{\lambda'}}\, d\lambda' - j\frac{\pi}{\sqrt{a}}\, e^{j(kra + \frac{\pi}{4})} \tag{76}$$

The integral in this equation can be expressed as a complex Fresnel integral by means of the substitution $a\lambda' = \frac{\pi}{2} t^2$.

The result is

$$I_o(kr) = \frac{\pi\sqrt{2}\, e^{jkra}}{\sqrt{a}} \left[\frac{e^{-j\frac{\pi}{4}}}{\sqrt{2}} - \int_0^x e^{-j\frac{\pi}{2}\tau^2} d\tau \right], \tag{77}$$

where

$$x = \left(\frac{2kra}{\pi}\right)^{\frac{1}{2}}$$

This can also be written

$$I_o(kr) = \frac{2\sqrt{\pi}\, e^{jkra}}{\sqrt{a}} \int_{(kra)^{\frac{1}{2}}}^{\infty} e^{-jt^2} dt \quad . \tag{78}$$

The evaluation of the higher order integrals in Equation 68 is now quite straightforward. The integrand of the next even term can be expanded as follows:

$$\frac{u^2}{u^2 + ja} = 1 - \frac{ja}{u^2 + ja} \tag{79}$$

Therefore,

$$\int_{-\infty}^{\infty} \frac{u^2}{u^2 + ja} e^{-kru^2} du = \int_{-\infty}^{\infty} e^{-kru^2} du - jaI_o(kr) =$$

$$= \left(\frac{\pi}{kr}\right)^{\frac{1}{2}} - jaI_o(kr) \quad . \tag{80}$$

The integrand of the term corresponding to m = 4 can be written

$$\frac{u^4}{u^2 + ja} = u^2 - ja + \frac{(-ja)^2}{u^2 + ja} \tag{81}$$

so

$$\int_{-\infty}^{\infty} \frac{u^4}{u^2 + ja} = \frac{\sqrt{\pi}}{2(kr)^{\frac{3}{2}}} - ja \frac{\sqrt{\pi}}{(kr)^{\frac{1}{2}}} + (-ja)^2\, I_o(kr) \quad . \tag{82}$$

The integral of the general $2m^{th}$ term can be written

$$\int_{-\infty}^{\infty} \frac{u^{2m}}{u^2 + ja} e^{-kru^2}\, du = \sum_{k=1}^{m} \frac{1\cdot3\cdot5\cdots(2(m-k)-1)\sqrt{\pi}}{2^{(m-k)}(kr)^{m-k+\frac{1}{2}}} \cdot$$

$$\cdot (-ja)^{k-1} + (-ja)^m\, I_o(kr) \tag{83}$$

or, in more compact form,

$$\int_{-\infty}^{\infty} \frac{u^{2m}}{u^2 + ja} e^{-kru^2} du = \sum_{k=1}^{m} \frac{\Gamma(m - k + \frac{1}{2})(-ja)^{k-1}}{(kr)^{(m - k + \frac{1}{2})}} +$$

$$+ (-ja)^m I_o(kr) \qquad (84)$$

Substitution of this into Equation 68 yields

$$I_{-\pi}(kr, \beta, n) \sim - \frac{e^{-j(kr + \frac{\pi}{4})}}{j2\sqrt{2}\, n\pi} \sum_{m=0}^{\infty} B_{2m}^{-} (\beta, n) \cdot$$

$$\left[\sum_{k=1}^{m} \frac{\Gamma(m - k + \frac{1}{2})(-ja)^{k-1}}{(kr)^{(m - k + \frac{1}{2})}} + \right.$$

$$\left. + (-ja)^m I_o(kr) \right] \qquad (85)$$

The coefficients, B_{2m}^{-} (β, n), are related in a simple manner to those of series developed in the previous section.

It follows from Equations 65, 67, 69, and 50 that

$$B_{2m}^{-}(\beta, n) = \frac{1}{(2m)!} \frac{d^{(2m)}}{du^{(2m)}} \left\{ jG(u)(u^2 + ja) \right\} \Bigg|_{u = 0} \qquad (86)$$

This yields the following relations:

$$B_0^{-}(\beta, n) = -aC_0^{-}(\beta, n) \qquad (87)$$

and

$$B_{2m}^{-}(\beta, n) = jC_{2(m-1)}^{-}(\beta, n) - aC_{2m}^{-}(\beta, n) . \qquad (88)$$

Since $H(u)$ is analytic when $z = -\beta$, all of these coefficients are finite so long as only the pole at $z = -\beta$ approaches the saddle at $z = -\pi$. In particular, they are finite when $\beta = \pi$. The following analysis reveals the value of these coefficients for this value of β. $H(u)$ can be written as the sum of an even and odd function of u, that is,

$$H(u) = H^e(u) + H^o(u) \quad , \qquad (89)$$

where

$$H^e(u) = \frac{H(u) + H(-u)}{2} \qquad (90)$$

and

$$H^{o}(u) = \frac{H(u) - H(-u)}{2} \tag{91}$$

In order to find the form of $H^{e}(u)$ and $H^{o}(u)$ it is most convenient to make the change of variable

$$z(u) = \omega(u) - \pi \tag{92}$$

so that

$$u = -e^{-j\frac{\pi}{4}}\sqrt{2}\cos\frac{z}{2} = -e^{-j\frac{\pi}{4}}\sqrt{2}\sin\frac{\omega}{2} \tag{93}$$

The allowed values of ω are restricted to the shaded strip of the ω-plane shown in Figure 12. Therefore, a change in the sign of ω corresponds to a change in the sign of u. This permits $H^{e}(u)$ and $H^{o}(u)$ to be written as follows:

$$H^{e}(u) = \frac{\cos\omega(u) + \cos\beta}{2\cos\frac{\omega(u)}{2}}\left[\cot\frac{\omega(u) + \beta - \pi}{2n} + \right.$$

$$\left. + \cot\frac{-\omega(u) + \beta - \pi}{2n}\right] \tag{94}$$

and

$$H^{o}(u) = \frac{\cos\omega(u) + \cos\beta}{2\cos\frac{\omega(u)}{2}}\left[\cot\frac{\omega(u) + \beta - \pi}{2n} - \right.$$

$$\left. - \cot\frac{-\omega(u) + \beta - \pi}{2n}\right] \tag{95}$$

Now when $\beta = +\pi$, $H^e(u) = 0$ and, therefore, all of the even coefficients of the Maclaurin series expansion of $H(u)$ vanish, that is,

$$B^-_{2m}(\pi, n) = 0 \tag{96}$$

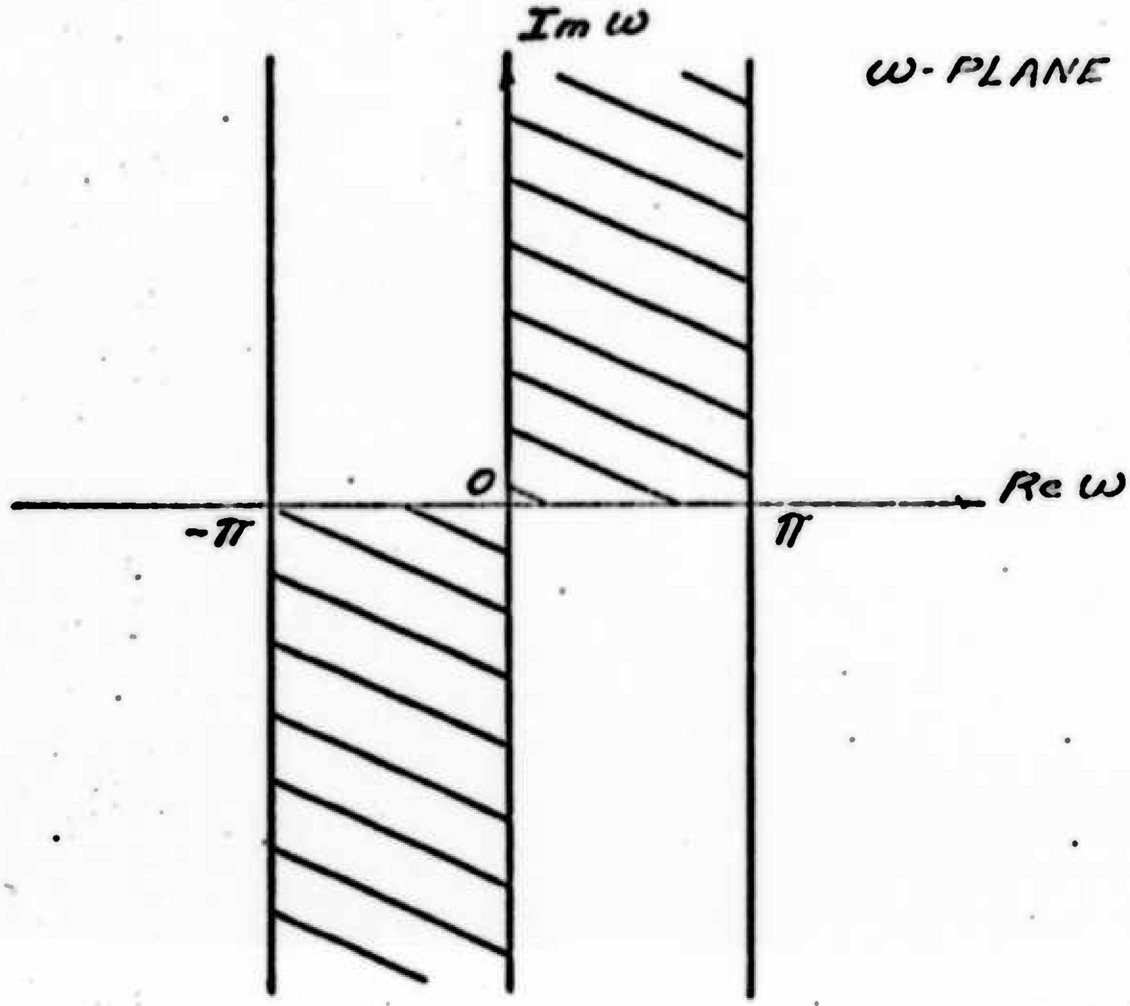

Figure 12. The complex ω-plane. The values of ω allowed in Equation 93 are restricted to the shaded regions.

For this case of $\beta = \pi$ Equation 85 reduces to

$$I_{-\pi}(kr, \pi, n) \sim \frac{e^{-j(kr + \frac{\pi}{4})}}{j2\sqrt{2}\,n\,\pi} B_o(\pi, n)\, I_o(kr) \tag{97}$$

This first term must be retained since the pole in $I_o(kr)$ at $\beta = \pi$ just cancels the zero in $B_o(\beta, n)$ to yield a finite value. That value is found by writing $\beta = \pi \pm \epsilon$ and taking the limit as $\epsilon \rightarrow 0$. The details are shown here.

$$B_o(\pi \pm \epsilon, n) = -(1 + \cos[\pi \pm \epsilon]) \cot \frac{\pm\epsilon}{2n}$$

$$\approx \mp n\epsilon \tag{98}$$

$$I_o(kr) \approx \frac{\pi\sqrt{2}}{\epsilon} e^{-j\frac{\pi}{4}} \tag{99}$$

so

$$\lim_{\epsilon \rightarrow 0} I_{-\pi}(kr, \pi \pm \epsilon, n) = \pm \frac{1}{2} e^{-jkr} \tag{100}$$

The plus sign applies when $\beta > \pi$, and the minus sign when $\beta < \pi$. This discontinuity in the diffracted field just compensates for the discontinuity at the boundaries of the incident and reflected fields, producing a continuous total field there. The value of Equation 100 directly on the field boundary is zero. The Cauchy principal value of the associated residue contribution is $\frac{1}{2}$, as was shown in Equation 31.

The pole at $z = -\beta = -(\phi - \phi')$ can lie near the saddle point at $z = +\pi$. When this situation occurs

$$I_{+\pi}(kr, \beta, n) = -\frac{1}{4\pi n j} \int_{SDP_{\pi}} \cot\left(\frac{\beta + z}{2n}\right) e^{jkr \cos z}\, dz \qquad (34)$$

must be evaluated in the manner just illustrated. This evaluation yields

$$I_{+\pi}(kr, \beta, n) \sim -\frac{e^{-j(kr + \frac{\pi}{4})}}{j2\sqrt{2}\, n\pi} \sum_{m=0}^{\infty} B_{2m}^{+}(\beta, n) \cdot$$

$$\left[\sum_{k=1}^{m} \frac{\Gamma(m - k + \frac{1}{2})(-ja)^{k-1}}{(kr)^{(m - k + \frac{1}{2})}} + (-ja)^{m} I_0(kr)\right] \qquad (101)$$

With

$$\lim_{\epsilon \to 0} I_{+\pi}(kr, \pi \pm \epsilon, n) = \pm \frac{1}{2} e^{-jkr}, \qquad (102)$$

$$B_o^+(\beta, n) = -aC_o^+(\beta, n) \quad , \tag{103}$$

and

$$B_{2m}^+(\beta, n) = jC_{2(m-1)}^+(\beta, n) - aC_{2m}^+(\beta, n) \quad . \tag{104}$$

Figures 5, 6, 7, and 8 illustrate that the poles of $F(z)$ located at $z = -\beta + 2N\pi n$ can lie near the saddle point at $z = -\pi$ when N is a negative integer. When this situation occurs $I_{-\pi}(kr, \beta, n)$ can be evaluated by the method used for the case in which the pole at $z = -\beta$ approaches that saddle. However, the method must be modified slightly to account for the fact that the pole is described by arbitrary negative N. This modification entails simply replacing the term $(\cos z - \cos\beta)$ of Equations 62 and 63 by $(\cos z - \cos(-\beta + 2n\pi N))$. This substitution makes $H(z)$ analytic at $z = -\beta + 2n\pi N$ and allows expansion of $H(u)$ in a Maclaurin series. This substitution puts Equation 66 into the form $a = 1 + \cos(-\beta + 2n\pi N)$. All other equations of the analysis remain unchanged in form. Therefore, when G_p is to be determined at field points for which $-\beta + 2n\pi N$ is near $-\pi$, Equation 85 should be used to evaluate $I_{-\pi}(kr, \beta, n)$. In Equation 85 and the allied equations, that is, 87 and 88, $a = 1 + \cos(-\beta + 2n\pi N)$.

It also can be shown that when G_p is to be determined at field points for which $-\beta + 2n\pi N$ is near π, (see Figure 8, for example) Equation 101 should be used to evaluate

$I_{+\pi}(kr, \beta, n)$. In this equation $a = 1 + \cos(-\beta + 2nN\pi)$. In this case N is a positive integer.

If n is close to zero, that is, if the exterior angle between the faces of the scattering wedge is small, a large number of poles will lie near the saddles at $z = \pm\pi$. In this case the radius of convergence of the Maclaurin series for H(u) will be very small and Equations 85 and 101 will fail.

A number of examples illustrating the use of the equations developed in this section are discussed in Chapter IV. However, before proceeding with this the relation between the expressions developed here and those given by Pauli and Oberhettinger will be examined further.

Relation to Pauli's Asymptotic Series

Pauli was the first to introduce the method of steepest descents used in this work. He applied this method to the evaluation of G_p in a manner much like that used in this study. Pauli, however, performed one operation at the beginning of his evaluation which caused his resulting asymptotic expression to be of less general applicability than the one derived here. The starting point for Pauli's derivation was Sommerfeld's *ansatz* which is given by Equation 17. Pauli's path of integration for this equation was closed in the manner shown in Figure 4, and the pole contributions to G_p were evaluated. This reduced G_p to the form

$$G_p = \int_{SDP_{-\pi}} F(z, n, \phi - \phi')dz + \int_{SDP_{+\pi}} F(z, n, \phi - \phi')dz \pm$$

$$\pm \int_{SDP_{-\pi}} F(z, n, \phi + \phi')dz \pm \int_{SDP_{+\pi}} F(z, n, \phi + \phi')dz$$

$$+ \text{ Residue contributions} \quad , \tag{105}$$

where

$$F(z, n, \phi \pm \phi') = -\frac{1}{2\pi n} \frac{e^{j\frac{z}{n}}}{e^{j\frac{z}{n}} - e^{-j\frac{\phi \pm \phi'}{n}}} e^{jkr \cos z} \tag{106}$$

By making the substitution $z = \omega - \pi$ in the first and third integrals and $z = \omega + \pi$ in the second and fourth, Pauli reduced G_p to the sum of two integrals.

$$G_p = \frac{1}{2\pi jn} \sin\frac{\pi}{n} \int_{SDP_o} \frac{e^{-jkr\cos\omega}}{\cos\frac{\pi}{n} - \cos\frac{\omega + (\phi - \phi')}{n}} d\omega \pm$$

$$\pm \frac{1}{2\pi jn} \sin\frac{\pi}{n} \int_{SDP_o} \frac{e^{-jkr\cos\omega}}{\cos\frac{\pi}{n} - \cos\frac{\omega + (\phi + \phi')}{n}} d\omega +$$

$$+ \text{ Residue contributions} \quad . \tag{107}$$

The contour SDP_o in the ω-plane is illustrated in Figure 13.

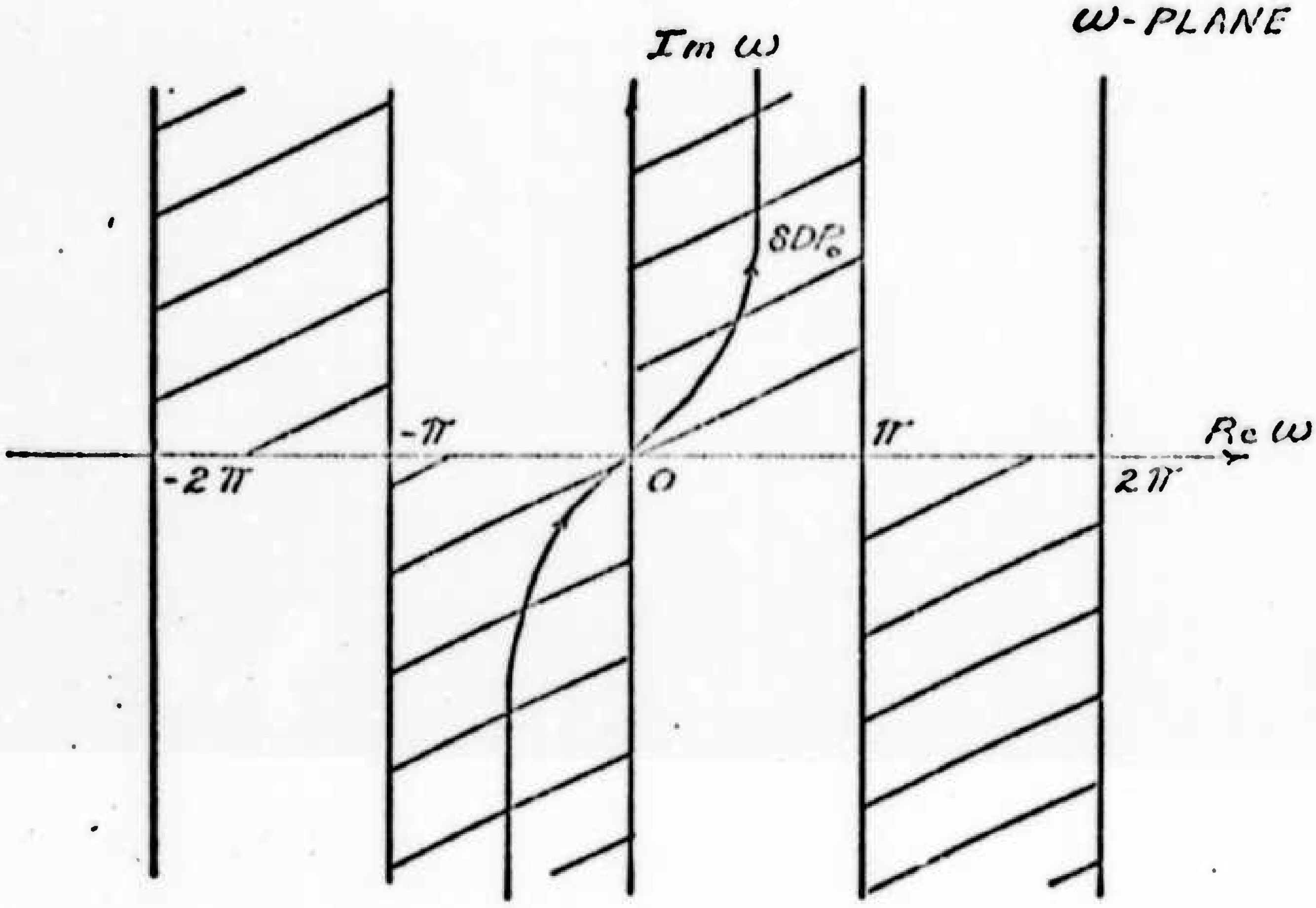

Figure 13. Integration contour SDP_o used by Pauli to evaluate G_p.

Pauli then evaluated this equation by the method described in the previous section.

Consider now the poles of the integrands of Equation 107. The poles which lie near $+\pi$ or $-\pi$ in the z-plane will lie near the origin in the ω-plane. If a pole lies near

$z = \pi$ (or $-\pi$) but none lies near $z = -\pi$ (or π), then a single pole will lie near $\omega = 0$ and Pauli's method of steepest descents yields a useful result for G_p. If, however, one pole lies near $z = +\pi$ and another near $z = -\pi$, two poles will lie near $\omega = 0$. In this case Pauli's method fails and his asymptotic expansion for G_p is not valid.

Pauli reduced the generality of his result when he combined the integrations over $SDP_{-\pi}$ and $SDP_{+\pi}$ into a single equation. The generalized form of Pauli's expression developed in this work can be applied to cases in which poles simultaneously lie near $z = +\pi$ and $z = -\pi$, since the integrations over $SDP_{-\pi}$ and $SDP_{+\pi}$ were evaluated individually.

Pauli's asymptotic expansion for the integrals in Equation 107 is

$$\frac{1}{2\pi j n} \sin\frac{\pi}{n} \int_{SDP_0} \frac{e^{-jkr\cos\omega}}{\cos\frac{\pi}{n} - \cos\frac{\omega+\beta}{n}}\, d\omega =$$

$$= U_B = \frac{1}{\sqrt{2\pi a}\, n} \sin\frac{\pi}{n}\, e^{-j(kr - \frac{\pi}{4})} \cdot$$

$$\sum_{m=0}^{\infty} j^m \frac{\Gamma(m + \frac{1}{2})}{\sqrt{\pi}} A_{2m}(\beta) S_m(kra) \frac{1}{(kr)^m} \tag{108}$$

where

$$S_m(kra) = (m - \tfrac{1}{2})^{-1}(kra)^{\frac{1}{2}} F_2(1, -m + \tfrac{3}{2}, jkra) \quad , \tag{109}$$

$$A_{2m}(\beta) = \frac{e^{-jm\frac{\pi}{2}}}{(2m)!} \frac{d^{(2m)}}{d\omega^{(2m)}}\left[\frac{\cos\omega + \cos\beta}{\cos\frac{\pi}{n} - \cos\frac{\omega+\beta}{n}} \quad \frac{1}{\cos\frac{\omega}{2}}\right]\Bigg|_{\omega = 0} \tag{110}$$

and $a = 1 + \cos \quad = 1 + \cos (\quad \pm \quad ')$. The functions $F_2(1, -m + \frac{3}{2}, jkra)$ are confluent hypergeometric functions. These can be written in the form

$$F_2(1, -m + \tfrac{3}{2}, jkra) = (m - \tfrac{1}{2})(kra)^{m - \frac{1}{2}} e^{jkra} \int_{kra}^{\infty} \frac{e^{-jt}}{t^{m + \frac{1}{2}}} dt \; . \tag{111}$$

If (as Ott[110] has shown) the integrals in this equation are repeatedly integrated by parts Equation 108 can be written in the form shown below.

$$U_B = \frac{1}{\pi\sqrt{2}} \frac{\sin\frac{\pi}{n}}{n} e^{-j(kr - \frac{\pi}{4})} \cdot \sum_{m=0}^{\infty} A_{2m}(\beta) j^m \left[\sum_{k=1}^{m} (-ja)^{k-1} \frac{\Gamma(m - k + \frac{1}{2})}{(kr)^{m-k+\frac{1}{2}}} + (-ja)^m I_0(kr)\right] \; . \tag{112}$$

Pauli's expression for U_B can be derived by combining Equations 85 and 101 for a common value of N, such as N = 0. Combining these equations results in

$$U_B^* = I_{+\pi}(kr, n, \beta) + I_{-\pi}(kr, n, \beta) =$$

$$= \frac{e^{-j(kr - \frac{\pi}{4})}}{\pi\sqrt{2}\,n} \sum_{m=0}^{\infty} \frac{(B_{2m}^{+}(\beta, n) + B_{2m}^{-}(\beta, n))}{2} \cdot$$

$$\sum_{k=1}^{m} \frac{(-ja)^{k-1}\,\Gamma(m - k + \frac{1}{2})}{(kr)^{(m - k + \frac{1}{2})}} + (-ja)^m\, I_0(kr) \quad . \quad (113)$$

It can easily be shown that

$$\frac{B_{2m}^{+}(\beta, n) + B_{2m}^{-}(\beta, n)}{2} = j^m \sin\frac{\pi}{n}\, A_{2m}(\beta, n) \quad ;$$

hence $U_B^* = U_B$ and the relationship of the Pauli series to the generalized series is established.

<u>Relation to Oberhettinger's Asymptotic Series</u>

Oberhettinger has studied the diffraction of plane waves by wedges which have exterior angles greater than 180 degrees. He showed that the total field can be expressed as the sum of four integrals plus a number of plane wave terms. The integrals describe the diffracted field and the plane wave terms describe the incident and reflected fields; as in the solutions previously described, Oberhettinger's expression for G_p is

$$G_p = I(kr, (\pi - (\phi - \phi')), n) + I(kr, (\pi + (\phi - \phi')), n) \pm$$
$$\pm I(kr, (\pi - (\phi + \phi')), n) \pm I(kr, (\pi + (\phi + \phi')), n) +$$
$$+ e^{jkr\cos(\phi - \phi')} U(\pi - |\phi - \phi'|) \pm e^{jkr\cos(\phi + \phi')} \cdot$$
$$\cdot U(\pi - |\phi + \phi'|) + e^{jkr\cos(\phi + \phi' - 2n\pi)} \cdot$$
$$\cdot U(\pi - |\phi + \phi' - 2n\pi|) \qquad (114)$$

where

$$I(kr, \delta, n) = \frac{-1}{2n\pi} \sin\left(\frac{\delta}{n}\right) \int_0^\infty \frac{e^{-jkr\cosh x}}{\cosh\frac{x}{n} - \cos\frac{\delta}{n}}\, dx \quad . \qquad (115)$$

The relation between this integral and the integrals given in Equations 33 and 34 will now be established. Equations 33 and 34 have the form

$$I_{\mp\pi}(kr, \beta, n) = \frac{-1}{4\pi n j} \int_{SDP_{\mp\pi}} \cot\left(\frac{\beta + z}{2n}\right) e^{jkr\cos z}\, dz \quad . (116)$$

Replacing z by $\omega - \pi$ in the integral over $SDP_{-\pi}$ and by $\omega + \pi$ in the integral over $SDP_{+\pi}$ yields

$$I_{\mp\pi}(kr, \beta, n) = \frac{\pm 1}{4\pi n j} \int_{SDP_o} \cot\left(\frac{\beta + \omega \mp \pi}{2n}\right) e^{-jkr\cos\omega}\, d\omega \quad (117)$$

The path SDP_o is shown in Figure 13. The integrand of Equation 117 can be written as the sum of an even and odd function of ω. The integral of the odd part over SDP_o vanishes, leaving

$$I_{\mp\pi}(kr, \beta, n) = \frac{\pm 1}{4\pi n j} \int_{SDP_o} \frac{1}{2} \left\{ \cot \frac{\beta \mp \pi + \omega}{2n} + \right.$$

$$\left. + \cot \frac{\beta \mp \pi - \omega}{2n} \right\} e^{-jkr\cos\omega}\, d\omega \quad (118)$$

Combining the terms of the integrand reduces this to

$$I_{\mp\pi}(kr, \beta, n) = \frac{\pm 1}{4\pi n j} \int_{SDP_o} \frac{\sin \frac{\beta \mp \pi}{n}}{\cos \frac{\omega}{n} - \cos \frac{\beta \mp \pi}{n}} \cdot$$

$$\cdot\, e^{-jkr\cos\omega}\, d\omega$$

If SDP_o is deformed so as to be coincident with the $\mathrm{Im}\,\omega$-axis, and then is rotated by 90 degrees, by replacing ω by jx, Equation 118 takes the form

$$I_{\mp\pi}(kr, \beta, n) = \frac{\pm 2j}{4\pi n j} \int_0^\infty \frac{\sin \frac{\beta \mp \pi}{n} \, e^{-jkr \cosh x}}{\cosh \frac{x}{n} - \cos \frac{\beta \mp \pi}{n}} dx \qquad (119)$$

Reversing the order of the argument to $\pi \pm \beta$ and replacing this by δ reduces the integral to that used by Oberhettinger, that is, Equation 115. The following notational correspondence exists then between the integrals used in this work and those used by Oberhettinger.

$$I_{-\pi}(kr, (\phi - \phi'), n) = I(kr, \pi - (\phi - \phi'), n) \qquad (120)$$

$$I_{+\pi}(kr, (\phi - \phi'), n) = I(kr, \pi + (\phi - \phi'), n) \qquad (121)$$

$$I_{-\pi}(kr, (\phi + \phi'), n) = I(kr, \pi - (\phi + \phi'), n) \qquad (122)$$

$$I_{+\pi}(kr, (\phi + \phi'), n) = I(kr, \pi + (\phi + \phi'), n) \qquad (123)$$

Oberhettinger used Watson's lemma to derive an asymptotic expression for Equation 115 valid for cases in which ϕ, the angular coordinate of the field point, does not fall near a field boundary. That expression is given in Equation 124.

$$I(\delta, n) \sim - e^{-j(kr + \frac{\pi}{4})} \sum_{m=0}^{\infty} A_m^0(\delta, n)(j)^{-m} \Gamma(m + \tfrac{1}{2}) \cdot$$

$$\cdot \frac{1}{(kr)^{\frac{1}{2} + m}} \qquad (124)$$

with

$$A_o^o(\delta, n) = \frac{1}{2\pi\sqrt{2n}} \cot\left(\frac{\delta}{2n}\right) \tag{125}$$

$$A_1^o(\delta, n) = -\frac{1}{2\pi n\sqrt{2}} \cot\left(\frac{\delta}{2n}\right)\left\{\frac{1}{4} + \frac{1}{2n^2}\csc^2\left(\frac{\delta}{2n}\right)\right\} \tag{126}$$

and

$$A_2^o(\delta, n) = \frac{1}{2\sqrt{2}\, n\pi} \frac{1}{4} \cot\left(\frac{\delta}{2n}\right)\left\{\frac{3}{8} + \left(\frac{5}{6n^2} - \frac{1}{3n^4}\right)\csc^2\left(\frac{\delta}{2n}\right) + \right.$$

$$\left. + \frac{1}{n^4}\csc^4\left(\frac{\delta}{2n}\right)\right\}. \tag{127}$$

This coefficient differs from the form given by Oberhettinger by a factor of one-half. Oberhettinger's coefficient is in error. These coefficients have the same form as the $C_m^{\pm}(\beta, n)$'s derived in this work; in fact,

$$A_o^o(\delta, n) = \frac{1}{2\pi n\sqrt{2}}\, C_o^{\pm}(\beta, n) \tag{128}$$

$$A_1^o(\delta, n) = \frac{1}{2\pi\sqrt{2n}}\, C_2^{\pm}(\beta, n) \tag{129}$$

$$A_2^o(\delta, n) = \frac{(j)^2}{2\pi\sqrt{2n}}\, C_4^{\pm}(\beta, n) \tag{130}$$

and in general

$$A_m^o(\delta, n) = \frac{(j)^m}{2\pi\sqrt{2n}} C_{2m}^{\pm}(\beta, n) \tag{131}$$

Equation 124 is, of course, identical to Equation 55. They were derived from different forms of the same integral. Equation 55 was derived by a direct application of the method of steepest descents; Equation 124 was derived by Watson's lemma. Both equations fail on and near field boundaries.

In order to derive a more general asymptotic form for $I(\delta, n)$, valid near field boundaries, Oberhettinger split Equation 115 into two parts. The first part was associated with the diffraction by a half-plane; the second described the modification of this half-plane diffraction term caused by the finite wedge angle. The first part reduces to the Fresnel integral and an infinite series in inverse power of kr. Oberhettinger applied Watson's lemma to the second integral to form an asymptotic series in inverse powers of kr. Oberhettinger's series is shown in Equation 132.

$$I(\delta, n) \sim -\frac{e^{-jkr\cos\delta + j\frac{\pi}{4}}}{\sqrt{\pi}}\,\mathrm{sgn}\,\delta \int_{(2kr)^{\frac{1}{2}}\sin\frac{\delta}{2}}^{\infty} e^{-j\tau^2}\,d\tau - \qquad (132)$$

$$- e^{-jkr - j\frac{\pi}{4}} \sum_{m=0}^{\infty} (j)^{-m}\,\Gamma(m + \tfrac{1}{2}) \Big[A_m(\delta, n) -$$

$$- \chi_m(\delta)\Big] \frac{1}{(kr)^{m+\frac{1}{2}}}$$

where $\chi_m(\delta) = A_m(\delta, 2) + A_m(2\pi - \delta, 2) =$

$$= \frac{(-1)^m}{2\pi 2^{n+\frac{1}{2}} (\sin\frac{\delta}{2})^{2n+1}}$$

Although it is not mentioned explicitly by Oberhettinger, if $|\delta| > \alpha$ then δ must be replaced by $\delta - 2\alpha$ in Equation 132. If δ is replaced by $\pi \pm \beta$ this series takes the form

$$I(\beta, n) \sim -\frac{e^{jkr\cos\beta + j\frac{\pi}{4}}}{\sqrt{\pi}} \operatorname{sgn}(\pi \pm \beta) \int_{(kra)^{\frac{1}{2}}}^{\infty} e^{-j\tau^2}\, d\tau -$$

$$- e^{-jkr - j\frac{\pi}{4}} \sum_{m=0}^{\infty} (j)^{-m}\, \Gamma(m + \tfrac{1}{2}) \Big[A_n(\delta, n) -$$

$$- \chi_m(\beta) \Big] \frac{1}{(kr)^{m + \frac{1}{2}}} \tag{133}$$

where

$a = 1 + \cos\beta$

and

$$\chi_m(\beta) = \frac{(-1)^m \cos\frac{\beta}{2}}{\sqrt{2}\,\pi a^{m+1}} \tag{134}$$

Substituting Equation 131 and 134 into (133) results in

$$I(\beta, n) \sim - \frac{e^{jkr \cos\beta + j\frac{\pi}{4}}}{\sqrt{\pi}} \, \mathrm{sgn}\,(\pi \pm \beta) \int_{(krn)^{\frac{1}{2}}}^{\infty} e^{-j\tau^2} \, d\tau -$$

$$- e^{-jkr - j\frac{\pi}{4}} \sum_{m=0}^{\infty} \frac{\Gamma(m + \frac{1}{2})}{(kr)^{m + \frac{1}{2}}} \left[\frac{C^{\pm}_{2m}(\beta, n)}{2\pi\sqrt{2n}} - \right.$$

$$\left. - j^m \frac{\cos\frac{\beta}{2}}{\pi\sqrt{2}\, n^{m+1}} \right] \qquad (135)$$

The correspondence between Oberhettinger's expansion and the generalized Pauli expansion will now be investigated, and it will be shown that they are simply different arrangements of the same series. Consider again Equations 85 and 101. These equations are written below in a slightly modified form.

$$I_{\pm\pi}(kr, \beta, n) \sim - \frac{e^{-j(kr + \frac{\pi}{4})}}{j2\sqrt{2}\, n\pi} \left\{ I_0(kr, \beta) \sum_{m=0}^{\infty} B^{\pm}_{2m}(\beta, n)(-jn)^m + \right.$$

$$\left. + \sum_{m=1}^{\infty} \left[B^{\pm}_{2m} \sum_{k=1}^{m} \frac{\Gamma(m - k + \frac{1}{2})(-jn)^{k-1}}{(kr)^{(m - k + \frac{1}{2})}} \right] \right\} \qquad (136)$$

As before, $a = 1 + \cos(-\beta + 2n\pi N)$, but here the Fresnel integral has been factored out of the summation. The summation multiplying this integral can be written in closed form by setting

$$(-ja)^m = (\sqrt{-ja})^{2m} ,$$

so that the summation has the form

$$\sum_{m=0}^{\infty} B_{2m}^{\pm}(\beta, n)(\sqrt{-ja})^{2m} .$$

This is just equal to the even part of $H(u)$ (see Equations 65, 89, and 94) evaluated at $u = \sqrt{-ja}$. This value of u corresponds to $z = -\beta + 2n\pi N$ or to $\omega = -\beta + \pi + 2n\pi N$ (see Equation 92). The even part of $H(u)$ can be therefore evaluated as follows:

$$H^e(u = \sqrt{-ja}) = \frac{(\cos\omega(u) + \cos(-\beta + 2n\pi N))}{2\cos\frac{\omega(u)}{2}} \cdot \left. \frac{\cos\frac{\omega(u) + \beta - \pi}{2n}}{\sin\frac{\omega(u) + \beta - \pi}{2n}} \right|_{\omega = \pi - \beta + 2n\pi N} + \frac{(\cos\omega(u) + \cos(-\beta + 2n\pi N))}{2\cos\frac{\omega(u)}{2}} \cdot \left. \frac{\cos\frac{-\omega(u) + \beta - \pi}{2n}}{\sin\frac{-\omega(u) + \beta - \pi}{2n}} \right|_{\omega = \pi - \beta + 2n\pi N} \tag{137}$$

The second term of this equation vanishes. Application of L'Hospital's rule to the first term yields

$$H^e(u = \pm\sqrt{-ja}) = -2n \sin \frac{\omega(u)}{2}\Bigg|_{\omega = \pi - \beta + 2n\pi N} =$$

$$= -2n \cos\left[\frac{\beta}{2} - n\pi N\right] \tag{138}$$

Therefore,

$$\sum_{m=0}^{\infty} B_{2m}(\beta, n)(-ja)^m = -2n \cos\left[\frac{\beta}{2} - n\pi N\right] \tag{139}$$

When this and Equation 78 are substituted into Equation 136 the first term in the expression for $I_{\pm\pi}(kr, \beta, n)$ takes the form

$$\frac{-\sqrt{2}\cos\left(\frac{\beta}{2} - n\pi N\right)}{\sqrt{\pi}\sqrt{a}}\, e^{jkr\cos(\beta - 2n\pi N) + j\frac{\pi}{4}} \int_{(kra)^{\frac{1}{2}}}^{\infty} e^{-jt^2}\, dt = \tag{140}$$

$$= -\operatorname{sgn}(\pi \pm (\beta - 2n\pi N))\, \frac{e^{jkr\cos(\beta - 2n\pi N) + j\frac{\pi}{4}}}{\sqrt{\pi}} \cdot$$

$$\int_{(kra)^{\frac{1}{2}}}^{\infty} e^{-jt^2}\, dt$$

The factor sgn $(\pi \pm (\beta - 2n\pi N))$ arises here because

$$\frac{\cos\left(\frac{\beta}{2} - n\pi N\right)}{\sqrt{a}} = \pm \frac{1}{\sqrt{2}} .$$

The minus sign applies if $|\beta - 2n\pi N| > \pi$; otherwise the plus sign applies.

The second term in Equation 136, that is, the double summation, can be rearranged and written as a series of coefficients multiplying terms of the form

$$(kr)^{\frac{-M}{2}} .$$

That is,

$$\sum_{m=1}^{\infty} B_{2m}^{\pm}(\beta, n) \sum_{k=1}^{m} \frac{\Gamma(m - k + \frac{1}{2})(-ja)^{k-1}}{(kr)^{(m - k + \frac{1}{2})}} =$$

$$= \left[\frac{\Gamma(\frac{1}{2})}{(kr)^{\frac{1}{2}}} \sum_{m=1}^{\infty} B_{2m}^{\pm}(\beta, n)(-ja)^{m-1} + \frac{\Gamma(1 + \frac{1}{2})}{(kr)^{\frac{3}{2}}} \cdot \sum_{m=2}^{\infty} B_{2m}^{\pm}(\beta, n)(-ja)^{m-2} + \cdots\cdots\cdot \right.$$

$$+ \frac{\Gamma(M + \frac{1}{2})}{(kr)^{M + \frac{1}{2}}} \sum_{m = M + 1}^{\infty} B_{2m}^{\pm}(\beta, n)(-ja)^{m - M - 1} + \ldots\ldots$$

$$= \sum_{p = 0}^{\infty} \frac{\Gamma(p + \frac{1}{2})}{(kr)^{p + \frac{1}{2}}} S_p(\beta, n) \quad . \tag{141}$$

The typical coefficient $S_p(\beta, n)$ can be expressed as a finite sum by making use of the series form of the even part of $H(u)$ as shown here.

$$S_p(\beta, n) = (-ja)^{-p + 1} \sum_{m = p + 1}^{\infty} B_{2m}^{\pm}(\beta, n)(-ja)^m =$$

$$= (-ja)^{-(p + 1)} \left[H^e(u = \sqrt{-ja}) - \right.$$

$$\left. - \sum_{m = 0}^{p} B_{2m}^{\pm}(\beta, n)(-ja)^m \right] \tag{142}$$

The final sum in this expression can be simplified using Equations 87, 88, 103, and 104. Substituting these equations into the sum yields,

$$\sum_{m=0}^{P} B_{2m}^{\pm}(\beta, n)(-ja)^m = -aC_o^{\pm} + (aC_o^{\pm} + ja^2C_2^{\pm}) + (-ja^2C_2^{\pm} + a^3C_4^{\pm}) +$$

$$+ (-a^3C_4^{\pm} - ja^4C_6^{\pm}) + \cdots + (-j)^P \cdot$$

$$\cdot a^{P+1}C_{2P}^{\pm} = (-j)^P a^{P+1}C_{2P}^{\pm} \quad , (143)$$

since all but the last term cancel. Substitution of this result and the expression for the even part of $H(u)$ into Equation 142 produces

$$S_P(\beta, n) = (-ja)^{-(P+1)} (-2n \cos (\frac{\beta}{2} - n\pi N)) + jC_{2P}^{\pm}(\beta, n) (144)$$

This equation can now be inserted into Equation 141 and that along with 140 and 136. These substitutions yield

$$I_{\pm\pi}(kr, \beta, n) \sim - \operatorname{sgn} (\pi \pm (\beta - 2n\pi N)) \frac{e^{jkr \cos (\beta - 2n\pi N) + j\frac{\pi}{4}}}{\sqrt{\pi}}$$

$$\int_{(kra)^{\frac{1}{2}}}^{\infty} e^{-j\tau^2} d\tau - e^{-j(kr + \frac{\pi}{4})} \cdot$$

$$\sum_{P=0}^{\infty} \frac{\Gamma(P + \frac{1}{2})}{(kr)^{P+\frac{1}{2}}} \left[\frac{C_{2P}^{\pm}(\beta, n)}{2\sqrt{2}\, n\pi} - \frac{j^P \cos(\frac{\beta}{2} - n\pi N)}{\pi\sqrt{2}\, a^{P+1}} \right] \quad . (145)$$

This is just Oberhettinger's series as given in Equation 135, but here written for arbitrary wedge angle. Thus, the Oberhettinger series is simply the generalized Pauli series written in a different form.

Summary of Equations

In this chapter, five series expressions for G_p have been presented. The first of these was the eigenfunction series, and the other four were asymptotic series. These five expressions are summarized below, and their range of application is discussed.

Eigenfunction Series

$$G_p = \frac{1}{n} \sum_{m=0}^{\infty} \epsilon_m J_{\frac{m}{n}}(kr) e^{j \frac{m}{n} \frac{\pi}{2}} \left[\cos \frac{m}{n} (\phi - \phi') \pm \cos \frac{m}{n} (\phi + \phi') \right] \tag{146}$$

This equation is perfectly general and can be employed to compute G_p for arbitrary wedge angles (α), angles of incidence (ϕ'), and observation coordinates (r, ϕ).

The four asymptotic expressions for G_p all have the following basic form:

$$G_p = e^{jkr \cos (\phi - \phi')} U(\pi - |\phi - \phi'|) +$$

+ (plane wave terms corresponding to reflected field components)

$$+ I_{+\pi}(kr, n, (\phi - \phi')) + I_{-\pi}(kr, n, (\phi - \phi')) \pm$$

$$\pm I_{+\pi}(kr, n, (\phi + \phi')) \pm I_{-\pi}(kr, n, (\phi + \phi')) \qquad (147)$$

The first term in this expression describes the incident plane wave field. The second term contains the plane wave fields arising from the reflection of the incident field by the faces of the wedge. These fields are described by terms of the form

$$e^{jkr \cos (2n\pi N - (\phi \pm \phi'))} \; U(\pi - |2n\pi N - (\phi \pm \phi')|)$$

The value of N and the range of existence of these higher order components are most easily determined from the z-plane pole diagrams. The unit step functions appearing in this equation describe the locations of the plane wave field boundaries. On the field boundaries, the unit step has the value one-half.

The four final terms in Equation 147 describe the diffracted component of the total field, and it is these terms which are expressed as asymptotic series. Each field boundary has associated with it one of these four terms. The four asymptotic forms for these terms are listed below.

Uncorrected Asymptotic Series

$$I_{\pm\pi}(kr, (\phi \pm \phi'), n) \sim - \frac{e^{-j(kr + \frac{\pi}{4})}}{2\sqrt{2n}\,\pi} \cdot$$

$$\sum_{m=0}^{\infty} C_{2m}^{\pm}((\phi \pm \phi'), n) \frac{\Gamma(m + \frac{1}{2})}{(kr)^{m + \frac{1}{2}}} \qquad (148)$$

$$C_0^{\pm} = \cot\left(\frac{\pi \pm \beta}{2n}\right) \qquad (149)$$

$$C_2^{\pm} = jC_0^{\pm}\left\{\frac{1}{4} + \frac{1}{2n^2}\csc^2\left(\frac{\beta \pm \pi}{2n}\right)\right\} \qquad (150)$$

$$C_4^{\pm} = -\frac{1}{4}C_0^{\pm}\left\{\frac{3}{8} + \frac{1}{n^4}\csc^4\left(\frac{\beta \pm \pi}{2n}\right) + \right.$$

$$\left. + \left[\frac{5}{6n^2} - \frac{1}{3n^4}\right]\csc^2\left(\frac{\beta \pm \pi}{2n}\right)\right\} \qquad (151)$$

This expression can be used to compute the four final terms in Equation 147 so long as the values of ϕ, ϕ', and n are such that no poles lie near the saddle points associated with the evaluation of these terms. If the values of ϕ, ϕ', and n are such that a pole lies near the saddle associated with a particular $I_{\pm\pi}$, Equation 148 is not valid.

When kr is increased, the effective distance between the poles and saddle points is increased. Therefore, for given values of ϕ, ϕ' and n, the validity of Equation 148 increases with increasing kr. Stated in physical terms, Equation 148 can be used to compute the diffracted components of G_p at field points at which the product of the angular distance from field boundaries and the radian distance from the vertex of the wedge is large.

Generalized Pauli Asymptotic Series

$$I_{\pm\pi}(kr, (\phi \pm \phi'), n) \sim - \frac{e^{-j(kr + \frac{\pi}{4})}}{j2\sqrt{2}\, n\pi} \sum_{m=0}^{\infty} B^{\pm}_{2m}\left[(\phi \pm \phi'), n\right] \cdot$$

$$\left[\sum_{k=1}^{m} \frac{\Gamma(m - k + \frac{1}{2})(-ja)^{k-1}}{(kr)^{(m - k + \frac{1}{2})}} + (-ja)^{m} I_0(kr) \right] \tag{152}$$

$$B^{\pm}_{0}((\phi \pm \phi'), n) = -aC^{\pm}_{0}((\phi \pm \phi'), n) \tag{153}$$

$$B^{\pm}_{2m}((\phi \pm \phi'), n) = jC^{\pm}_{2(m-1)}((\phi \pm \phi'), n) - aC^{\pm}_{2m} \cdot ((\phi \pm \phi'), n) \tag{154}$$

$$a = 1 + \cos(2n\pi N - (\phi \pm \phi')) \tag{155}$$

$$I_0(kr) = \frac{2\sqrt{\pi}}{\sqrt{a}} e^{jkra} \int_{(kra)^{\frac{1}{2}}}^{\infty} e^{-jt^2}\, dt \tag{156}$$

N denotes the z-plane pole nearest the saddle point used in the evaluation of $I_{\pm\pi}$. Equation 152 can be used to evaluate the last four terms in Equation 147 for arbitrary values of ϕ, ϕ' and α, and, in particular, for values of ϕ near the boundaries of the plane wave fields. The value of N to be used in each term is most easily determined from a pole diagram. The accuracy of this expression increases with increasing kr.

Pauli Asymptotic Series

$$I_{-\pi}(kr, \beta, n) + I_{+\pi}(kr, \beta, n) \sim \frac{1}{\pi\sqrt{2}} \frac{\sin\frac{\pi}{n}}{n} e^{-j(kr - \frac{\pi}{4})} \cdot$$

$$\sum_{m=0}^{\infty} A_{2m}(\beta, n) j^m \left[\sum_{k=1}^{m} (-ja)^{k-1} \frac{\Gamma(m - k + \frac{1}{2})}{(kr)^{m - k + \frac{1}{2}}} - \right.$$

$$\left. - (-ja)^m I_o(kr) \right] \qquad (157)$$

$$A_{2m}(\beta, n) = \frac{B^{+}_{2m}(\beta, n) + B^{-}_{2m}(\beta, n)}{2}$$

The expressions for $B^{\pm}_{2m}(\beta, n)$ are given by Equations 153 and 154, and $I_o(kr)$ is given by 156.

Equation 157 may be used to compute the final terms of Equation 147 in cases in which a pole lies near either the saddle point at $z = \pi$ or at $z = -\pi$ but not near both. This equation is a sum of two series of the form given by Equation 152 for equal values of β and $N = 0$.

Generalized Oberhettinger Series

$$I_{\pm\pi}(kr, \beta, n) \sim - \operatorname{sgn}(\pi \pm \beta - 2n\pi N) \cdot$$

$$\frac{e^{jkr\cos(\beta - 2n\pi N) + j\frac{\pi}{4}}}{\sqrt{\pi}} \int_{(kra)^{\frac{1}{2}}}^{\infty} e^{-j\tau^2}\, d\tau -$$

$$- e^{-j(kr + \frac{\pi}{4})} \sum_{p=0}^{\infty} \frac{\Gamma(p + \frac{1}{2})}{(kr)^{p + \frac{1}{2}}} \left[\frac{C^{\pm}_{2p}(\beta, n)}{2\sqrt{2}\, n\pi} - \right.$$

$$\left. - \frac{j^p \cos(\frac{\beta}{2} - n\pi N)}{\pi\sqrt{2}\, a^{p+1}} \right] \qquad (158)$$

$$a = 1 + \cos(\beta - 2n\pi N)$$

The equation can be used to evaluate the last four terms in Equation 147 for arbitrary values of ϕ, ϕ' and α. The accuracy increases with increasing kr. This series is simply a rearrangement of the generalized Pauli series.

CHAPTER IV

NUMERICAL EXAMPLES

Some typical numerical examples are presented here to illustrate the type of results which are obtainable with the equations developed in the previous chapter. Some conclusions regarding the relative merit of the ordinary Pauli series, the generalized Pauli series, and the Oberhettinger series are summarized at the end of this chapter.

In each example, the wedge angle, the angle of incidence of the plane wave field, the angle of observation, and the boundary conditions were fixed, and the total field was calculated as a function of kr. In all the examples, the calculations were made on or near a field boundary for relatively small values of kr; in most cases, $0 < kr < 15$. It is near the field boundaries and for small values of kr that the greatest deviation between the results given by the asymptotic series and the eigenfunction series is expected. In the examples, the amplitude and phase of G_p were calculated by means of the eigenfunction series, and these values were taken to be the reference or true ones. These calculations were performed on the OSU - IBM - 7094 digital computer. In the examples involving wedges with α greater than 180 degrees, the fields were also calculated by means of the ordinary Pauli series, the generalized Pauli series, and the Oberhettinger series. In the examples involving wedges with α less than 180 degrees, the fields were calculated using the generalized Pauli series and the generalized Oberhettinger series. The results of these computations are compared with those given by the eigenfunction series. In all cases, the values of G_p have been divided by 2 in order to bring them into correspondence with the values published by Wait.[121]

Each example is preceded by a description of the assumed geometry and brief summary of the results. The wedge angle and the angles of incidence and observation are denoted on the graphs as are the boundary conditions. The Neumann boundary condition is denoted by the acoustically equivalent term "hard," while the Dirichlet condition is described by "soft." The particular asymptotic series used in each calculation is also denoted on the graphs.

The eigenfunction results are represented by a heavy dashed line. The asymptotic series results are denoted by solid or dashed lines or by circles. The results obtained using the leading term as well as higher order terms of the asymptotic series are illustrated on the graphs. The results given by the first term of a series are denoted by (1); those obtained with the first and second by (2); by the first, second, and third by (3); etc.

The results obtained for G_p from the "first term" of any of the asymptotic series include all the plane wave contributions plus the sum of two or four Fresnel integral terms which describe the leading term of the particular asymptotic series. The ordinary Pauli series requires two such integrals, while the other series require four. The results obtained from the "first and second terms" include the contributions listed above plus the sum of two or four terms given by the second term in the appropriate series. The uncorrected asymptotic series, Equation 148, was not used in these calculations.

Example 1

In this example a plane wave is assumed to be incident on a hard wedge having an exterior angle $\alpha = 330^\circ$. The assumed angle of incidence is $\phi' = 0^\circ$. The field is calculated along the shadow boundary at $\phi = 180^\circ$. The first term of the generalized Pauli series and the first two terms of the ordinary Pauli series describe this field accurately for values of kr as small as 1.0. Four terms are required in the Oberhettinger series to produce good agreement with the eigenfunction series for $5 < kr < 15$. Below $kr = 5$ even four terms do not produce good agreement.

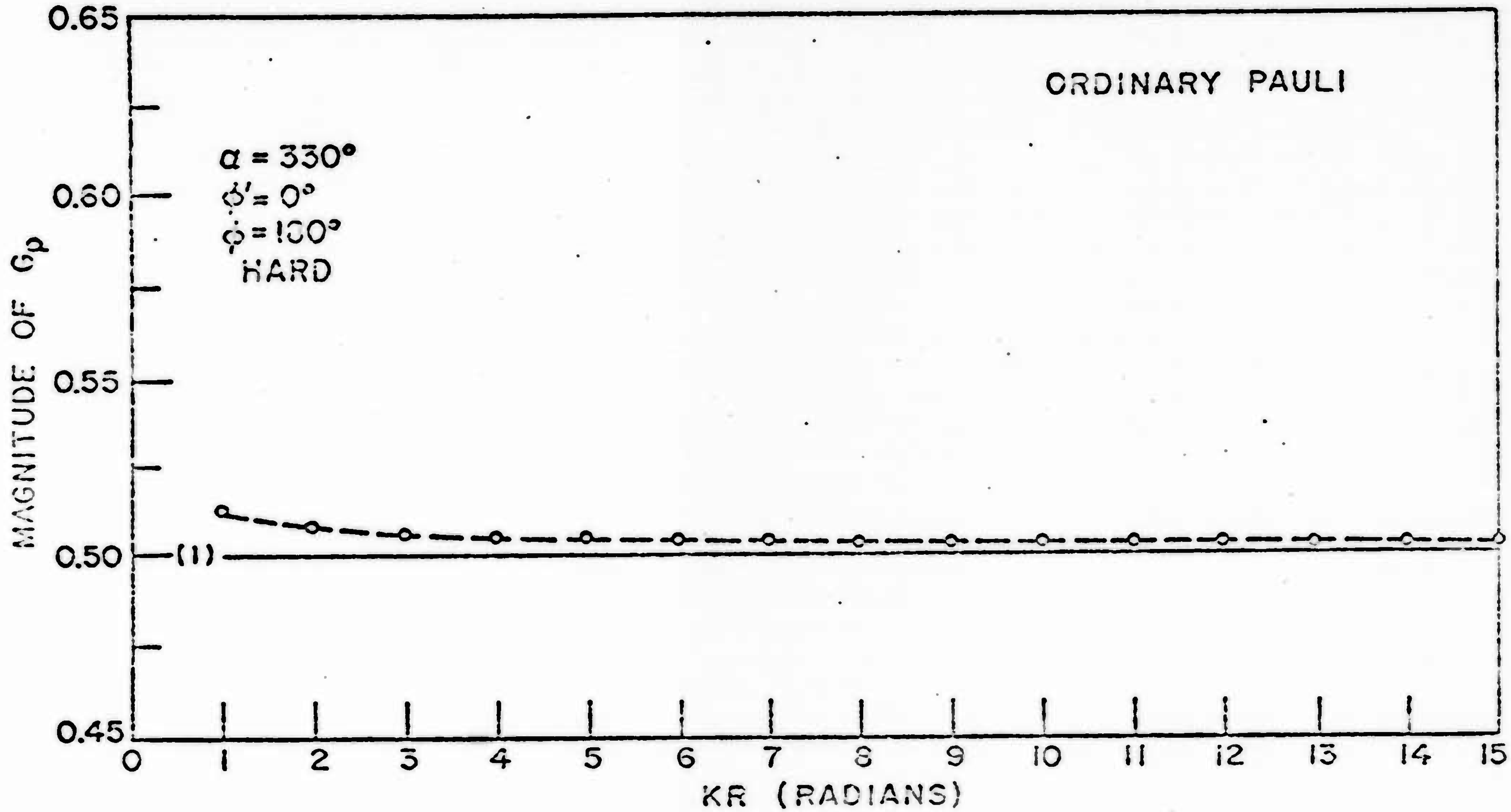

Figure 14. Magnitude of G_p for a 330 degree, hard wedge (a comparison of the results given by the ordinary Pauli series and the eigenfunction series). The solid line denotes the values given by the first term of the ordinary Pauli series. The circles describe the results given by the first and second terms. The third term produces insignificant variations in these results.

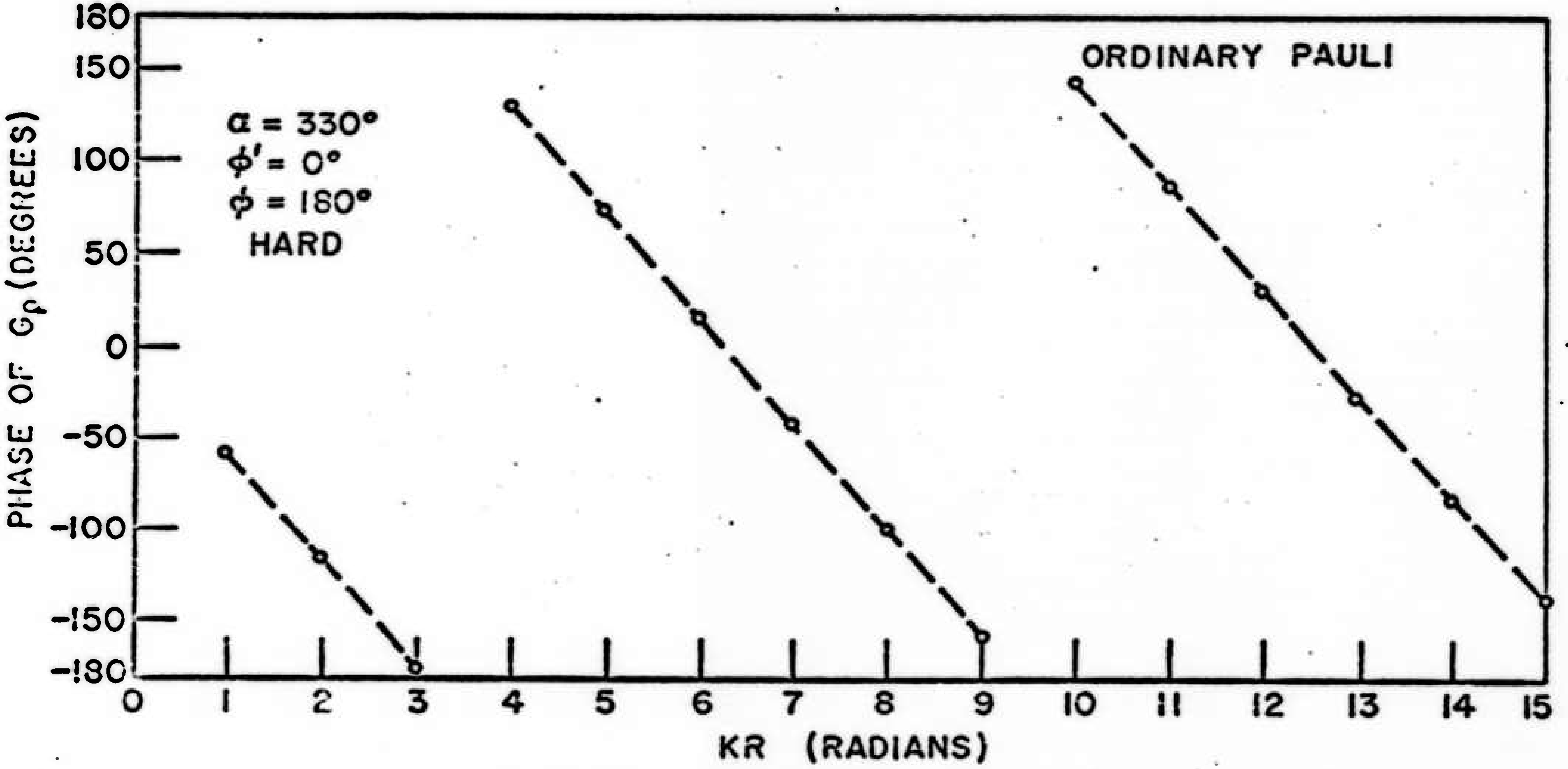

Figure 15. Phase of G_p for a 330 degree, hard wedge (a comparison of the results given by the ordinary Pauli series and the eigenfunction series). The circles describe the values given by the first term of the Pauli series. The second and third terms produce insignificant variations in these values.

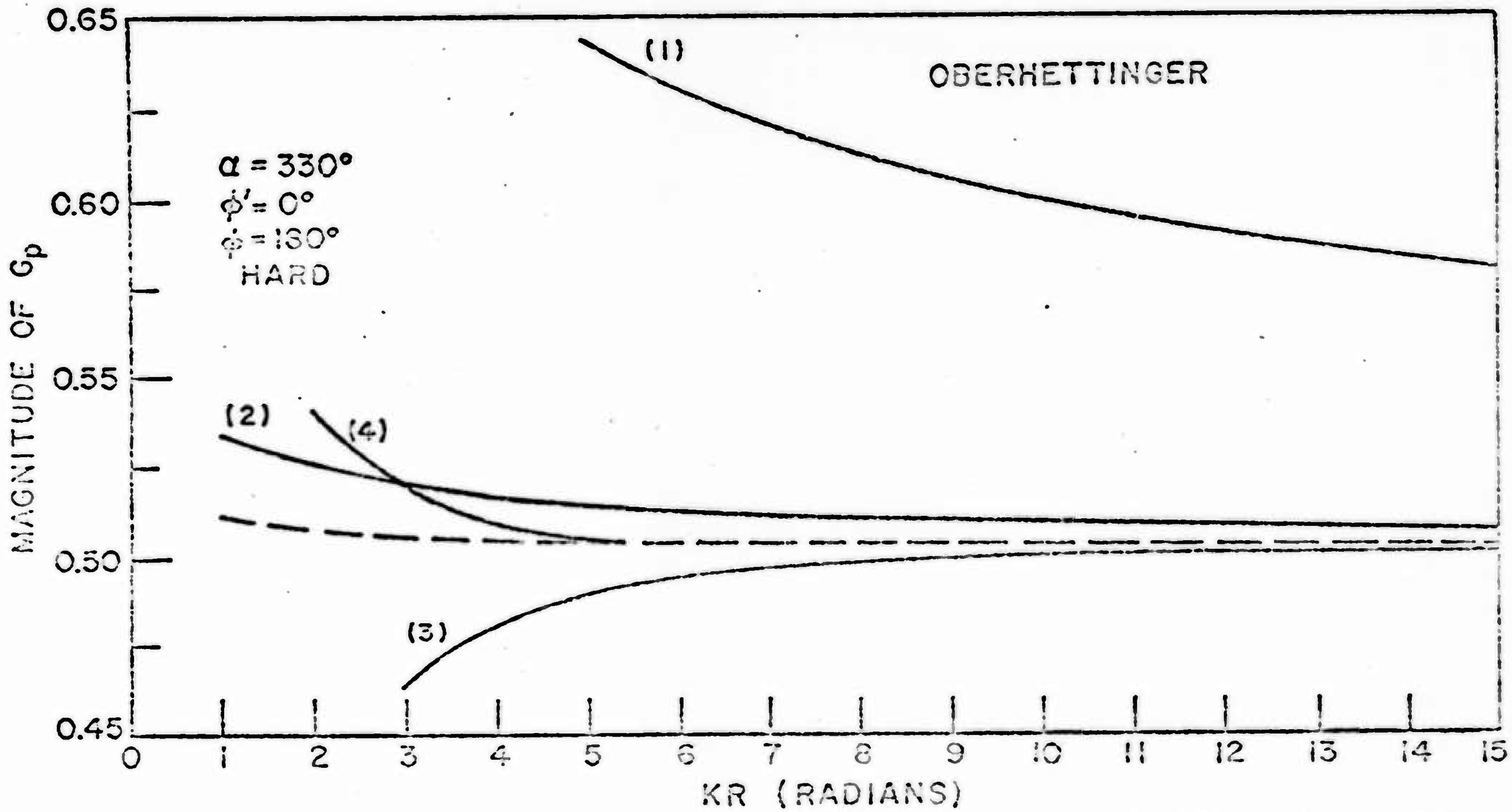

Figure 16. Magnitude of Gp for a 330 degree, hard wedge (a comparison of the Oberhettinger and eigenfunction series). The solid lines denote the values given by the first (1), the first and second (2), etc. terms of the Oberhettinger series. The values given by the first four terms of this series correspond with the eigenfunction values for kr greater than 5 .

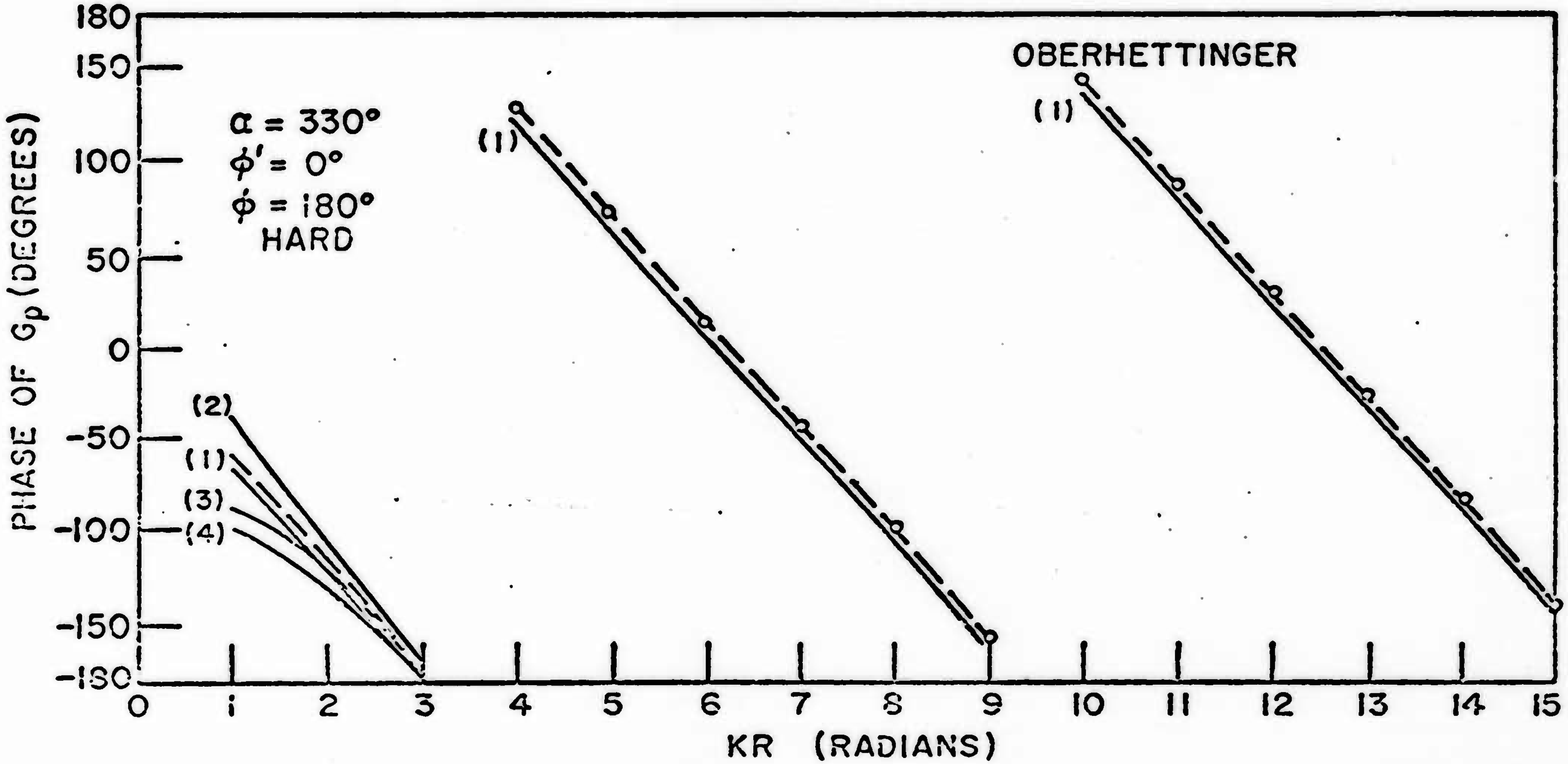

Figure 17. Phase of Gp for a 330 degree, hard wedge (a comparison of the Oberhettinger and eigenfunction series). In the range $1 < kr < 3$, the solid lines denote the values of Gp given by the first four terms of the Oberhettinger series. In the range $3 < kr < 15$, the solid line denotes the values obtained by the first term. The circles describe the values obtained with the first two terms. The third and fourth terms contribute insignificant variations in the value of Gp in this range.

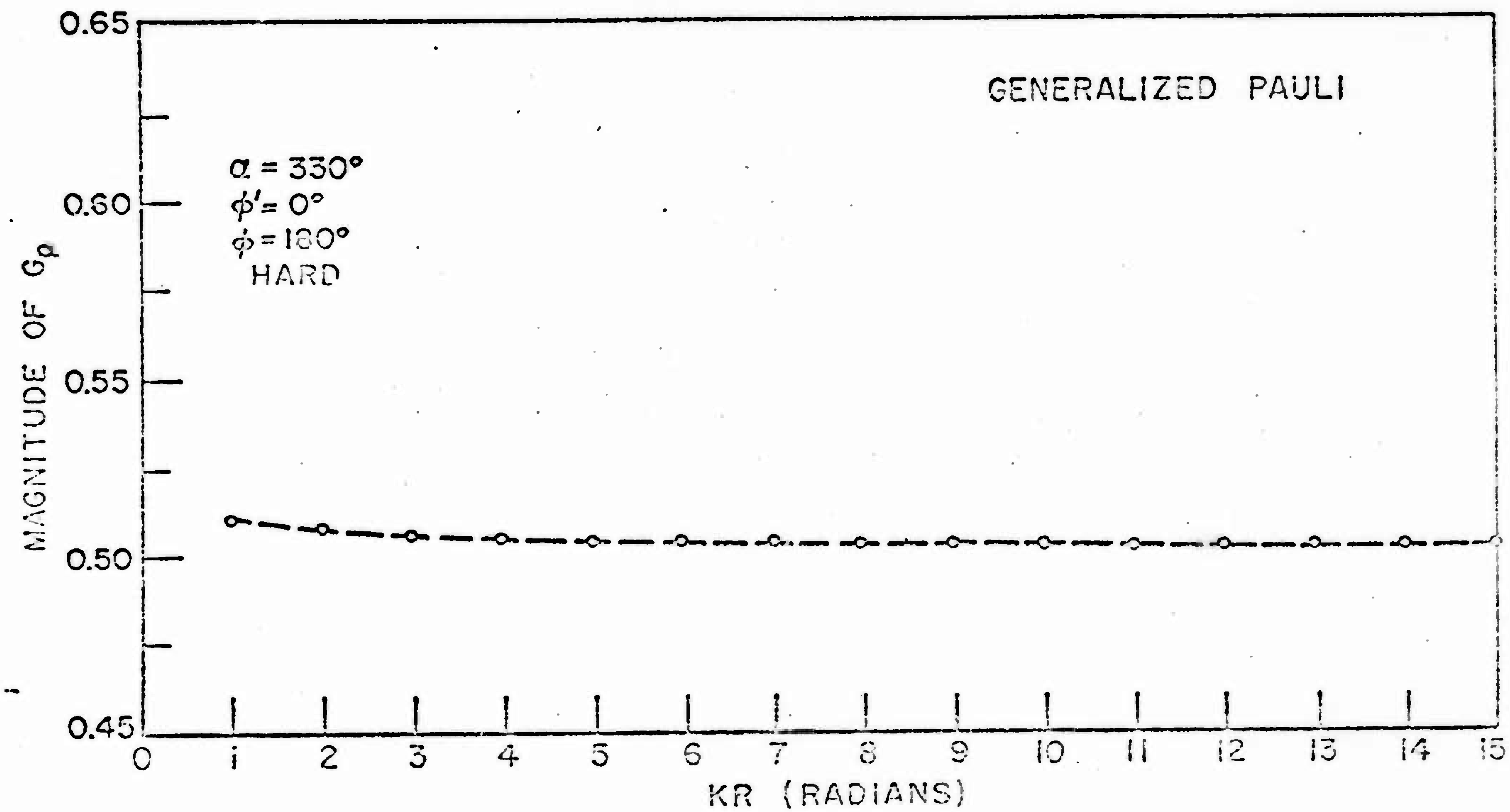

Figure 18. Magnitude of Gp for a 330 degree, hard wedge (a comparison of the generalized Pauli and the eigenfunction series). The values given by the first term of the generalized Pauli series are denoted by the circles. The second and third terms of the series contribute insignificant variations in these values.

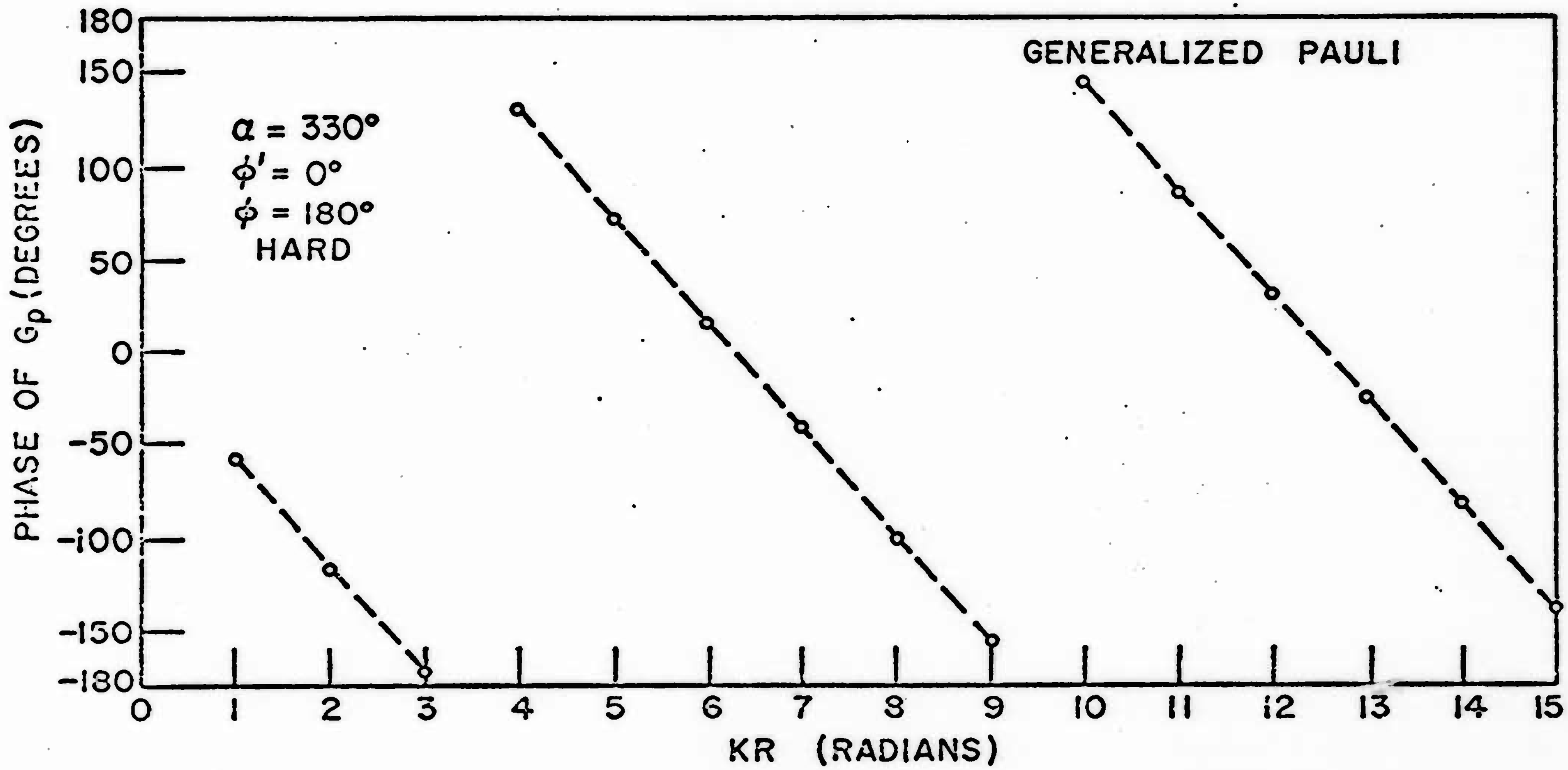

Figure 19. Phase of Gp for a 330 degree, hard wedge (a comparison of the generalized Pauli and the eigenfunction series). The values given by the first term of the generalized Pauli series are denoted by the circles. The second and third terms of the series contribute insignificant variations in these values.

Example 2

A plane wave field is assumed to be propagating along the $\phi' = 0^{\circ}$ face of a 270 degree, hard wedge in this example. The shadow boundary field is calculated. The leading term of the generalized Pauli series produces good agreement with the eigenfunction series over the range of kr examined. The ordinary Pauli series and the Oberhettinger series require several terms to produce good agreement even at large values of kr.

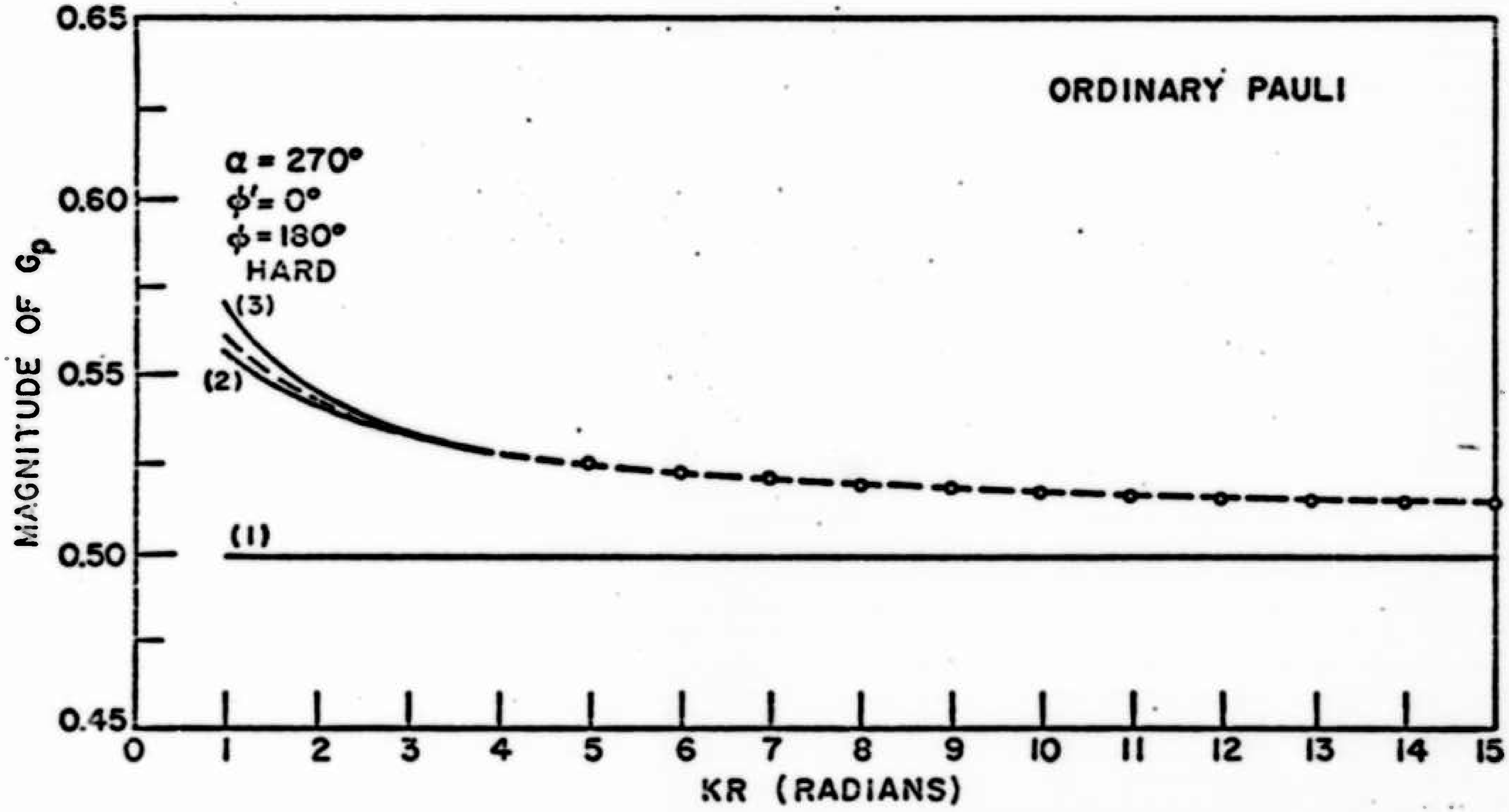

Figure 20. Magnitude of Gp for a 270 degree, hard wedge (a comparison of the ordinary Pauli series and the eigenfunction series). The small circles denote the values given by the first two terms of the Pauli series for values of kr greater than 5.0. The third term produces insignificant variation in these values.

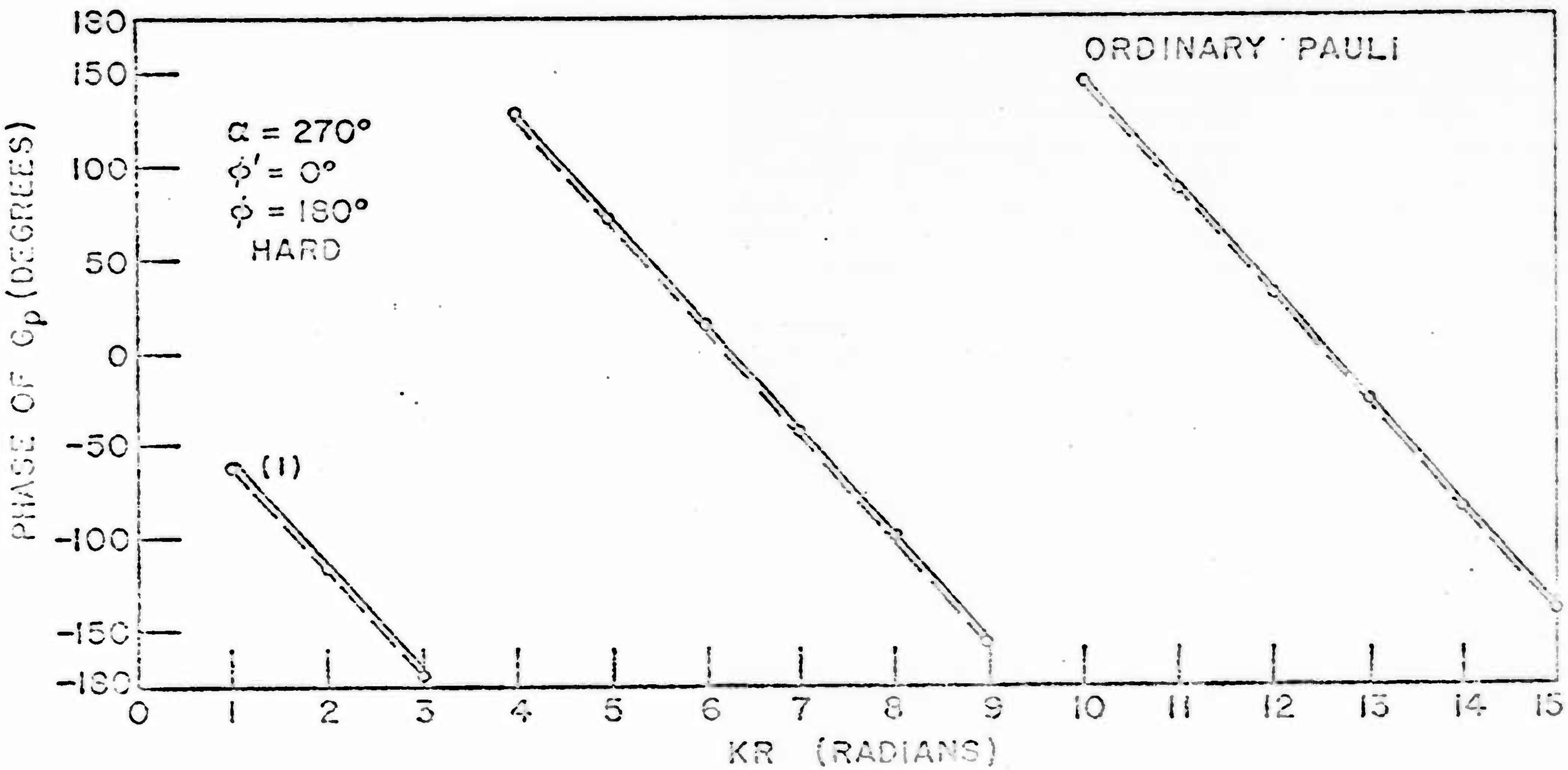

Figure 21. Phase of G_p for a 270 degree, hard wedge (a comparison of the ordinary Pauli series and the eigenfunction series). The solid line denotes the values given by the first term of the Pauli series. The small circles denote the values given by the sum of the first and second terms. The third term produces a small variation in these values.

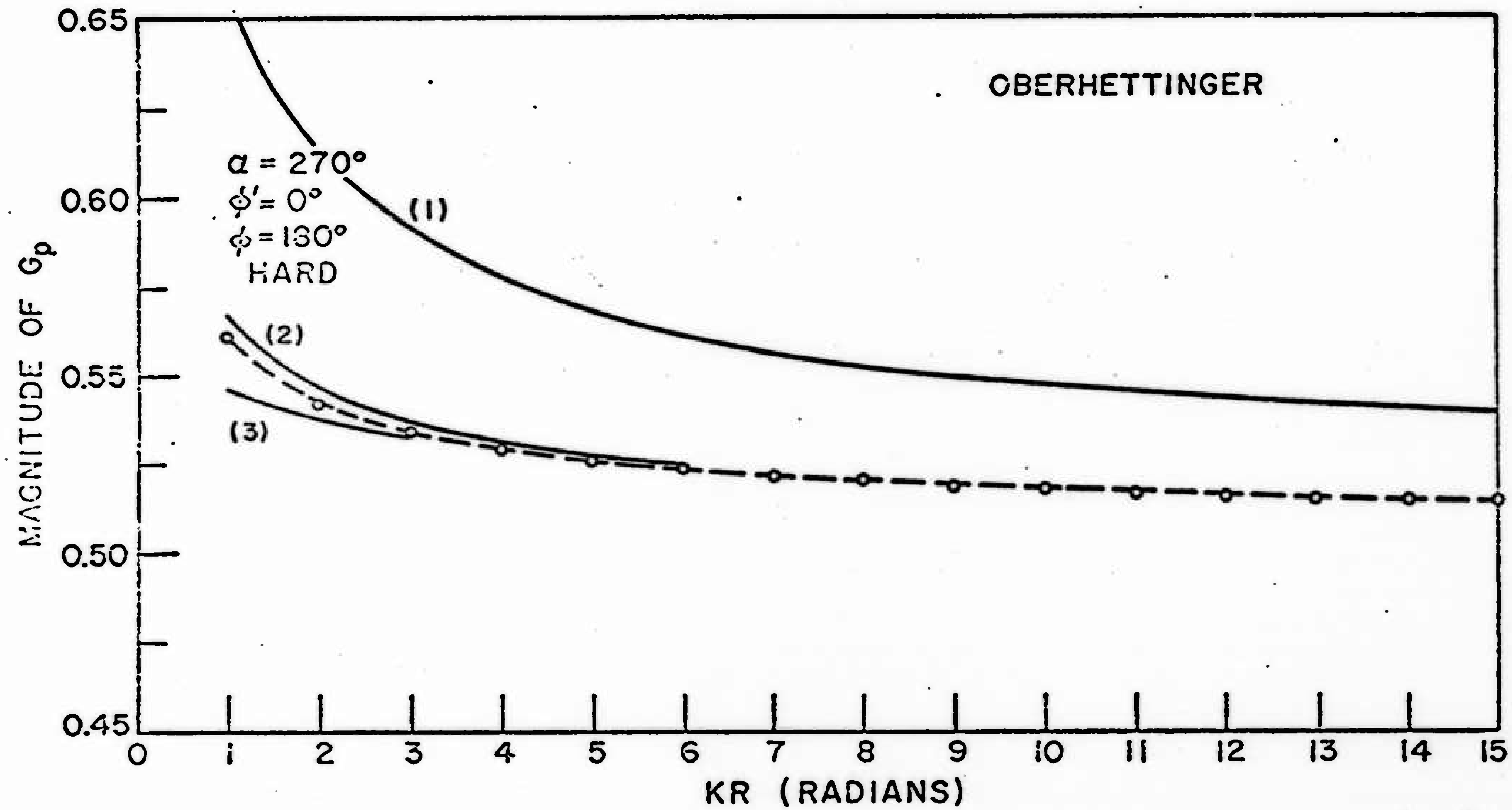

Figure 22. Magnitude of Gp for a 270 degree, hard wedge (a comparison of the Oberhettinger series and the eigenfunction series). The solid lines denote the values given by the first three terms of the series. The circles denote the values given by the first four terms.

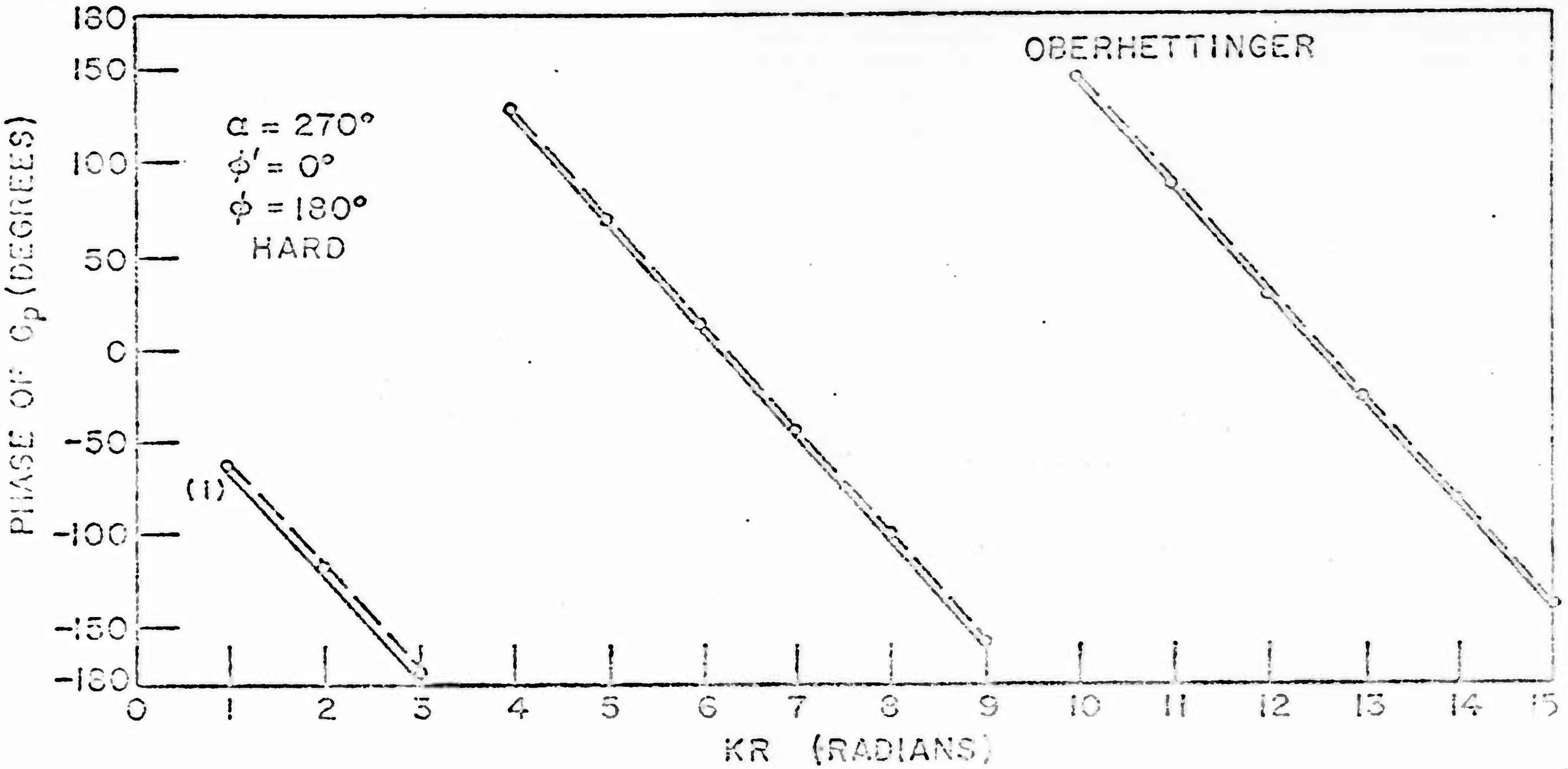

Figure 23. Phase of G_p for a 270 degree, hard wedge (a comparison of the Oberhettinger series and the eigenfunction series). The solid line denotes the value given by the first term. The circles denote the values given by the sum of the first and second terms. The third and fourth terms produce insignificant variations in these values.

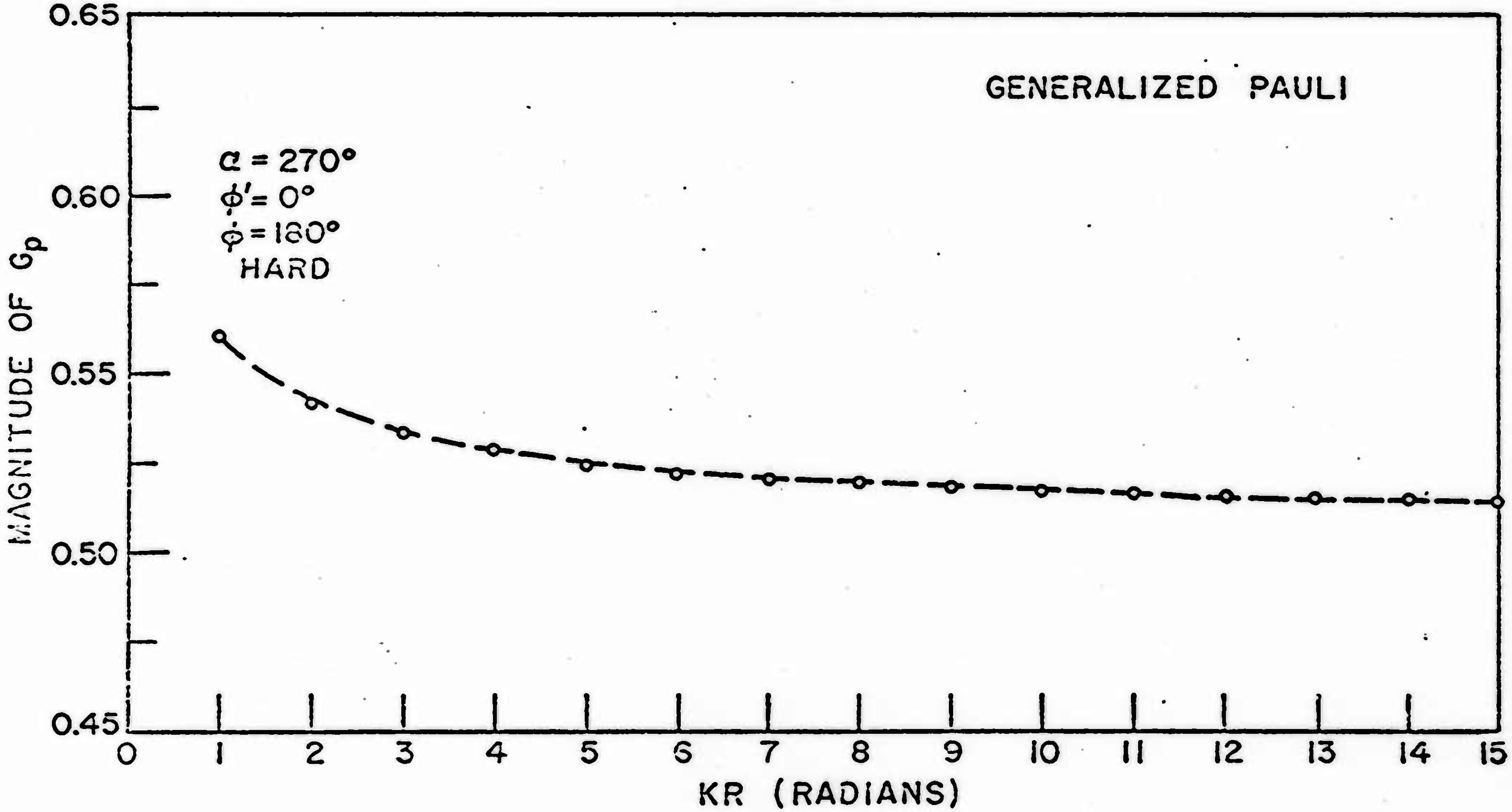

Figure 24. Magnitude of G_p for a 270 degree, hard wedge (a comparison of the generalized Pauli series and the eigenfunction series). The circles denote the values obtained with the first term of the generalized Pauli series. The second and third terms produce insignificant variations in these values.

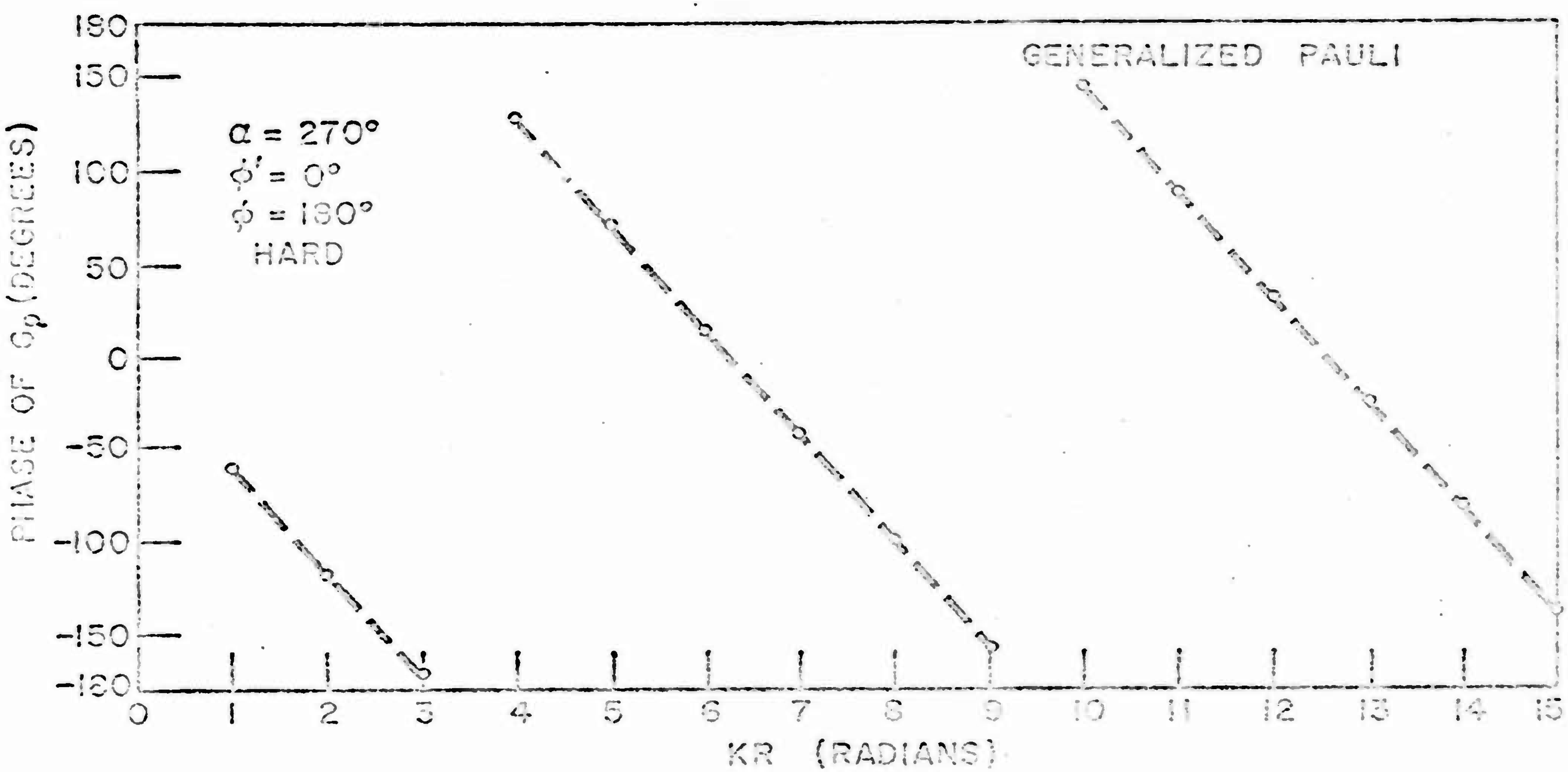

Figure 25. Phase of Gp for a 270 degree, hard wedge (a comparison of the generalized Pauli series and the eigenfunction series). The circles denote the values obtained with the first term of the generalized Pauli series. The second and third terms produce insignificant variations in these values.

Example 3

In this example the exterior wedge angle is assumed to be 190 degrees; the angle of incidence 0 degrees; and the field is calculated on the shadow boundary at 180 degrees. The Pauli series fails to yield an accurate value of G_P on the shadow boundary regardless of the number of terms used. Two terms are required in the generalized Pauli series and the Oberhettinger series to produce good agreement with the values given by the eigenfunction series for $kr < 5$. When kr is greater than 5 only one term is required in the generalized Pauli series, but two are required in the Oberhettinger series up to $kr = 15$.

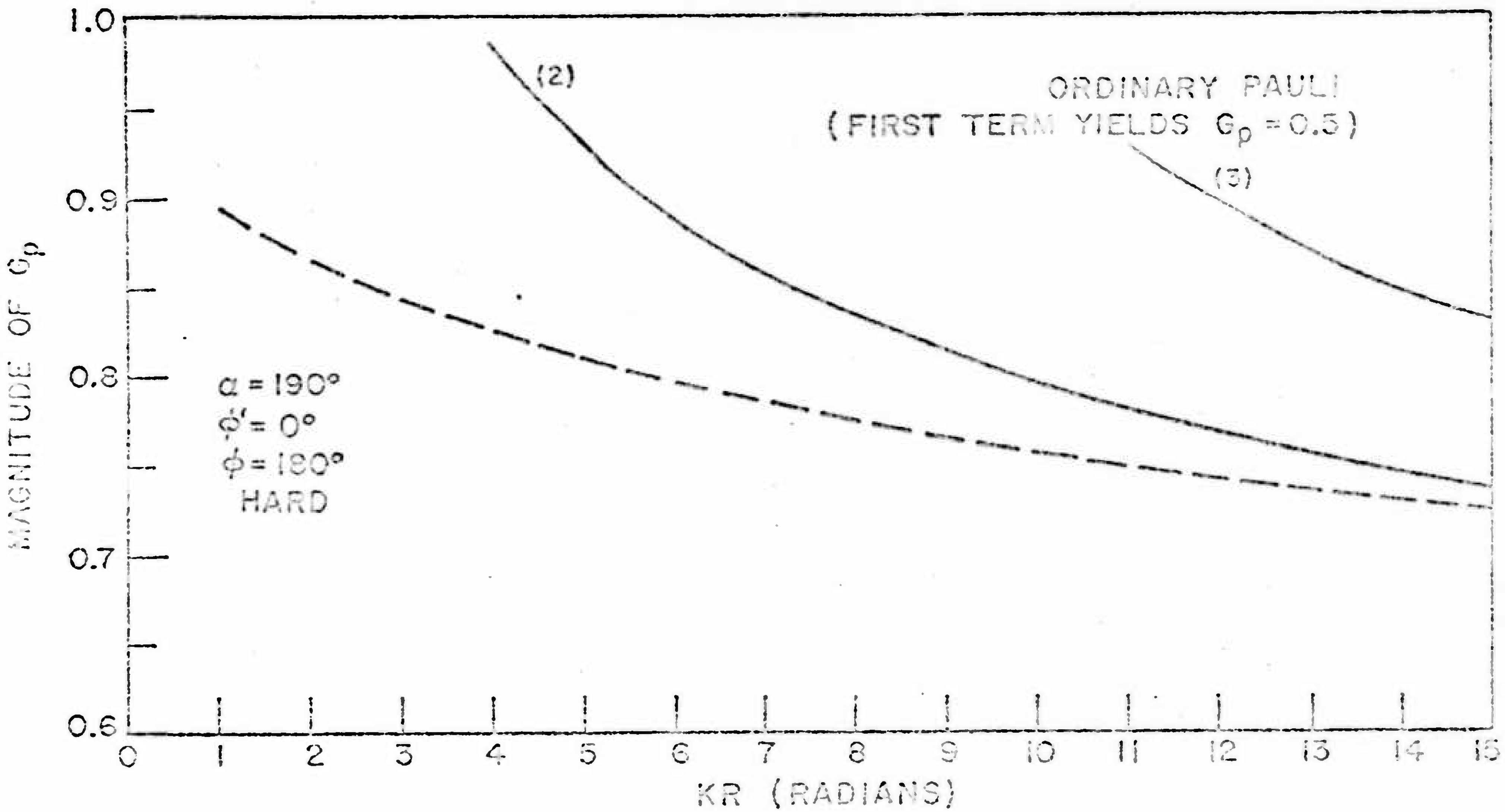

Figure 26. Magnitude of Gp for a 190 degree, hard wedge (a comparison of the ordinary Pauli series and the eigenfunction series). The solid lines denote the values given by the sum of the first two and first three terms of the Pauli series. The value given by the leading term of this series is 0.5 and is not shown on the graph.

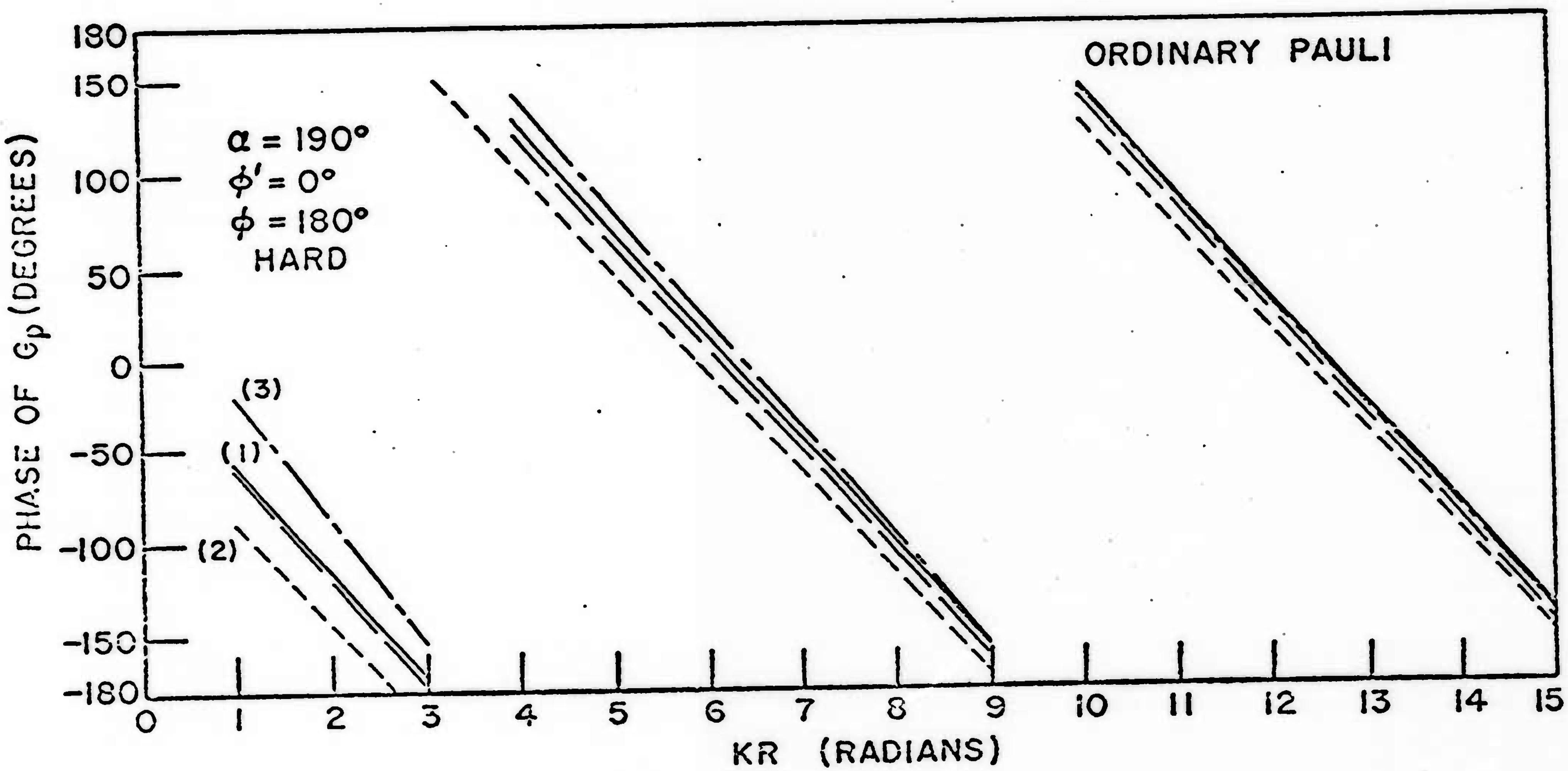

Figure 27. Phase of Gp for a 190 degree, hard wedge (a comparison of the ordinary Pauli series and the eigenfunction series). The numbered lines denote the values given by terms of the Pauli series.

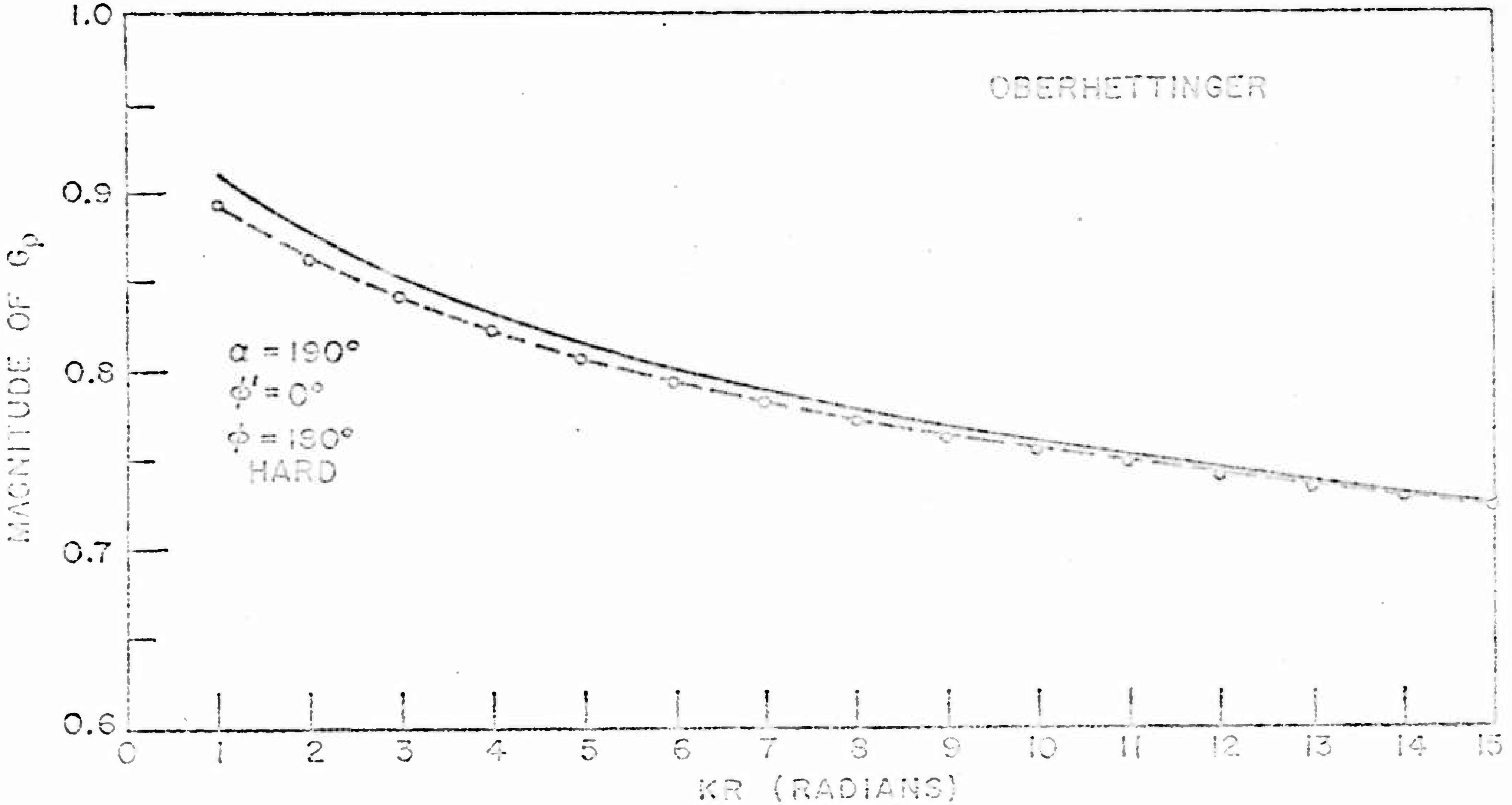

Figure 23. Magnitude of G_p for a 190 degree, hard wedge (a comparison of the Oberhettinger series and eigenfunction series). The solid line denotes the value given by the first term of the Oberhettinger series. The small circles denote the values given by the sum of the first two terms of the series. The third and fourth terms produce insignificant variations in these values.

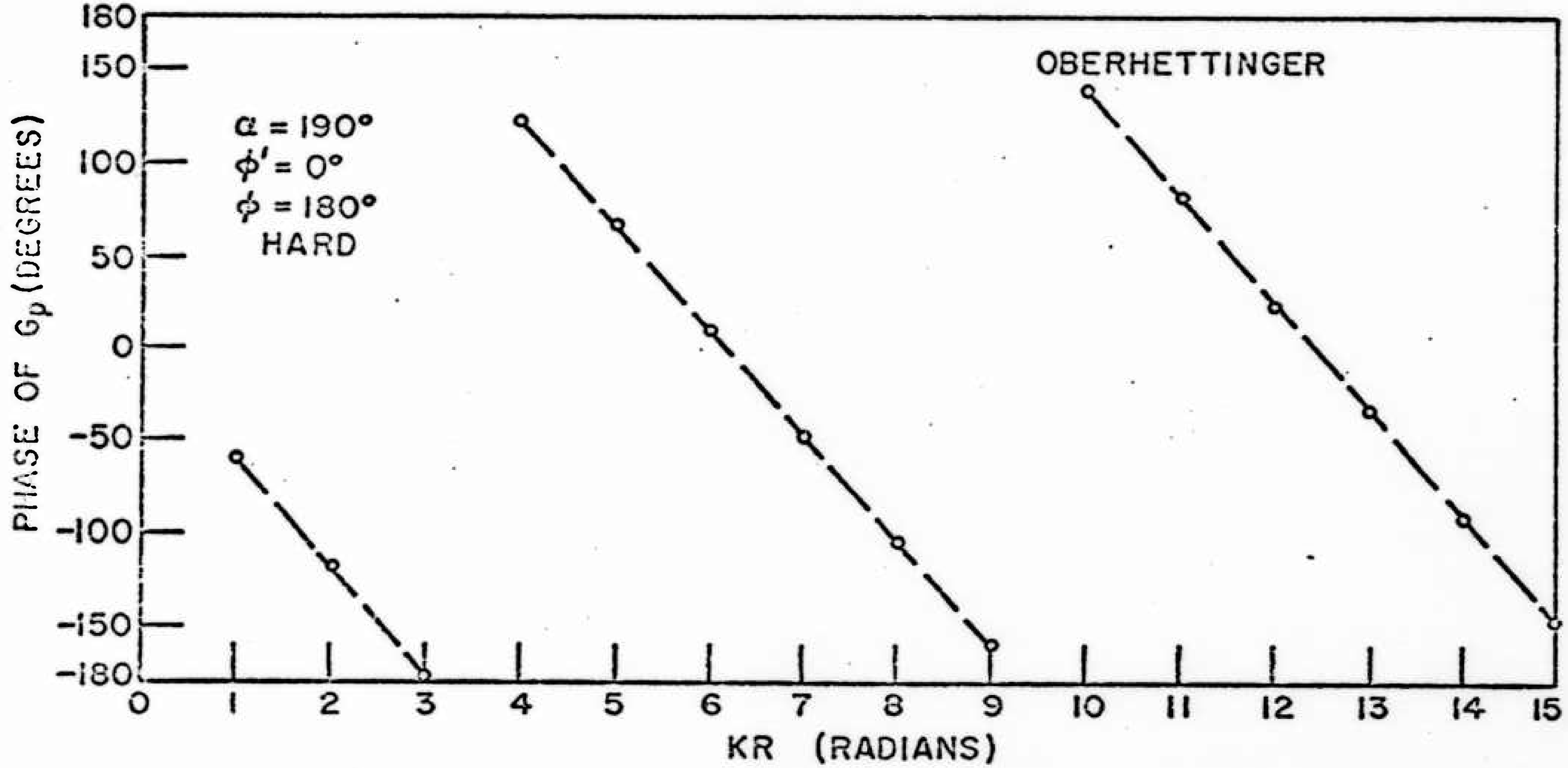

Figure 29. Phase of G_p for a 190 degree, hard wedge (a comparison of the Oberhettinger series and eigenfunction series). The small circles denote the values given by the first term of the Oberhettinger series. The second, third, and fourth terms of this series produce insignificant variations in these values.

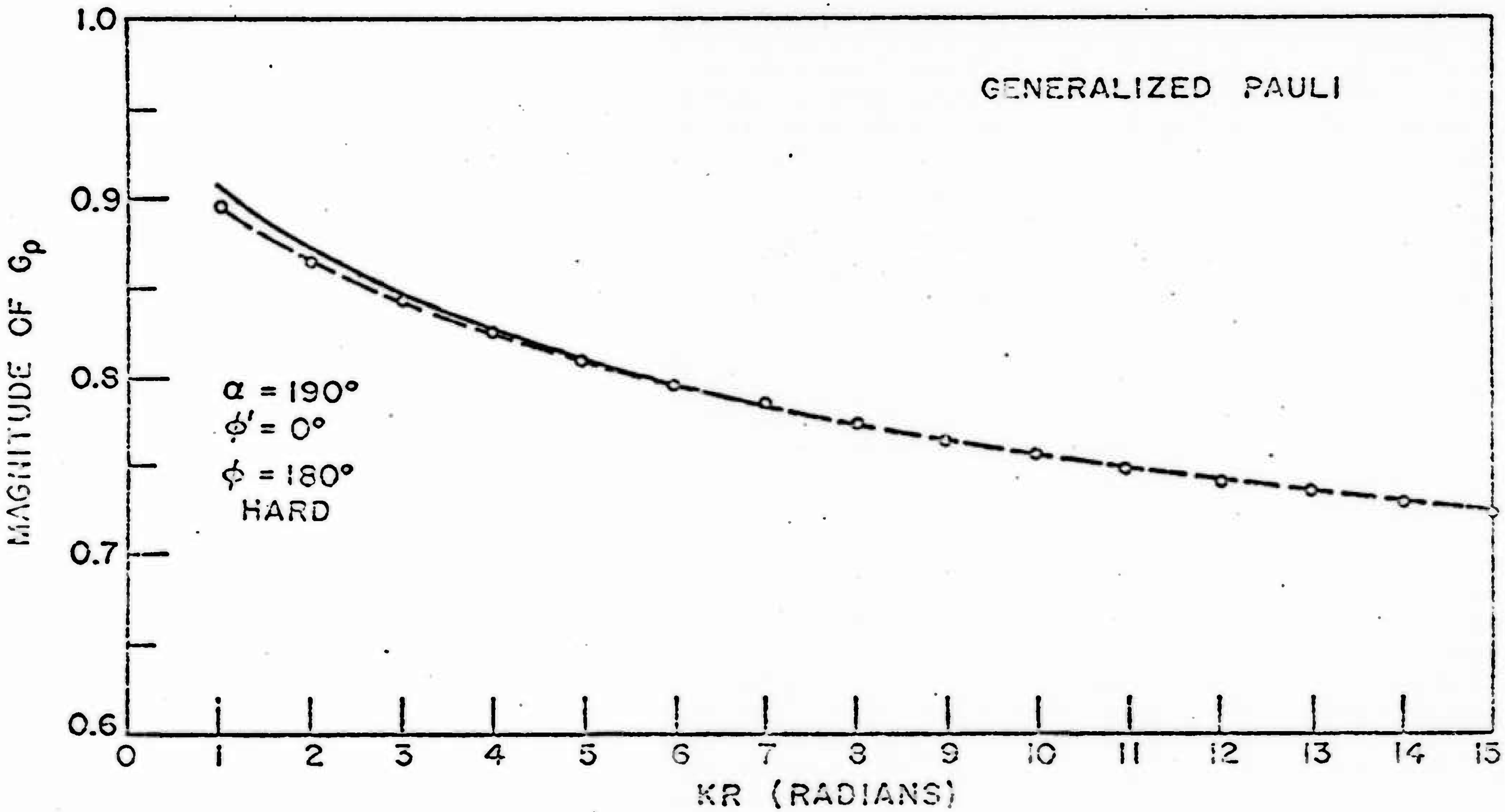

Figure 30. Magnitude of G_p for a 190 degree, hard wedge (a comparison of the generalized Pauli series and the eigenfunction series). The solid line denotes the values given by the first term of the series. The circles denote the values given by the sum of the first and second terms. The third term produces insignificant variations in these values.

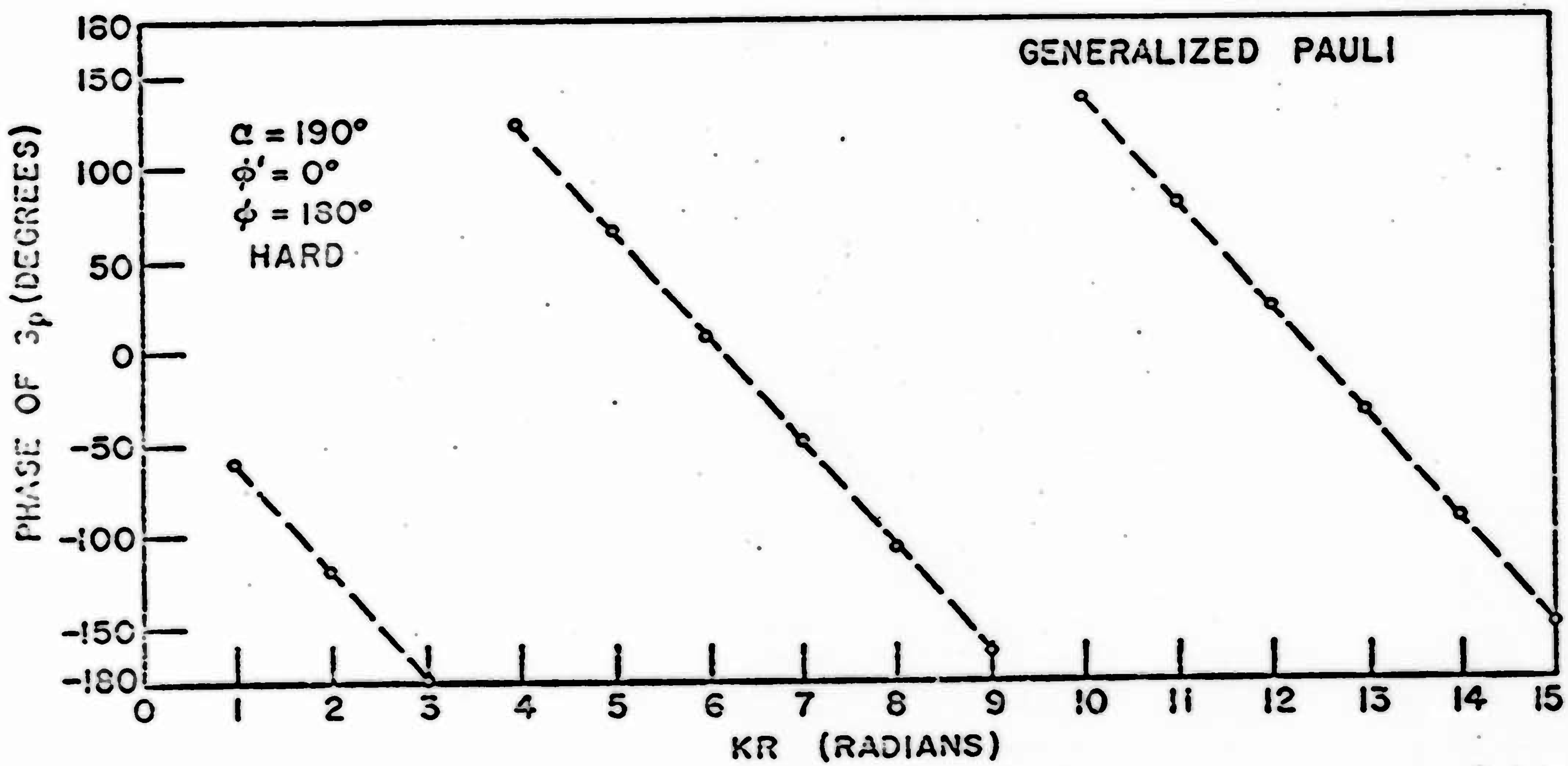

Figure 31. Phase of G_p for a 190 degree, hard wedge (a comparison of the generalized Pauli series and the eigenfunction series). The small circles denote the values given by the first term of the generalized Pauli series. The second and third terms of this series contribute insignificant variations in these values.

Example 4

The exterior wedge angle in this example is assumed to be 160 degrees. The angle of incidence is 10 degrees. The field is calculated at 155 degrees, midway between one of the faces of the wedge and a reflection boundary. This is the first example involving a wedge of angle less than 180 degrees. The field is calculated using the eigenfunction series, generalized Pauli series, and the generalized Oberhettinger series. Both hard and soft wedges are examined. The generalized Pauli and the generalized Oberhettinger series are equally useful in this case. The generalized Pauli is slightly better since it describes the amplitude of the field more accurately at small values of kr than the Oberhettinger series does. The phase of G_p is not shown in this or the following examples.

It can be shown that if $\alpha = \frac{\pi}{M}$, where M is an integer, the diffraction components of G_p vanish and the total field is described completely in terms of plane wave components. This corresponds to the fact that for these particular wedge angles the problem can be analyzed in terms of ordinary image theory.

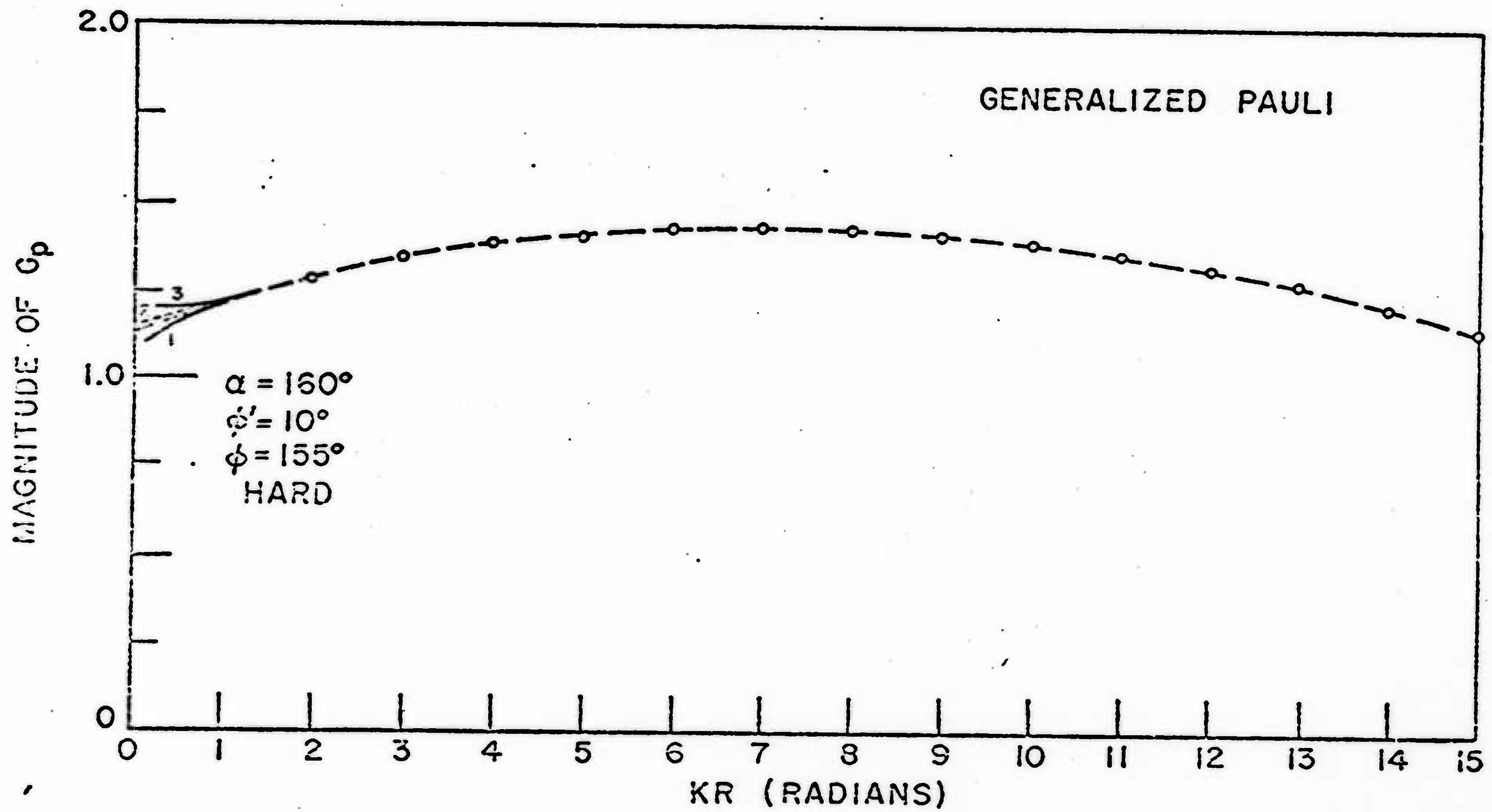

Figure 32. Magnitude of G_p for a 160 degree, hard wedge (a comparison of the generalized Pauli series and the eigenfunction series). The circles denote the values of G_p given by the first term of the generalized Pauli series for values of kr greater than 2.0. For these values of kr, the second and third terms of this series produce minor variations in the results.

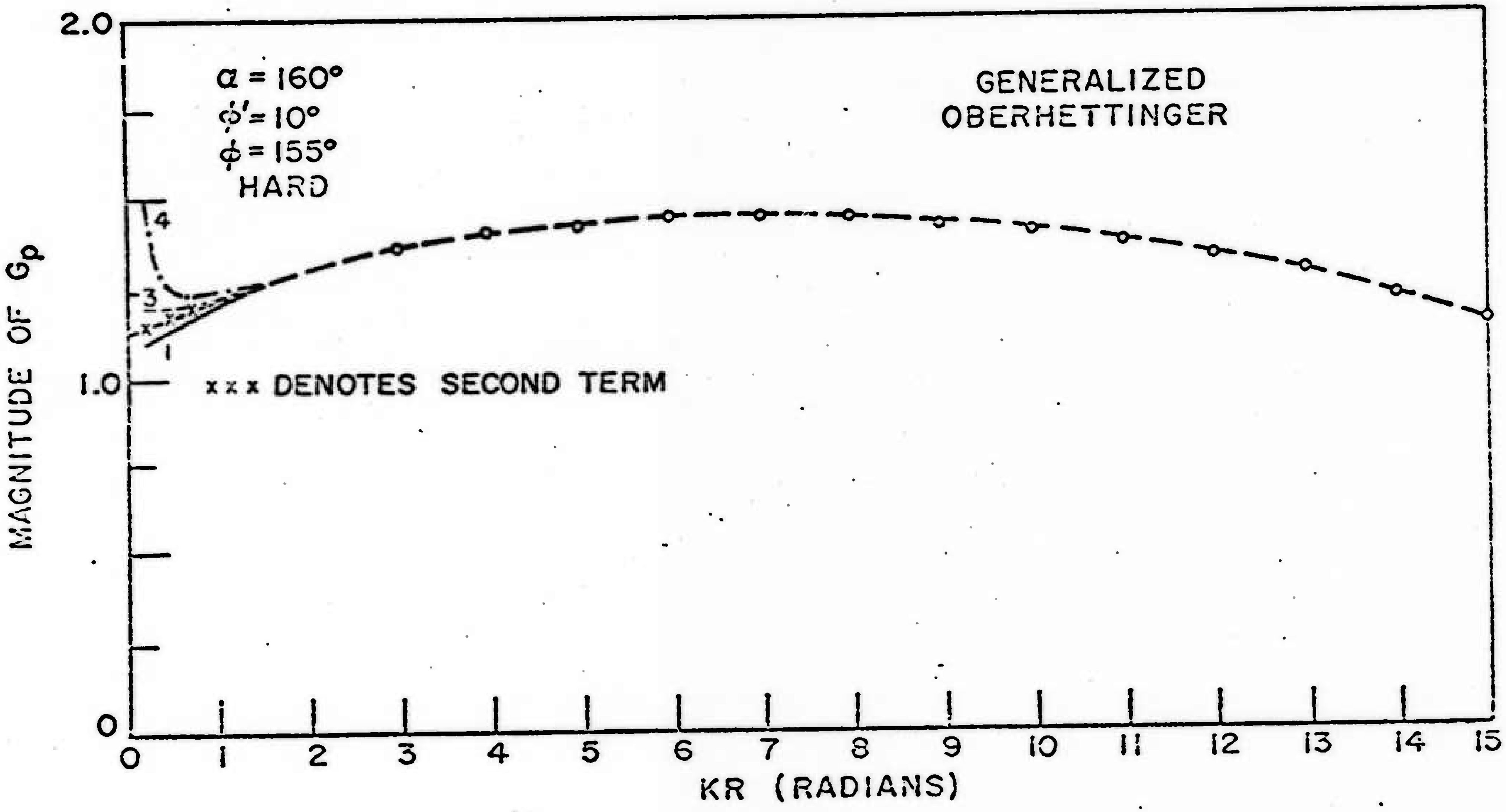

Figure 33. Magnitude of Gp for a 160 degree, hard wedge (a comparison of the generalized Oberhettinger series and the eigenfunction series). The circles denote the values for Gp given by the first term of the Oberhettinger series for kr greater than 3. The second, third, and fourth terms produce insignificant variations in these values.

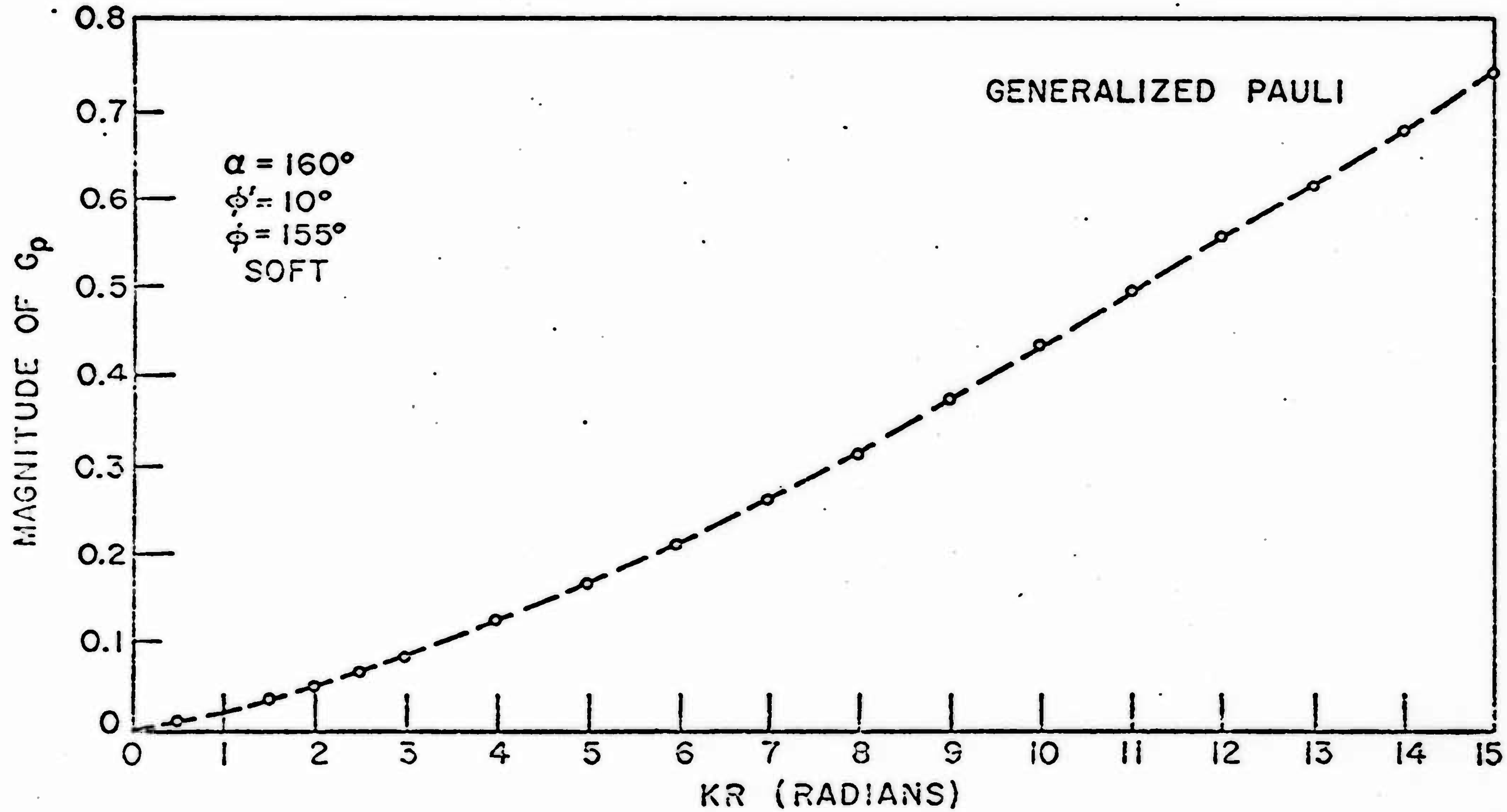

Figure 34. Magnitude of G_p for a 160 degree, soft wedge (a comparison of the generalized Pauli series and the eigenfunction series). The circles denote the values given by the first term of the generalized Pauli series. The second and third terms produce insignificant variations in these values.

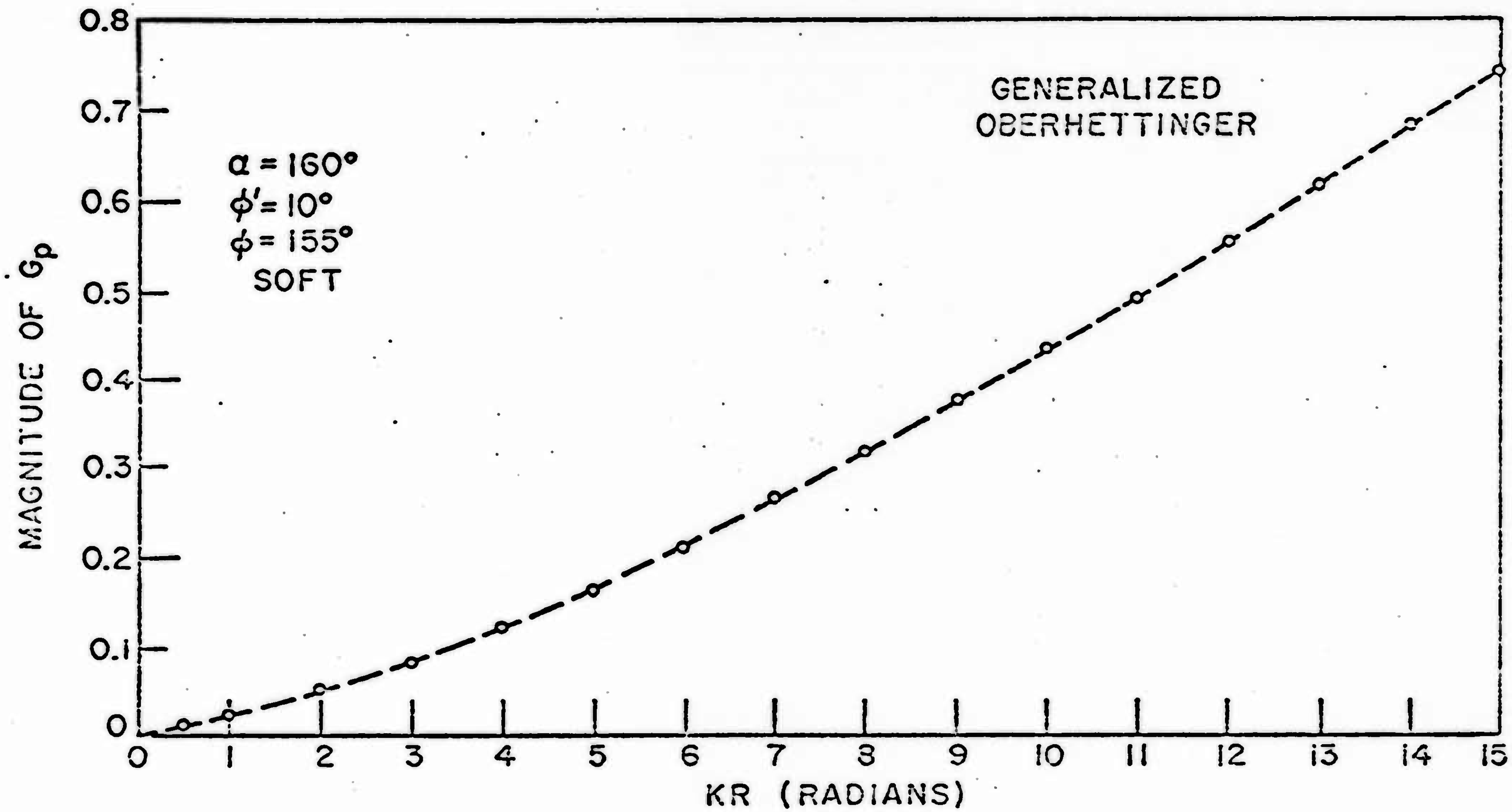

Figure 35. Magnitude of Gp for a 160 degree, soft wedge (a comparison of the generalized Oberhettinger series and eigenfunction series). The small circles denote the values given by the first term of the generalized Oberhettinger series. The second, third, and fourth terms of this series produce insignificant variations in these values.

Example 5

The assumed wedge angle is 100 degrees in this example; the angle of incidence is 30 degrees; and the field is calculated along the reflection boundary at $\phi = 10^{\circ}$. The first term of the generalized Pauli series accurately describes the field for kr as small as 1 in the case of the hard wedge. In the case of the soft wedge, two terms of this series are required to produce good agreement with the eigenfunction series at small values of kr. Two terms are required in the Oberhettinger series to describe the field of the hard wedge. In the case of the soft wedge, one term suffices except at small values of kr.

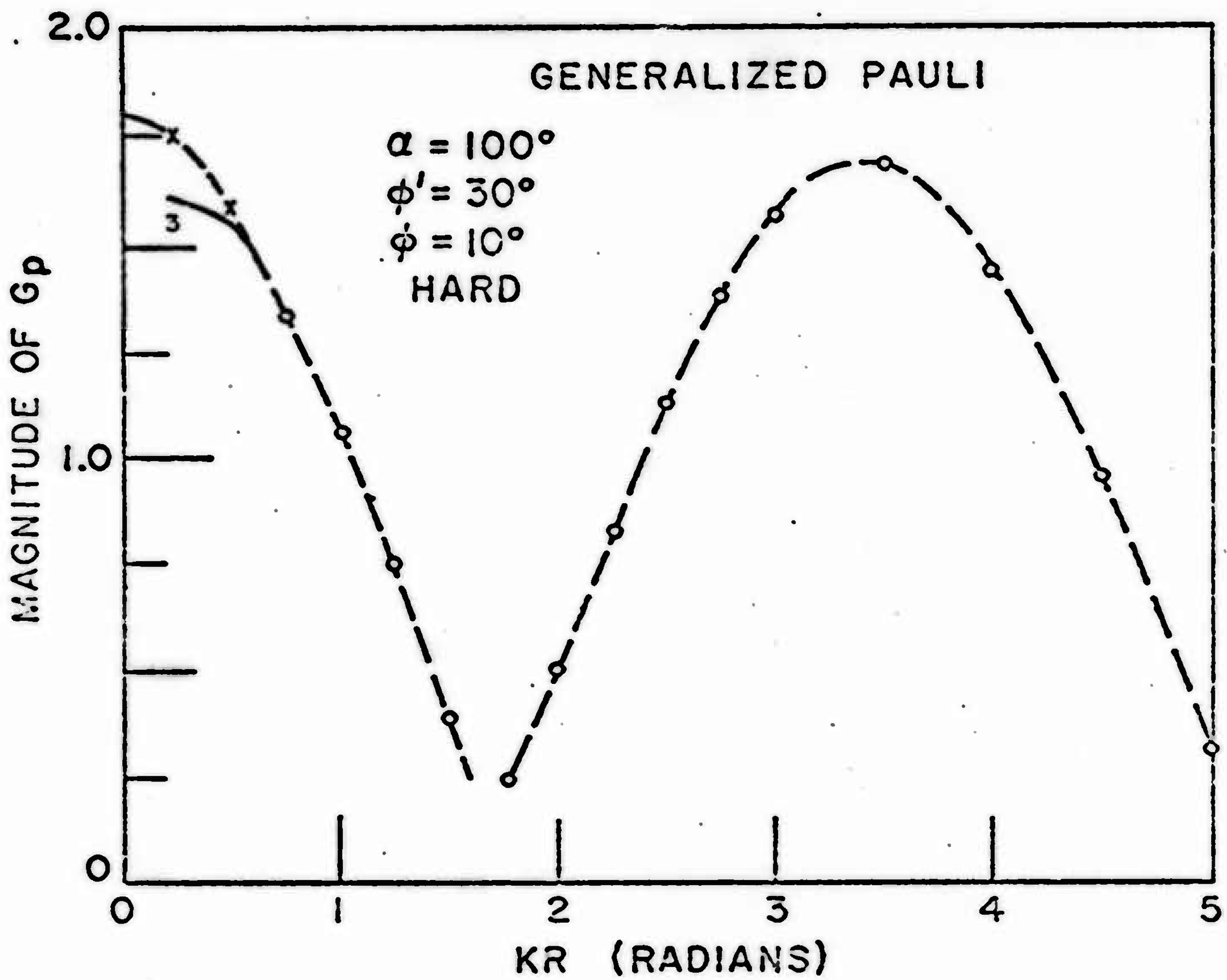

Figure 36. Magnitude of G_p for a 100 degree, hard wedge (a comparison of the generalized Pauli and the eigenfunction series). The small crosses at $kr = 0.25$ and 0.5 denote the values given by the first term of the ordinary Pauli series. The second term of this series produces insignificant variations in these values. The values given by the third term are denoted by the solid line. The small circles denote the values given by the first term for kr greater than 0.75. The second and third terms produce insignificant variations in these values.

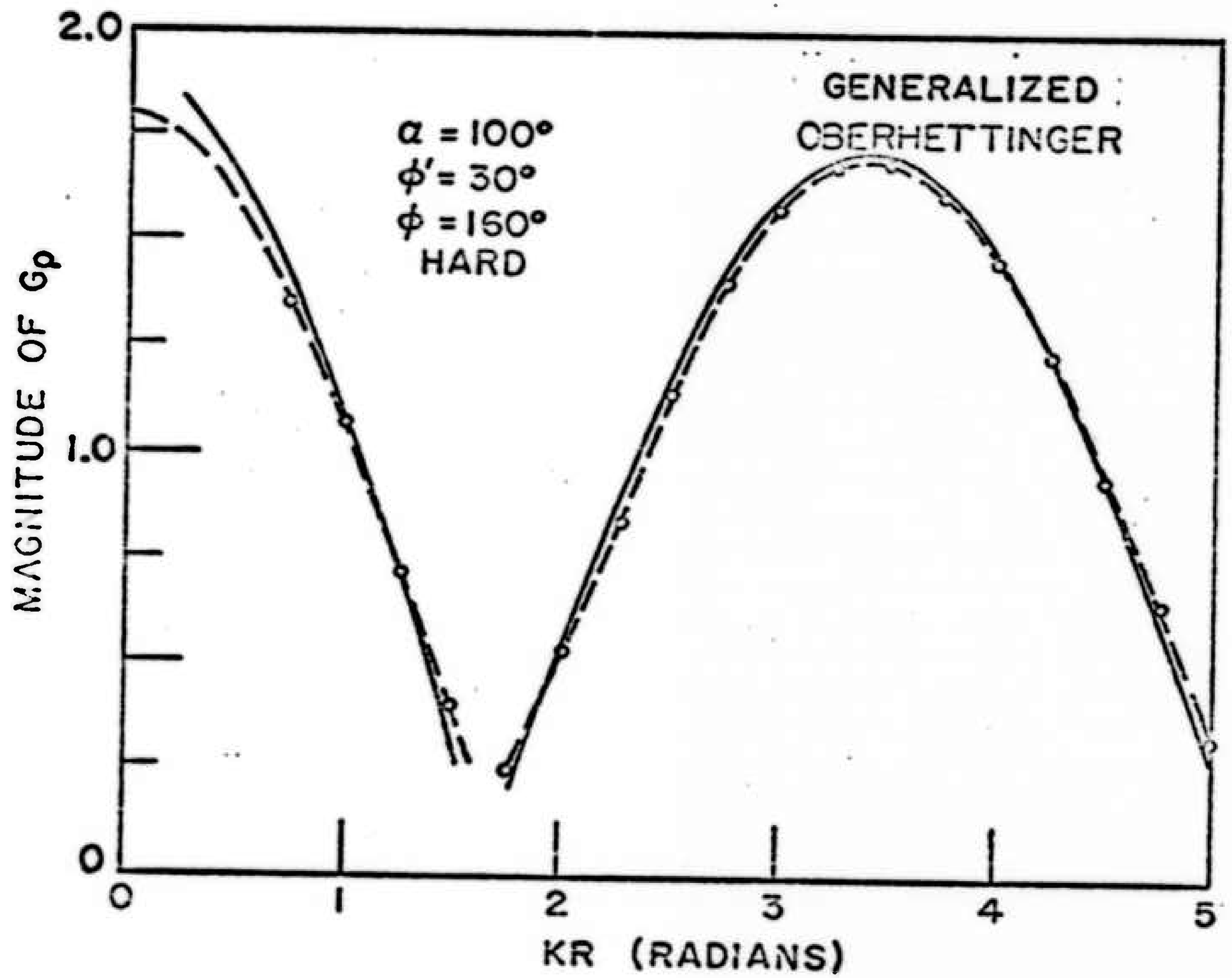

Figure 37. Magnitude of G_p for a 100 degree, hard wedge (a comparison of the generalized Oberhettinger and the eigenfunction series). The solid line denotes the values given by the first term of the series. The circles represent the values given by the first two terms for $kr > 0.75$. The third and fourth terms produce insignificant variations in these values.

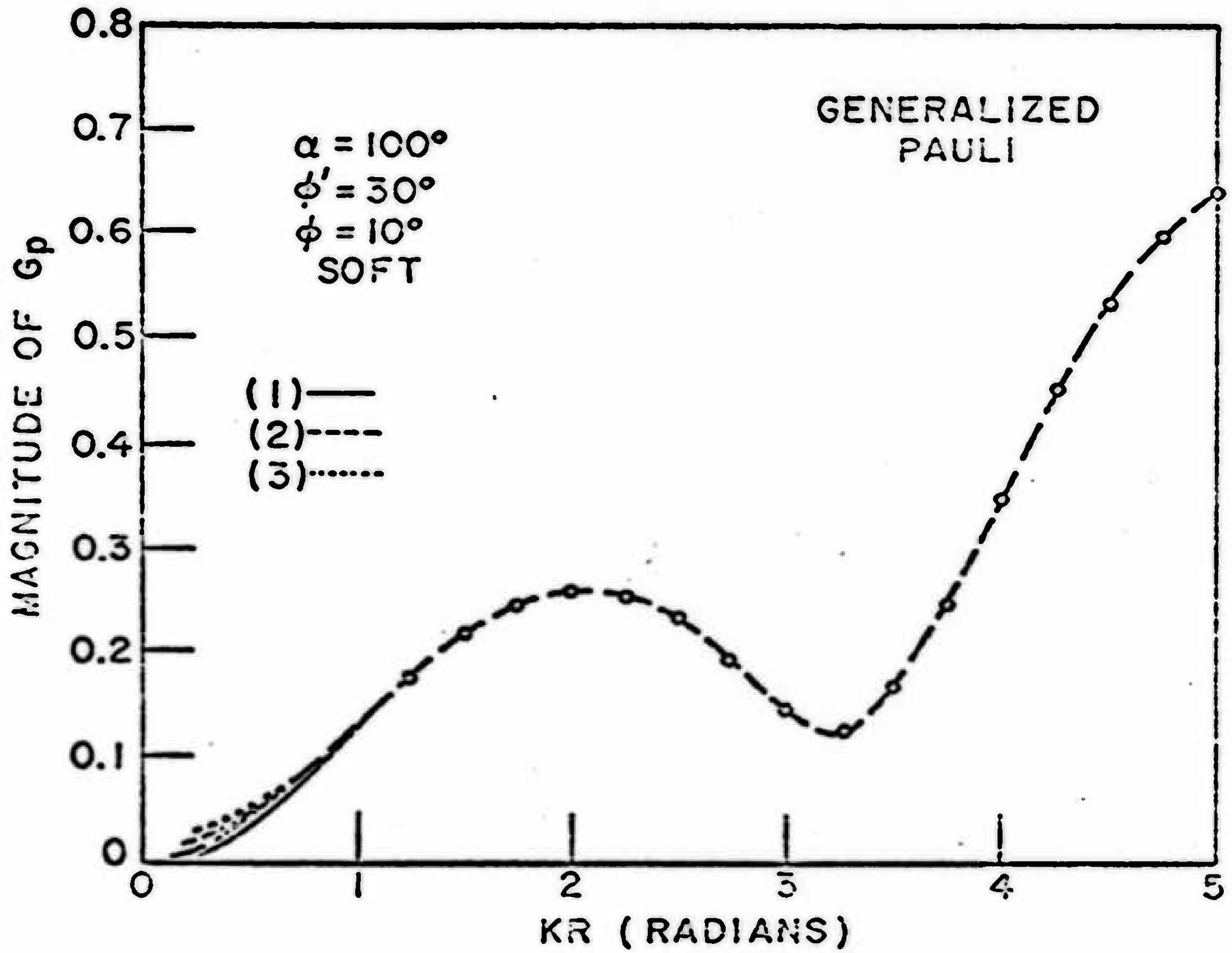

Figure 38. Magnitude of G_p for a 100 degree, soft wedge (a comparison of the generalized Pauli series and the eigenfunction series). For kr greater than 1.0, the values given by the first term of the series are denoted by small circles. The second and third terms produce insignificant variations in these values.

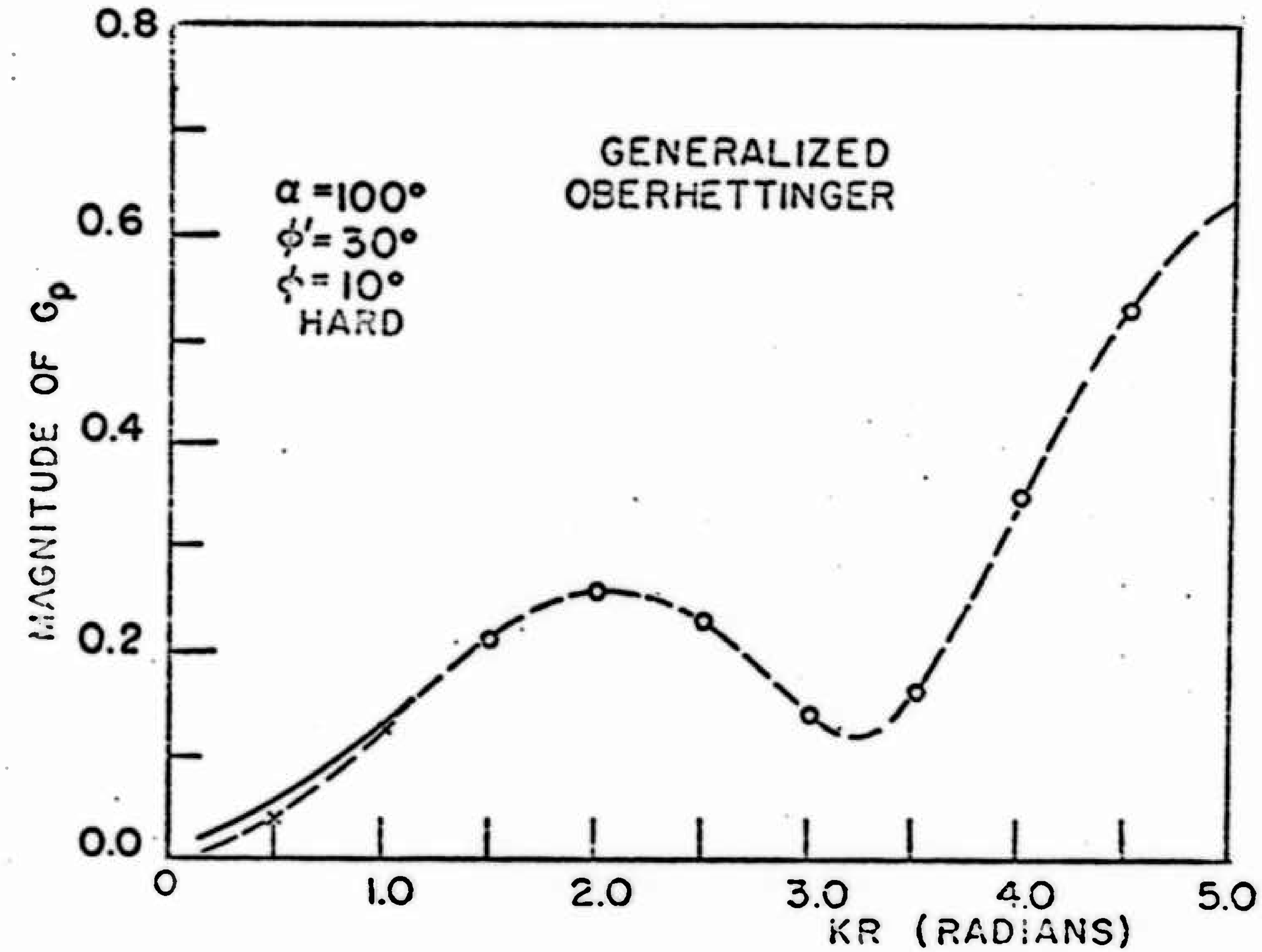

Figure 39. Magnitude of G_p for a 100 degree, soft wedge (a comparison of the generalized Oberhettinger and eigenfunction series). The small circles denote the values given by the first term of the series for $kr > 1$. The second, third, and fourth terms produce insignificant variations in these values. The small crosses denote the values given by the first and second terms of the series. The third and fourth terms produce insignificant variations in these values.

Example 6

The exterior wedge angle α is assumed to be 70 degrees; and the angle of incidence 10 degrees. In this example, the field was calculated at $\phi = 60^{\circ}$, midway between one face of the wedge and the reflection boundary at $\phi = 50^{\circ}$. In the case of the hard wedge, two terms are required in the generalized Pauli series to produce good agreement with the eigenfunction series for $kr < 2.5$. In the case of the soft wedge, only one term is required. The first term of the Oberhettinger series describes the field of the soft wedge quite well. This series does not yield particularly good results in the case of the hard wedge.

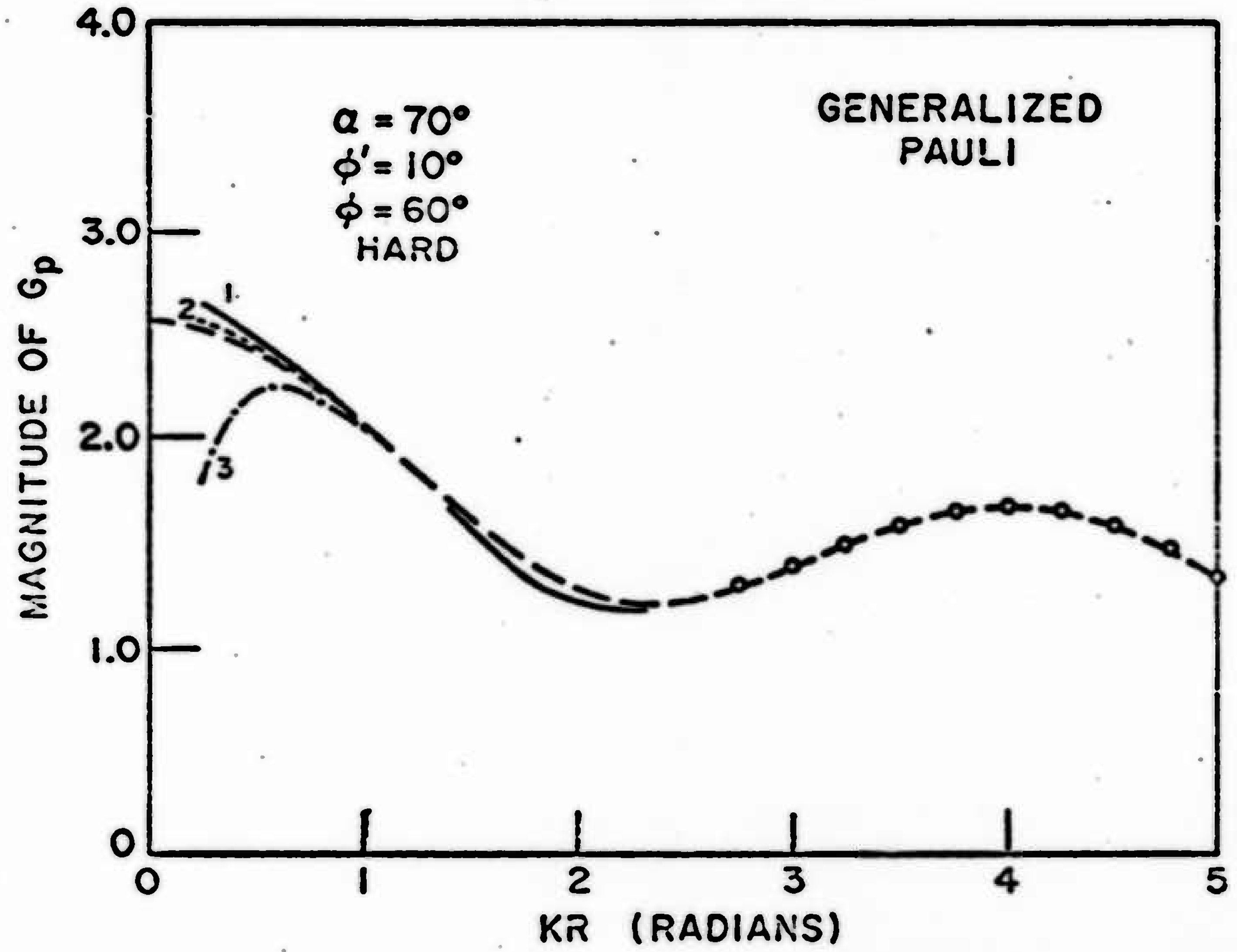

Figure 40. Magnitude of G_p for a 70 degree, hard wedge (a comparison of the generalized Pauli and the eigenfunction series). The solid line and the circles denote the values given by the first term of the generalized Pauli series. For values of kr less than 2.5, two terms are required in the Pauli series to achieve good agreement with the eigenfunction series.

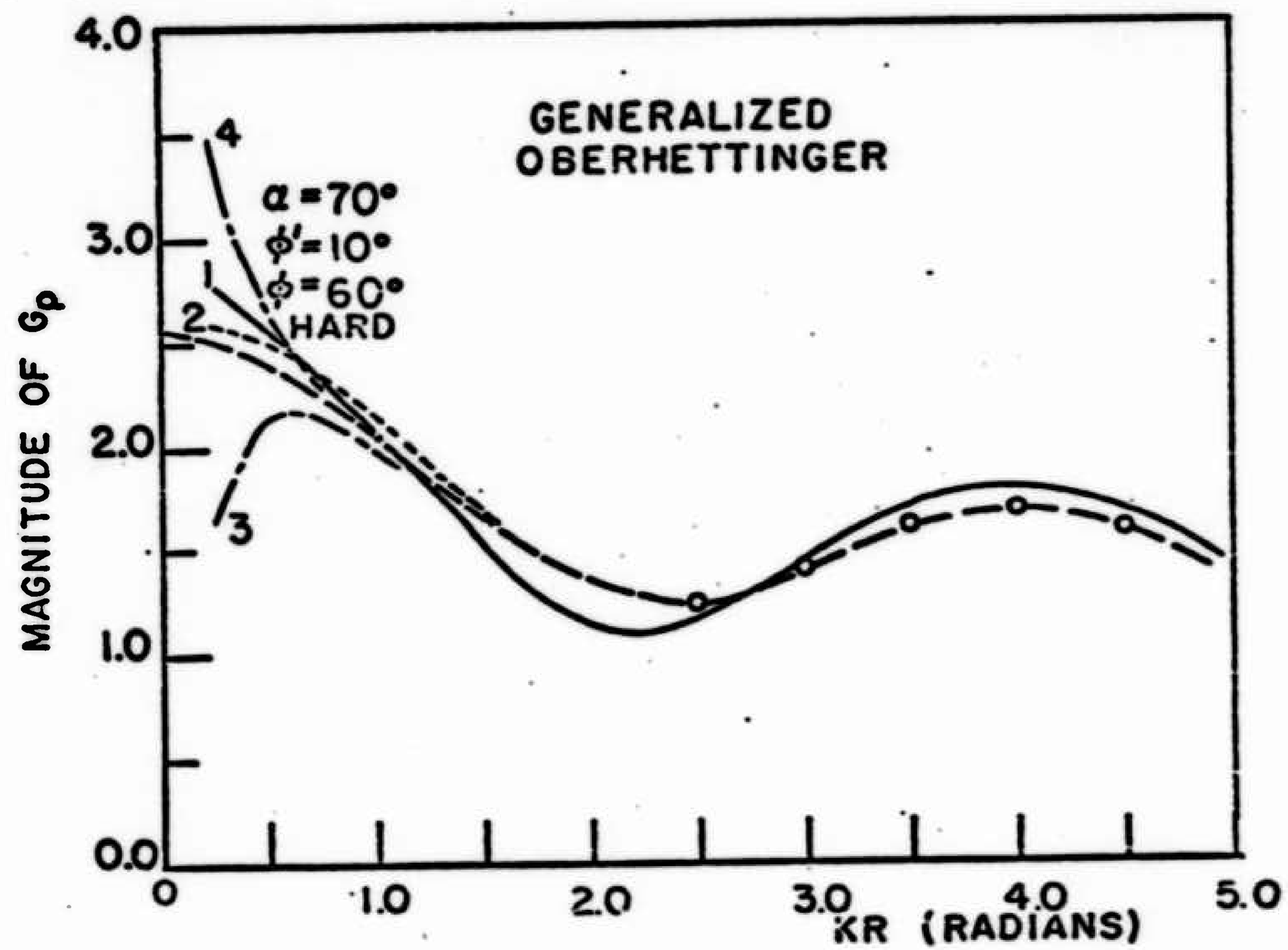

Figure 41. Magnitude of Gp for a 70 degree, hard wedge (a comparison of the generalized Oberhettinger and the eigenfunction series). The circles denote the values given by the first two terms of the series for kr 3.5. The third and fourth terms produce insignificant variations in these values.

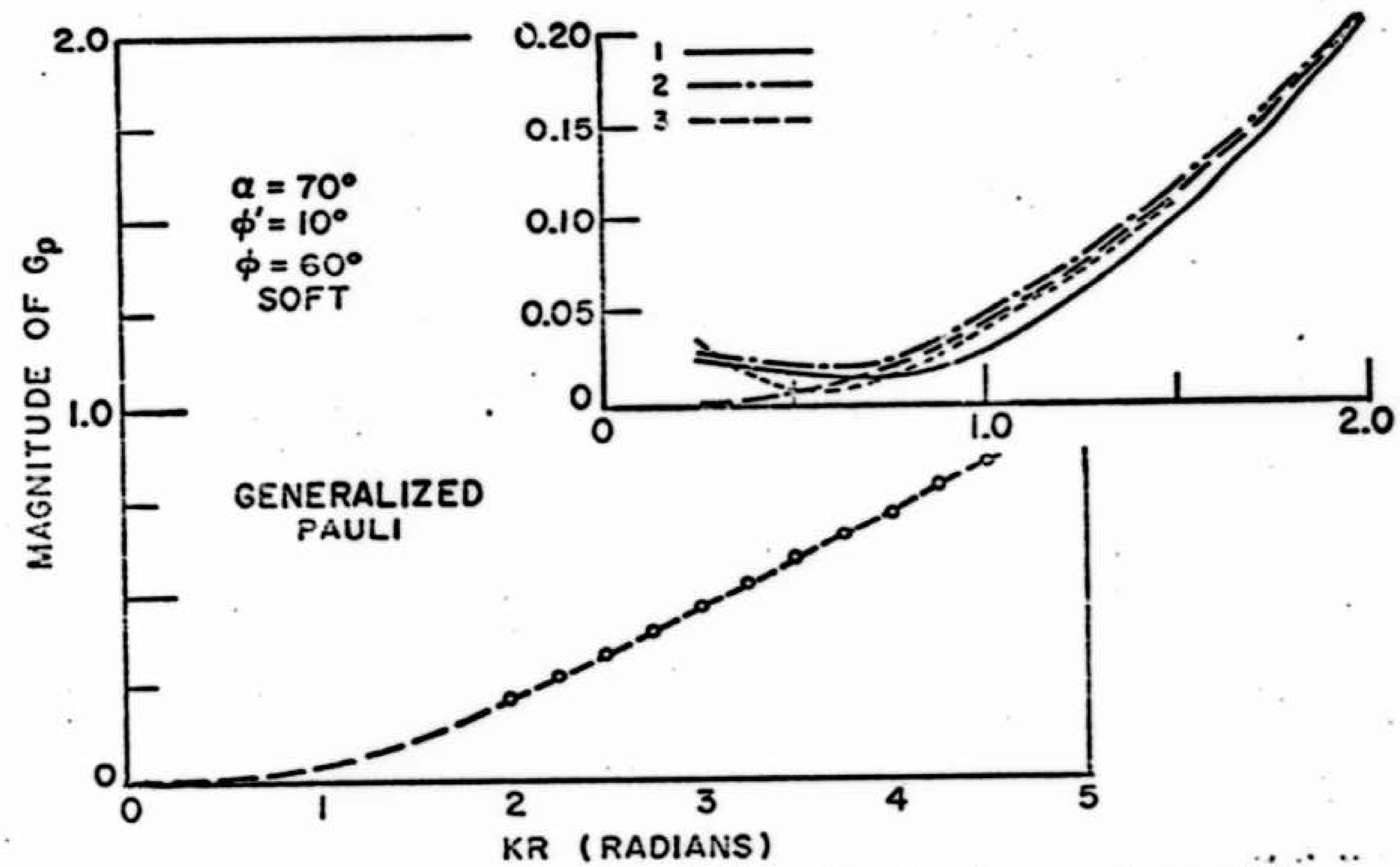

Figure 42. Magnitude of Gp for a 70 degree, soft wedge (a comparison of the generalized Pauli series and the eigenfunction series). The circles denote the values given by the first term of the generalized Pauli series for values of kr greater than 2. The second and third terms produce insignificant variations in these values. The inset graph describes the values obtained with the first three terms of the generalized Pauli series for small values of kr.

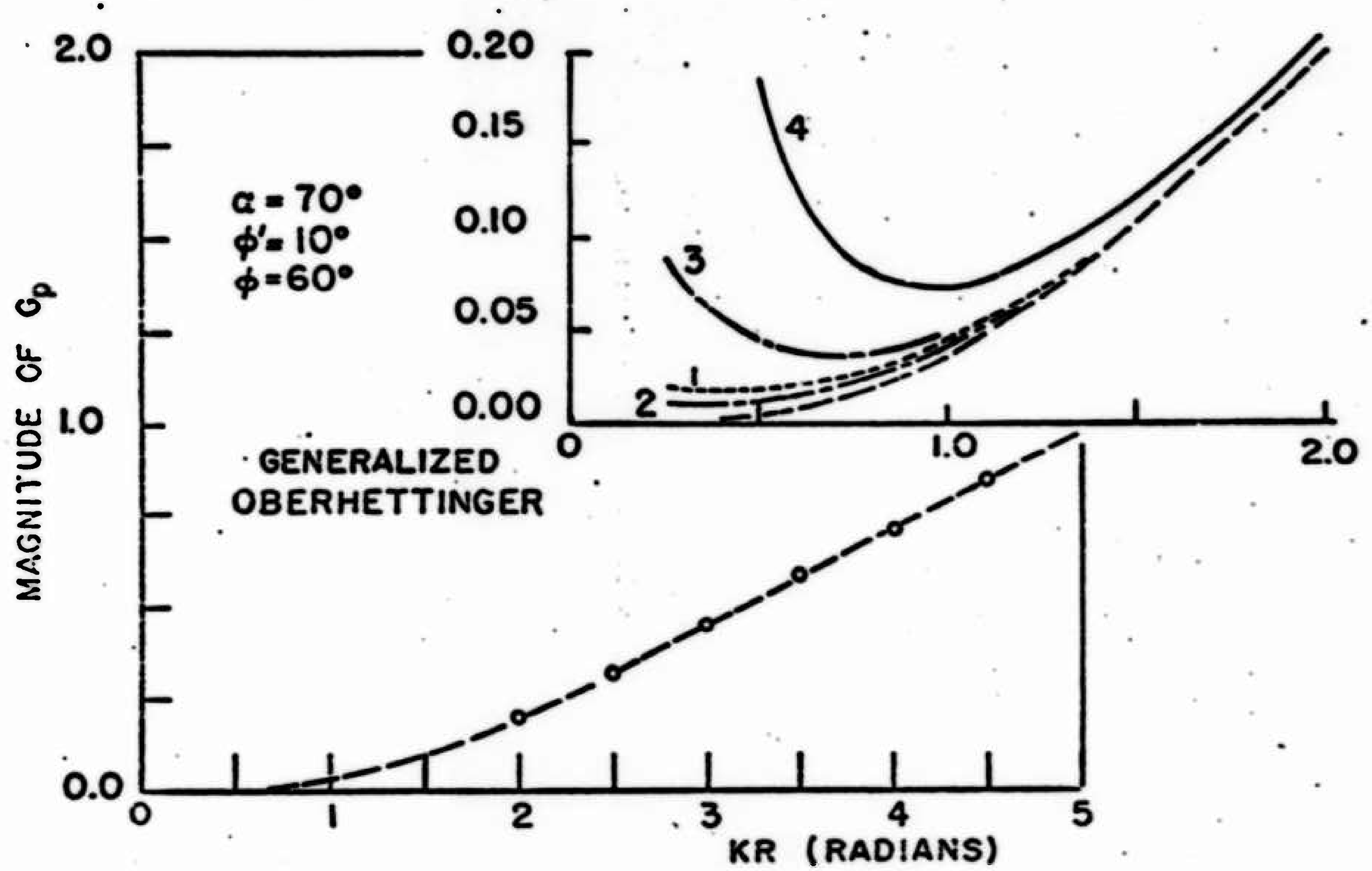

Figure 43. Magnitude of G_p for a 70 degree, soft wedge (a comparison of the generalized Oberhettinger and the eigenfunction series). The circles denote the values given by the first term of the generalized Oberhettinger series for values of kr greater than 2.0. The second, third, and fourth terms produce insignificant variations in these values. The inset graph describes the values obtained with the first four terms of the generalized Oberhettinger series for small values of kr.

Example 7

In this final example, the exterior wedge angle is assumed to be 40 degrees; the angle of incidence 20 degrees; and the angle of observation 10 degrees. In the case of the hard wedge, the values for G_p obtained with the first term of the generalized Pauli and Oberhettinger series are in excellent agreement with those given by the eigenfunction series. In this case, the diffracted component of the field is very small, and a simple superposition of the plane wave terms of Equation 153 is sufficient to describe the field. In the case of the soft wedge, the first term of the generalized Pauli series describes the field accurately for values of kr greater than 3.5. For smaller values of kr this series fails. The generalized Oberhettinger series does not describe the field adequately for the soft wedge case over the range tested. This example illustrates that both the generalized Pauli and the generalized Oberhettinger series fail for small values of α, but that the generalized Pauli series fails more gracefully than does the generalized Oberhettinger.

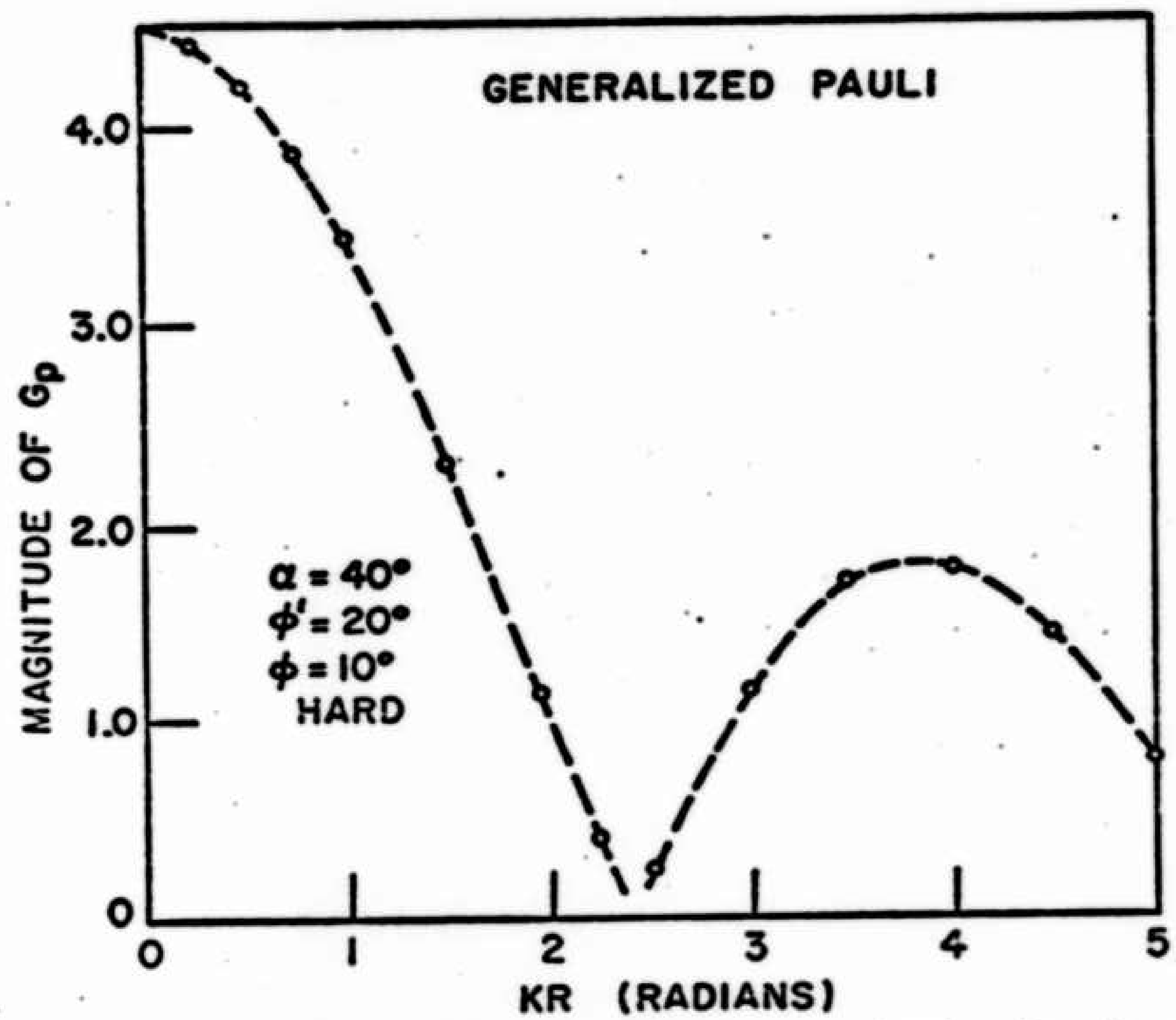

Figure 44. Magnitude of G_p for a 40 degree, hard wedge (a comparison of the generalized Pauli series and the eigenfunction series). The small circles denote the values given by the first term of the generalized Pauli series. The second and third terms of this series produce insignificant variations in these values.

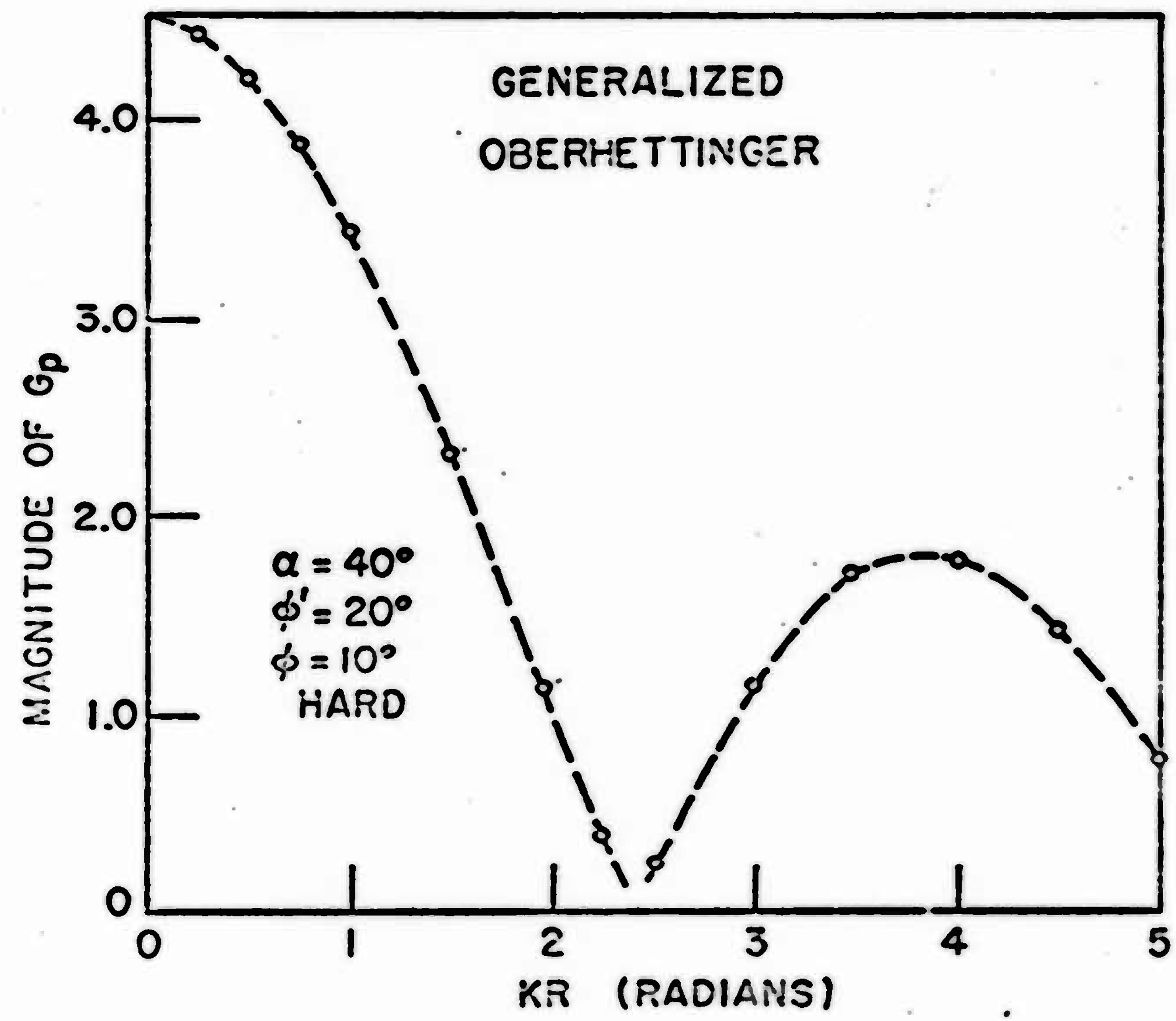

Figure 45. Magnitude of G_p for a 40 degree, hard wedge (a comparison of the generalized Oberhettinger and the eigenfunction series). The small circles denote the values given by the first term of the series. The second, third, and fourth terms produce insignificant variations in these values.

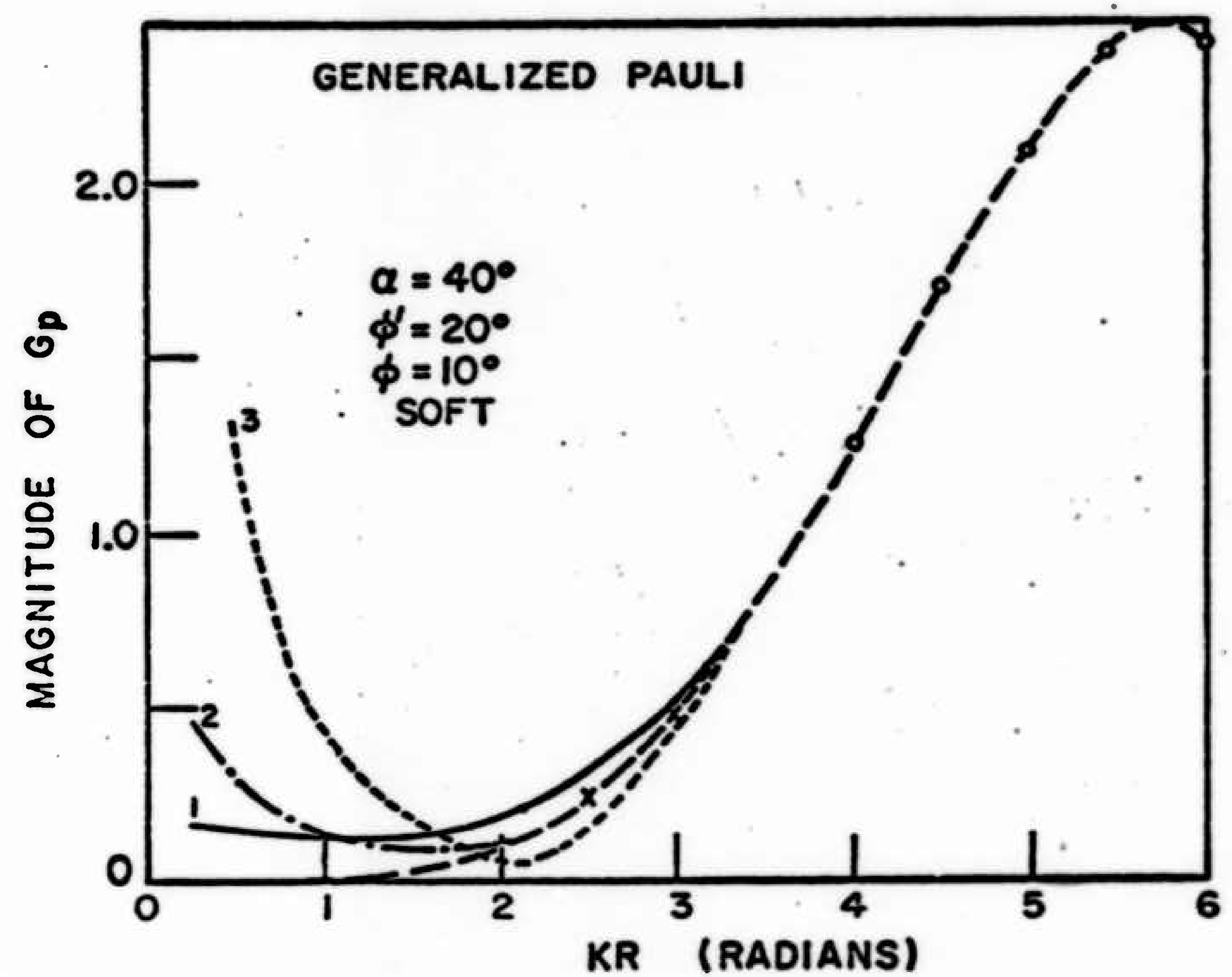

Figure 46. Magnitude of Gp for a 40 degree, soft wedge (a comparison of the generalized Pauli and the eigenfunction series). The circles denote the values given by the first term of the generalized Pauli series. The second and third terms produce insignificant variations in these values.

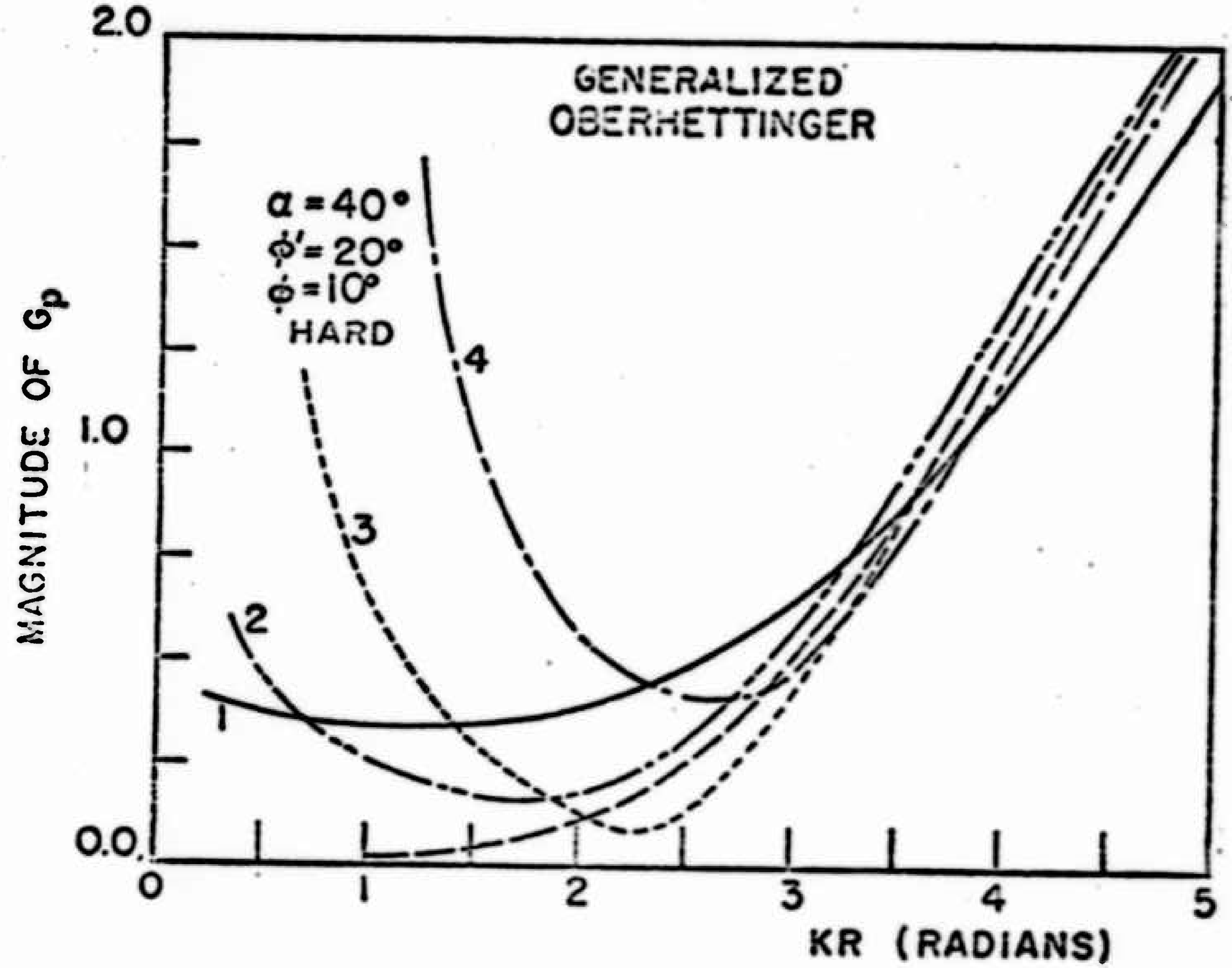

Figure 47. Magnitude of G_p for a 40 degree, soft wedge (a comparison of the generalized Oberhettinger and eigenfunction series).

Conclusions

The important results of this work can be summarized as follows:

a) The integral expression for the total field produced by the diffraction of a plane wave by a two-dimensional wedge can be expanded asymptotically by a variety of techniques, but the resulting expansions can be shown to be intimately related. In particular, the generalized Pauli series and the generalized Oberhettinger series are simply different arrangements of the same series, and the ordinary Pauli series represents a special form of the generalized Pauli series.

b) Of the asymptotic series examined in this work, the generalized Pauli series is the most satisfactory for computing the field near transition regions. The first term in this series provides an accurate description of the amplitude and phase of the field over a wide range of values of α and kr. It is particularly superior to the Oberhettinger series in cases involving wedges having angles quite different from 180 degrees.

c) The ordinary Pauli series is superior to the Oberhettinger series for calculating the fields diffracted by wedges having large exterior angles, while the Oberhettinger series is superior to the ordinary Pauli series for cases involving wedges with exterior angles in the neighborhood of and less than 180 degrees.

CHAPTER V

DIFFRACTION COEFFICIENTS

In this chapter the leading terms of the asymptotic expansions given in the summary of equations, pp. 79-85, are used to determine the diffraction coefficient for the wedge. In terms of the geometrical theory of diffraction the diffracted electric field for plane and cylindrical waves normally incident on the wedge is given by

$$\overline{E}^d(r,\phi) = \overline{E}^i \cdot [\hat{z}\hat{z}\, D_s(\phi,\phi') - \hat{\phi}'\hat{\phi}\, D_h(\phi,\phi')]\, \frac{e^{-jkr}}{\sqrt{r}} , \tag{159}$$

where $\overline{E}^i$ is the electric field incident on the edge,

$\hat{z}$ is a unit vector parallel to the edge,

D_s, D_h are the scalar diffraction coefficients for the Dirichlet (soft) and Neumann (hard) boundary conditions, respectively,

ϕ, ϕ' and r are defined in Figure 2.

In the discussion to follow E_z^d and E_ϕ^d correspond to the soft and hard diffracted components, respectively, of G_p in Equation 147, provided that E_z^i and $E_{\phi'}^i$, respectively, equal one. At this point it is convenient to introduce the definitions

$$D'(\phi \pm \phi') = \frac{e^{-j\frac{\pi}{4}}}{n\sqrt{2\pi k}} \; \frac{\sin \pi/n}{\cos \frac{\pi}{n} - \cos \frac{\phi \pm \phi'}{n}} , \tag{160}$$

$$d^{\pm}(\phi \pm \phi') = \frac{-e^{-j\frac{\pi}{4}}}{2n\sqrt{2\pi k}} \cot\left(\frac{\pi \pm (\phi \pm \phi')}{2n}\right) , \tag{161}$$

where the superscript $\pm$ is directly associated with the first $\pm$ sign in the argument of the cotangent,

$$F[kr\, a^{\pm}(\phi \pm \phi')]$$

$$= 2j\sqrt{kr\, a^{\pm}(\phi \pm \phi')}\; e^{jkr\, a^{\pm}(\phi \pm \phi')} \int_{\sqrt{kra^{\pm}(\phi \pm \phi')}}^{\infty} e^{-j\tau^2}\, d\tau \quad (162)$$

in which

$$a^{\pm}(\phi \pm \phi') = 1 + \cos(2\pi n N^{\pm} - (\phi \pm \phi')), \quad (163)$$

where $N^{\pm}$ is the integer which most nearly satisfies the equation

$$-(\phi \pm \phi') + 2\pi n N^{\pm} = \pm \pi . \quad (164)$$

The superscript $\pm$ is directly associated with the $\pm$ sign preceding the π. The positive branches of the square roots are taken in Equations 160 through 162.

The magnitude and phase of $F(kra^{\pm})$ are plotted in Figure 48, where it is seen that as $kra^{\pm}$ increases, $|F| \rightarrow 1$. For $kra^{\pm} > 10$, $F \simeq 1$.

From the preceding discussion and the leading term in the Generalized Pauli asymptotic series, Equation 153, the scalar diffraction coefficients

$$D_{\substack{s\\h}}(\phi, \phi') =$$

$$\left\{d^{+}(\phi-\phi')F[kra^{+}(\phi-\phi')] + d^{-}(\phi-\phi')F[kra^{-}(\phi-\phi')]\right\}$$

$$\mp\left\{d^{+}(\phi+\phi')F[kra^{+}(\phi+\phi')] + d^{-}(\phi+\phi')F[kra^{-}(\phi+\phi')]\right\} \quad (165)$$

in which the upper sign between the two bracketed terms is associated with the soft (s) boundary condition and the lower sign, with the hard (h) boundary condition. At points well removed from the transition regions adjacent to incident and reflected field shadow boundaries referred to as field boundaries earlier, where $kra^{\pm} > 10$, the correction factors F may be replaced by unity, and Equation 165 simplifies to

$$D_{\substack{s\\h}}(\phi,\phi') = D'(\phi-\phi') \mp D'(\phi+\phi'), \tag{166}$$

which is the well-known form of the wedge diffraction coefficient given by Keller.[3]

Next, using the leading term in the Pauli asymptotic series, Equation 157, the scalar diffraction coefficient

$$D_{\substack{s\\h}}(\phi,\phi') =$$

$$D'(\phi-\phi')\ F[kra(\phi-\phi')] \mp D'(\phi+\phi')\ F[kra(\phi+\phi')]; \tag{167}$$

in the Pauli solution $N^{\pm}$ is zero so that

$$a^{\pm}(\phi\pm\phi') = a(\phi\pm\phi') = 1 + \cos(\phi\pm\phi'). \tag{168}$$

Outside of the transition regions, where $kra > 10$, the correction factors may be replaced by unity and Equation 167 simplifies to Equation 166.

Finally using the leading term in the generalized Oberhettinger series, Equation 158, the scalar diffraction coefficients

$$D_{\substack{s\\h}}(\phi,\phi') =$$

$$[d^{+}(\phi-\phi') + \frac{\mathrm{sgn}(\pi-|(\phi-\phi')-2nN^{+}\pi|)e^{-j\frac{\pi}{4}}}{2\sqrt{\pi ka^{+}(\phi-\phi')}} \left\{1-F[ka^{+}(\phi-\phi')]\right\}$$

$$+ d^-(\phi-\phi') + \frac{\text{sgn}(\pi - |(\phi-\phi')-2nN^-\pi|)e^{-j\frac{\pi}{4}}}{2\sqrt{\pi ka^-(\phi-\phi')}} \left\{1-F[ka^-(\phi-\phi')]\right\}\Big]$$

$$\mp[d^+(\phi+\phi') + \frac{\text{sgn}(\pi - |(\phi+\phi')-2nN^+\pi|)e^{-j\frac{\pi}{4}}}{2\sqrt{\pi ka^+(\phi+\phi')}} \left\{1-F[ka^+(\phi+\phi')]\right\}$$

$$+ d^-(\phi+\phi') + \frac{\text{sgn}(\pi - |(\phi+\phi')-2nN^-\pi|)e^{-j\frac{\pi}{4}}}{2\sqrt{\pi ka^-(\phi+\phi')}} \left\{1-F[ka^-(\phi+\phi')]\right\}\Big] , \quad (169)$$

where $N^{\pm}$ is determined from Equation 164 and $a^{\pm}(\phi \pm \phi')$ from Equation 163. Outside of the transition regions, where $kra^{\pm} > 10$, the correction factors again may be replaced by unity and it is seen that Equation 169 simplifies to Equation 166.

Three expressions have been given for the scalar diffraction coefficients, Equations 165, 167, and 169. Unlike the earlier expression given by Keller[3] these are not restricted to the region outside the transition regions. It is natural to ask which is the most useful in the transition regions, in terms of its accuracy and simplicity. It is evident that Equation 169 is the most complicated representation of the diffraction coefficient, whereas Equation 167 is the most simple. On the other hand, a study of the examples in Chapter IV reveals that the most accurate results (assuming only the leading term is retained in each asymptotic series) are obtained with the Generalized Pauli series. A computer subroutine has been written for the diffraction coefficient described by Equation 165, and it has been used in a number of wedge diffraction problems[122,123,124,125] with good accuracy, provided r > 0.2 wavelength. It is definitely more accurate than the expression for the diffraction coefficient given in Equation 167. However, a computer subroutine is not essential to the use of the diffraction coefficients based on the Generalized Pauli series, since the corrections in the transition regions can be easily made using Figure 48.

The dyadic diffraction coefficient

$$\bar{D}(\phi,\phi') = \hat{z}\hat{z}\, D_s(\phi,\phi') - \hat{\phi}'\hat{\phi}\, D_h(\phi,\phi')$$

in Equation 159 can be applied to three-dimensional problems provided that the incident field at the point of diffraction is normal to the edge. Furthermore, it is applicable to cases where either the source point or the field point is close to the edge. This will be described in a later report[126] where the Generalized Pauli solution has been extended to obtain a dyadic diffraction coefficient for waves obliquely incident on a perfectly-conducting wedge. This dyadic diffraction coefficient can be used in the transition regions for plane, cylindrical or spherical wave illumination of the edge.

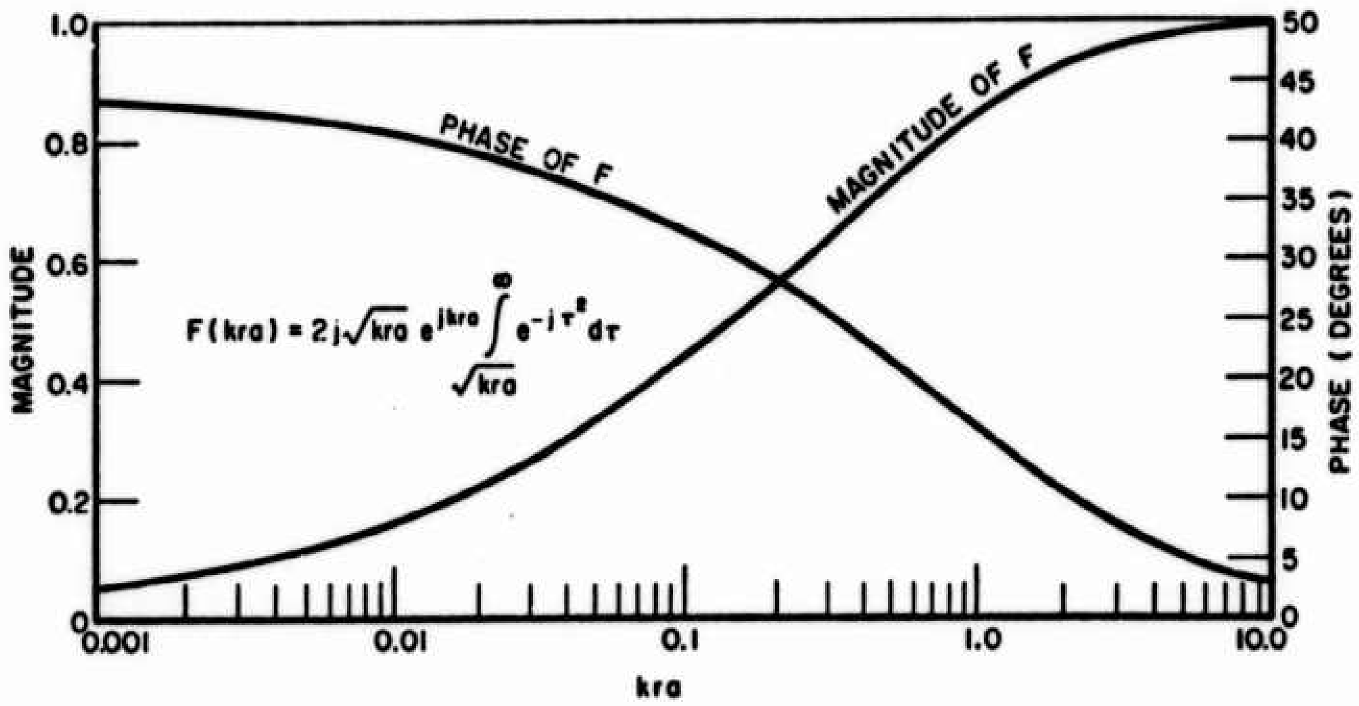

Fig. 48. The magnitude and phase of the correction factor.

BIBLIOGRAPHY

1. Pauli, Wolfgang. "On Asymptotic Series for Functions in the Theory of Diffraction of Light," Physical Review, 34 (December, 1938), 924-931.

2. Oberhettinger, F. "On Asymptotic Series Occurring in the Theory of Diffraction of Waves by a Wedge," Journal of Mathematics and Physics, 34 (1956), 245-255.

3. Keller, Joseph B. "Geometrical Theory of Diffraction," Journal of the Optical Society of America, 52 (February, 1962), 116-130.

4. Devore, R. V., and Kouyoumjian, R. G. "The Back-scattering from a Circular Disc." (Paper read before the Spring Meeting of the URSI-IRE, Washington, D.C., May, 1961.)

5. Peters, L., Jr., and Kilcoyne, T. E. "Radiating Mechanisms in a Reflector Antenna System," IEEE Transactions, EMC-7 (December, 1965), 368-374.

6. Rudduck, R. C. "Application of Wedge Diffraction to Antenna Theory." Report 1691-13, Antenna Laboratory, The Ohio State University Research Foundation, Columbus, Ohio, June, 1965.

7. Morse, Burt Jules. "Diffraction by Polygonal Cylinders," Journal of Mathematical Physics, 5 (February, 1964), 199-214.

8. Sommerfeld, Arnold. "Asymptotische Darstellung von Formeln aus der Beugungstheorie des Lichtes," Zeitschrift für Mathematik, 158 (1928), 199-208.

9. Sommerfeld, Arnold. Optics. New York: Academic Press, 1949. Pp. 247-272.

10. Carslaw, H. S. "Multiform Solutions of Certain Partial Differential Equations," Proceedings of the London Mathematical Society (1), 30 (1898), 121.

11. Poincaré, H. "Sur la polarisation par diffraction," Acta Mathematica, 16 (1892), 297-339.

12. MacDonald, H. M. "Diffraction of Light by an Opaque Plane," Proceedings of the London Mathematical Society (1), 14 (1915), 410-427.

13. MacDonald, H. M. Electric Waves. Cambridge: Cambridge University Press, 1902. Pp. 186-198.

14. Carslaw, H. S. "Diffraction of Waves by a Wedge of Any Angle," Proceedings of the London Mathematical Society (2), 18 (1919), 291-306.

15. Bromwich, T. J. "Diffraction of Waves by a Wedge," Proceedings of the London Mathematical Society (1), 14 (1916), 450-463.

16. Oberhettinger, F. "Diffraction of Waves by a Wedge," Communications on Pure and Applied Mathematics, 7 (1954), 551-563.

17. Kontorovich, M. J., and Lebedev, N. N. "On a Method of Solution of Some Problems in the Diffraction Theory," Journal of Physics (Moscow), 1 (1939), 229-241.

18. Karp, S. N. "Separation of Variables and Wiener-Hopf Techniques." Research Report No. E.M. 25, New York University Mathematical Research Group, New York, New York, 1950.

19. Harrington, R. F. "Current Element Near the Edge of a Conducting Half-Plane," Journal of Applied Physics, 24 (1953), 547-550.

20. Copson, E. T. "Diffraction by a Plane Screen," Proceedings of the Royal Society (A), 202 (1950), 277-284.

21. Magnus, W. "Über die Beugung elektromagnetischer Wellen an einer Halberbene," Zeitschrift für Physik, 117 (1941), 168-179.

22. Nomura, Yukichi. "On the Diffraction of Electric Waves by a Perfectly Reflecting Wedge," Science Reports of the Research Institutes, Tohoku University, 1 (January, 1951), 1-23.

23. Senior, T. B. A. "Diffraction of a Dipole Field by a Perfectly Conducting Half Plane," Quarterly Journal of Mechanics and Applied Mathematics, 6 (March, 1953), 101-114.

24. Heins, A. E. "The Excitation of a Perfectly Conducting Half-Plane by a Dipole Field," IRE Transactions on Antennas and Propagation, AP-4 (July, 1956), 294-296.

25. Oberhettinger, F. "On the Diffraction and Reflection of Waves and Pulses by Wedges and Corners," Journal of Research of the National Bureau of Standards, 61 (November, 1958), 343-365.

26. Friedlander, F. G. Sound Pulses. Cambridge: Cambridge University Press, 1958.

27. Keller, J. B., and Blank, A. "Diffraction and Reflection of Pulses by Wedges and Corners," Communications on Pure and Applied Mathematics, 4 (1951), 75-94.

28. Keller, J. B. "Diffraction of a Shock or an Electromagnetic Pulse by a Right-Angled Wedge," Journal of Applied Physics, 23 (1952), 1267-1268.

29. Miles, J. W. "Diffraction of Electromagnetic Pulses," Proceedings of the Royal Society (A), 212 (1952), 543-547.

30. Sollfrey, W. "Diffraction of Pulses by Conducting Wedges and Cones." Research Report No. E.M. 11, New York University Mathematical Research Group, New York, New York, 1952.

31. Kay, I. "Diffraction of an Arbitrary Pulse by a Wedge," Communications on Pure and Applied Mathematics, 6 (1953), 648-687.

32. Turner, R. D. "The Diffraction of a Cylindrical Pulse by a Half-Plane," Quarterly Journal of Applied Mathematics, 14 (1956), 63-73.

33. Papadopoulos, V. M. "The Diffraction and Refraction of Pulses," Proceedings of the Royal Society (A), 252 (October, 1959), 520-537.

34. Papadopoulos, V. M. "The Diffraction and Refraction of Plane Pulses," IRE Transactions on Antennas and Propagation, AP-7 (December, 1959), S78-S87.

35. Papadopoulos, V. M. "Diffraction of a Pulse by a Resistive Half-Plane. I. Normal Incidence," Proceedings of the Royal Society (A), 255 (May, 1960), 538-549.

36. Papadopoulos, V. M. "Diffraction of a Pulse by a Resistive Half-Plane. II. Oblique Incidence," Proceedings of the Royal Society (A), 255 (May, 1960), 550-557.

37. Williams, W. C. "Refraction and Diffraction of Pulses," Canadian Journal of Physics, 39 (February, 1961), 272-275.

38. Papadopoulos, V. M. "Diffraction of a Pulse by a Dielectric Wedge," IRE Transactions on Antennas and Propagation, AP-10 (July, 1962), 503.

39. Macedo, A. M. M. "Diffraction of a Pulse by a Half-Plane, Treated by the Fourier Method," Anuario du Academia Brasiliana du Ciencia, 35 (1963), 37-44.

40. Faulkner, T. R. "Diffraction of Singular Fields by a Wedge," Archive of Rational Mechanical Analysis, 18 (1965), 196-204.

41. Makhoul, John I. "Contour Plots for the Diffraction of a Pulse by a Wedge," Radio Science, 1 (May, 1966), 609-613.

42. Senior, T. B. A. "Diffraction by an Imperfectly Conducting Half-Plane at Oblique Incidence," Applied Science Research (B), 8 (1959), 35-61.

43. Senior, T. B. A. "Diffraction by an Imperfectly Conducting Wedge," Communications on Pure and Applied Mathematics, 12 (May, 1959), 337-372.

44. Jones, D. S., and Pidduck, F. B. "Diffraction by a Metal Wedge at Large Angles," Quarterly Journal of Mathematics (2), 1 (1950), 229-237.

45. Felsen, L. B. "Diffraction by an Imperfectly Conducting Wedge." Report on Symposium on Microwave Optics, McGill Symposium, McGill University, Montreal, Canada, 1953.

46. Williams, W. E. "Diffraction by an Imperfectly Conducting Right-Angled Wedge," Proceedings of the Cambridge Philosophical Society, 55 (April, 1959), 195-209.

47. Williams, W. E. "Diffraction of an Electromagnetic Plane Wave by a Metallic Sheet," Proceedings of the Royal Society (A), 257 (September, 1960), 413-419.

48. Malyuzinec, G. D. Annalen der Physik, 6 (1958), 107.

49. Lebedev, N. N., and Skal'skaya, I. P. "A New Method for Solving the Problems of Diffraction of Electromagnetic Waves by a Wedge with Finite Conductivity," Zh. Tekh. Fiz. (USSR), 32 (October, 1962), 1174-1183.

50. Radlow, J. "Diffraction of a Dipole Field by a Unidirectionally Conducting Semi-Infinite Plane Screen," Quarterly Journal of Applied Mathematics, 17 (July, 1959), 113-27.

51. Hurd, R. A. "An Electromagnetic Diffraction Problem Involving Unidirectionally Conducting Surfaces," Canadian Journal of Physics, 38 (October, 1960), 1229-1244.

52. Seshadri, S. R. "Diffraction of a Plane Wave by a Unidirectionally Conducting Half-Plane," Proceedings of the National Institute of Science of India (A), 27 (January, 1961), 1-10.

53. Seshadri, S. R. "Excitation of Surface Waves on a Unidirectionally Conducting Screen," IRE Transactions on Microwave Theory and Techniques, MTT-10 (July, 1962), 279-286.

54. Dmitriev, V. I. "Diffraction of Electromagnetic Waves at a Conducting Plate in a Conducting Medium," Akad. Nauk SSSR, Izvestiia, Ser. Geofiz., No. 6 (1962), 731-735.

55. Jull, E. V. "Diffraction by a Conducting Half-Plane in an Anisotropic Plasma," Canadian Journal of Physics, 42 (August, 1964), 1455-1468.

56. Williams, W. E. "Diffraction in an Anisotropic Medium," Quarterly Journal of Mechanics and Applied Mathematics, 18 (February, 1965), 121.

57. Seshadri, S. R., and Rajagopal, A. K. "Diffraction by a Perfectly Conducting Semi-Infinite Screen in an Anisotropic Plasma," IEEE Transactions on Antennas and Propagation, AP-11 (July, 1963), 497-502.

58. Karp, S. N., and Karal, F. C. "Surface Waves on a Right Angled Wedge." Research Report EM-116, New York University Institute of Mathematical Science, Division of Electromagnetic Research, New York, New York, August, 1958.

59. Karal, F. C., and Karp, S. N. "Diffraction of a Plane Wave by a Right Angled Wedge which Sustains a Surface Wave on One Face." Research Report EM-123 (ASTIA No. AD 208046), New York University Institute of Mathematical Sciences, Division of Electromagnetic Research, New York, New York, January, 1959.

60. Karp, S. N., and Karal, F. C. "Vertex Excited Surface Waves on Both Faces of a Right Angled Wedge." Research Report EM-124, New York University Institute of Mathematical Sciences, Division of Electromagnetic Research, New York, New York, 1959.

61. Karp, S. N., and Karal, F. C. "Vertex Excited Surface Waves on Both Faces of a Right Angled Wedge," Communications on Pure and Applied Mathematics, 12 (1959), 435-455.

62. Karal, F. C., and Karp, S. N. "Scattering of a Surface Wave by a Discontinuity in the Surface Reactance on a Right Angled Wedge." Research Report EM-146, New York University Institute for Mathematical Sciences, Division of Electromagnetic Research, New York, New York, February, 1960.

63. Karal, F. C., and Karp. S. N. "Diffraction of a Plane Wave by a Right-Angled Wedge which Sustains Surface Waves on One Face," Quarterly Journal of Applied Mathematics, 20 (July, 1962), 97-106.

64. Karal, F. C., Karp, S. N., Chu, T. S., and Kouyoumjian, R. G. "Scattering of a Surface Wave by a Discontinuity in the Surface Reactance on a Right-Angled Wedge," Communications on Pure and Applied Mathematics, 14 (February, 1961), 35-48.

65. Chu, T. S., and Kouyoumjian, R. G. "The Diffraction of a Surface Wave by a Right Angled Wedge." Report 1035-2, Antenna Laboratory, The Ohio State University Research Foundation, Columbus, Ohio, March, 1960.

66. Chu, T. S., Kouyoumjian, R. G., Karal, F. C., and Karp, S. N. "The Diffraction of Surface Waves by a Terminated Structure in the Form of a Right Angle Bend," IRE Transactions on Antennas and Propagation, AP-10 (November, 1962), 679-686.

67. Chu, T. S., and Kouyoumjian, R. G. "On the Surface Wave Diffraction by a Wedge," IRE Transactions on Antennas and Propagation, AP-13 (January, 1965), 159-164.

68. Williams, W. E. "Propagation of Electromagnetic Surface Waves Along Wedge Surfaces," Quarterly Journal of Mechanics and Applied Mathematics, 13 (August, 1960), 278-284.

69. Kalmykova, S. S., and Kurilko, V. I. "The Diffraction of Surface Waves by a Perfectly Conducting Wedge," Dokl. Akad. Nauk SSSR, 154 (February, 1964), 1066-68.

70. Spence, J. E. "Surface Wave Diffraction by a Wedge," IEEE Transactions on Antennas and Propagation, AP-13 (November, 1965), 995.

71. Karp, S., and Sollfrey, W. "Diffraction by a Dielectric Wedge with Application to Propagation through a Cold Front." Research Report EM-23, New York University Mathematical Research Group, New York, New York, 1950.

72. Karal, F. C., and Karp, S. N. "Diffraction of a Skew Plane Electromagnetic Wave by an Absorbing Right Angled Wedge." Research Report EM-11, New York University Institute of Mathematical Science, Division of Electromagnetic Research, New York, New York, February, 1958.

73. Karp, S. N., and Karal, F. C. "A New Method for the Determination of Far Fields with Application to the Problem of Radiation of a Line Source at the Tip of an Absorbing Wedge," IRE Transactions on Antennas and Propagation (Toronto Symposium on Electromagnetic Theory), AP-7 (1959).

74. Karp, S. N. "Two Dimensional Green's Function for a Right Angled Wedge Under an Impedance Boundary Condition." Research Report EM-129, New York University Institute for Mathematical Sciences, Division of Electromagnetic Research, New York, 1959.

75. Karp, S. N. "Two Dimensional Green's Function for a Right Angled Wedge under Impedance Boundary Conditions," Communications on Pure and Applied Mathematics, 13 (1960), 203-216.

76. Felsen, L. B. "High Frequency Diffraction by a Wedge with a Linearly Varying Surface Impedance," Applied Science Research, B9 (1951), 170-188.

77. Felsen, L. B. "Field Solutions for a Class of Corrugated Wedges and Cone Surfaces." Memo No. 32, Polytechnical Institute of Brooklyn, New York, July, 1957.

78. Felsen, L. B. "Radiation of Sound from a Vibrating Wedge." Report No. R-613-57, PIB, Microwave Research Institute, Polytechnical Institute of Brooklyn, New York, October, 1957.

79. Felsen, L. B. "Electromagnetic Properties of Wedges and Cone Surfaces with a Linearly Varying Surface Impedance," IRE Transactions on Antennas and Propagation (Special Supplement), AP-7 (December, 1959), 231-243.

80. Malyuzinec, G. D. "Radiation of Sound by Vibrating Boundaries of an Arbitrary Wedge," Acoustical Journal (USSR), 1 (1955), 144.

81. Derwin, C. C. "Diffraction by a Perfectly Absorbing Thin Screen," Journal of Applied Physics, 29 (June, 1958), 921-922.

82. Maluzhinets, G. D. "The Excitation, Reflection, and Emission of Surface Waves from a Wedge with Given Face Impedances," Soviet Physics Doklady, 3 (1958), 752-755.

83. Pistol'kors, A. A., Kaplun, V. A., Knyazeva, L. V., "The Diffraction of Electromagnetic Waves by Dielectric or Semiconducting Sheets," Radiotekhnika i Elektronika (USSR), 4 (June, 1959), 911-919.

84. Shmoys, J. "Diffraction by a Half-Plane with a Special Impedance Variation," IRE Transactions on Antennas and Propagation, AP-7 (December, 1959), S88-S91.

85. Papadopoulos, V. M. "Diffraction and Refraction by a Transparent Wedge," Applied Scientific Research (B), 9 (1961-63), 431.

86. Unz, H., and Sleator, F. B. "Scattering of a Plane Scalar Wave by Fundamental Surfaces with Mixed Boundary Conditions," Applied Science Research Bulletin, 10 (1963), 344-352.

87. Bobrovnikov, M. S., and Kislitsyna, V. N. "Problem of the Diffraction of a Uniform Plane Electromagnetic Wave by an Impedance Wedge," Radiotekhnika i Elektronika (USSR), 9 (September, 1964), 1696-1700.

88. Radlow, J. "Diffraction by a Right-Angled Dielectric Wedge," International Journal of Engineering Science, 2 (June, 1964), 275-290.

89. Felsen, L. B. "Comment on Radiation from Source Distributions Covering One Face of a Perfectly Conducting Wedge," IEEE Transactions on Antennas and Propagation, AP-12 (September, 1964), 653-655.

90. Kritikos, H. N. "Boundary Waves along an Impedance Plane with Linearly Varying Impedance," IRE Transactions on Antennas and Propagation, AP-13 (July, 1965), 577-583.

91. Russo, P. M., Rudduck, R. C., and Peters, L., Jr. "A Method for Computing E-Plane Patterns of Horn Antennas," IEEE Transactions on Antennas and Propagation," AP-13 (March, 1965), 219-224.

92. Chu, T. S. "Surface Wave Diffraction and Its Relationship to Surface Wave Antennas." Unpublished Ph.D. Dissertation, The Ohio State University, Columbus, Ohio, August, 1960.

93. Bazer, J., and Karp, S. N. "Propagation of Plane Electromagnetic Waves Past a Shoreline." Research Report EM-46, New York University Institute of Mathematical Sciences, Division of Electromagnetic Research, New York, New York, July, 1952.

94. Burke, J. E., and Keller, J. B. "Diffraction by a Thick Screen, a Step, and Related Axially Symmetric Objects." Engineering Report EDL-E98, Electronic Defense Laboratories, Mountainview, California, March 1, 1960.

95. Keller, J. B. "Application of GTD to Polygonal Cylinders," in Electromagnetic Waves, by R. E. Langer (Madison, Wisconsin: University of Wisconsin Press, 1962), pp. 129-137.

96. Yu, J. S., and Rudduck, R. C. "Diffraction by Conducting Walls of Finite Thickness." Report 1767-7, Antenna Laboratory, The Ohio State University Research Foundation, Columbus, Ohio, May, 1965.

97. Booker, H. G., Ratcliffe, J. A., and Shenn, D. H. "Diffraction by an Irregular Screen," Philosophical Transactions of the Royal Society (A), 242 (1950), 579.

98. Briggs, B. H. "Diffraction by an Irregular Screen of Limited Extent," Proceedings of the Physical Society, 77 (February, 1961), 494.

99. Nussenzveig, H. M. "Solution of a Diffraction Problem. I. The Wide Double Wedge." Philosophical Transactions of the Royal Society (A), 252 (1959), 1-51.

100. Dybdal, R. B. "Mutual Coupling between TEM and TE_{01} Parallel-Plate Waveguide Apertures." Report 1693-5, Antenna Laboratory, The Ohio State University Research Foundation, Columbus, Ohio, August 15, 1964.

101. Horton, C. W. "On the Diffraction of a Plane Wave by a Semi-Infinite Conducting Sheet," Physical Review, 75 (1949), 1263.

102. Horton, C. W., and Watson, R. B. "On the Diffraction of Radar Waves by a Semi-Infinite Conducting Screen," Journal of Applied Physics, 21 (1950), 16-21.

103. Artmann, K. "Beugung polarisierten Lichtes an Blenden endlicher Dicke im Gebiet der Schattengrenze," Zeitschrift für Physik, 127 (1950), 468-494.

104. Huang, C., and Kodis, R. D. "Diffraction by Spheres and Edges at 1.25 Centimeters." Technical Report No. 138, Cruft Laboratory, Harvard University, Cambridge, Massachusetts, 1951.

105. Hedgecock, N. E., and McKay, A. B. "Diffraction of Nearly Plane 3.2-cm EM Waves by 45° and 90° Conducting Wedges. Comparison with Theory," IRE Transactions on Antennas and Propagation, AP-7 (Dec., 1959), S284-S287.

106. Savornin, J. Annalen der Physik, 11 (1939), 129.

107. Clemmow, P. C. "Some Extensions to the Method of Integration by Steepest Descents," Quarterly Journal of Mechanics and Applied Mathematics, 3 (1950), 241-256.

108. Van der Waerden, B. L. "On the Method of Saddle Points," Applied Science Research (B), B2 (1951), 33-45.

109. Debye, P. "Näherungsformeln für die Zylinderfunktionen für grosse Werte des Arguments und unbeschränkt veränderliche Werte des Index," Math. Annalen, 67 (1909), 535-558.

110. Ott, H. "Die Sattelpunktsmethode in der Umgebung eines Poles mit Anwendung aus die Wellenoptik und Akustik," Annalen der Physik, 43 (1943), 393-403.

111. Oberhettinger, F. "On a Modification of Watson's Lemma," Journal of Research of the National Bureau of Standards, 63B (1959), 15-17.

112. Copson, E. T. Asymptotic Expansions. Cambridge: Cambridge University Press, 1965.

113. Jeffreys, Harold. Asymptotic Approximations. Oxford: Clarendon Press, 1962.

114. Sommerfeld, Arnold. Partial Differential Equations in Physics. New York: Academic Press, 1964.

115. Meixner, J. "Die Kantenbedingung in der Theorie der Beugung elektromagnetischer Wellen an Vollkommen leitenden ebenen Schirmen," Annalen der Physik, 6 (1949), 1.

116. Van Bladel, J. Electromagnetic Fields. New York: McGraw Hill, 1964, Pp. 382-393.

117. Heins, A. E., and Silver, S. "The Edge Conditions and Field Representation Theorems in the Theory of Electromagnetic Diffraction," Proceedings of the Cambridge Philosophical Society, 51 (1955), 149-161.

118. Poincelot, P. "On the Boundary Condition at Edges," Comptes Rendus Acad. Sci. (France), 247 (December, 1958), 2312-2313.

119. Poincelot, P. "The Edge Condition in Diffraction Problems," Comptes Rendus Acad. Sci. (France), 246 (June, 1958), 3324-3325.

120. Poincelot, P. "Generalization of the Condition at an Edge," Comptes Rendus Acad. Sci. (France), 250 (June, 1960), 4316-4318.

121. Wait, James R., and Jackson, Carolen M. "Calculations of the Fie d Near the Apex of a Wedge Surface." National Bureau of Standards Technical Note 204. November 21, 1963.

122. Jones, J.E., Tsai, L.L., Rudduck, R.C., Swift, C.T. and Burnside, W.D., "The Admittance of a Parallel-Plate Waveguide Aperture Illuminating a Metal Sheet," IEEE Transactions, AP-16, (1968) 528-535.

123. Wu, D.C.F., Rudduck, R.C., and Pelton, E.L., "Application of a Surface Integration Technique to a Parallel-Plate Waveguide Radiation Pattern," IEEE Transactions, AP-17, (1969), 280-285.

124. Burnside, W.D., Rudduck, R.C., and Tsai, L.L., "Reflection Coefficient of a TEM Mode Symmetric Parallel-plate Waveguide Illuminating a Dielectric Layer," Radio Science, 4, (1969), 545-556.

125. Burnside, W.D., Pelton, E.L., and Peters, L., "Wedge Diffraction Theory Analysis of Parallel Plate Waveguide Arrays," submitted to IEEE Transactions on Antennas and Propagation.

126. Pathak, P.H. and Kouyoumjian, R., "The Dyadic Diffraction Coefficient for a Perfectly-Conducting Wedge," Report 2183-4, ElectroScience Laboratory, Department of Electrical Engineering, The Ohio State University; prepared under Contract AF 19(628)-5929 for Air Force Cambridge Research Laboratories.

UNCLASSIFIED
Security Classification

DOCUMENT CONTROL DATA - R&D

(Security classification of title, body of abstract and indexing annotation must be entered when the overall report is classified)

1. ORIGINATING ACTIVITY (Corporate author)

ElectroScience Laboratory, Department of Electrical Engineering, The Ohio State University Research Foundation, Columbus, Ohio 43212

2a. REPORT SECURITY CLASSIFICATION

Unclassified

2b. GROUP

3. REPORT TITLE

ASYMPTOTIC SERIES DESCRIBING THE DIFFRACTION OF A PLANE WAVE BY A WEDGE

4. DESCRIPTIVE NOTES (Type of report and inclusive dates)

Scientific Interim

5. AUTHOR(S) (Last name, first name, initial)

David L. Hutchins
Robert G. Kouyoumjian

6. REPORT DATE	7a. TOTAL NO. OF PAGES	7b. NO. OF REFS
15 December 1969	155	126

8a. CONTRACT OR GRANT NO.

Contract AF 19(628)-5929

b. Project, Task, Work Unit No. 5635-02-01

c. DoD Element: 61102F

d. DoD Subelement: 681305

9a. ORIGINATOR'S REPORT NUMBER(S)

ElectroScience Laboratory 2183-3
Scientific Report No. 3

9b. OTHER REPORT NO(S) (Any other numbers that may be assigned this report)

AFCRL-69-0412

10. AVAILABILITY/LIMITATION NOTICES

This document has been approved for public release and sale; its distribution is unlimited.

11. SUPPLEMENTARY NOTES

TECH, OTHER

12. SPONSORING MILITARY ACTIVITY

Air Force Cambridge Research Laboratories (CRD)
L.G. Hanscom Field
Bedford, Massachusetts 01730

13. ABSTRACT

The Pauli and the Oberhettinger asymptotic expansions for the diffracted field produced by the scattering of a plane wave by a wedge are compared analytically and numerically, and their range of application is extended.

The Pauli-Clemmow method of steepest descents is used to evaluate Sommerfeld's complex integral expression for the total field produced by the scattering of a plane electromagnetic wave by a perfectly conducting wedge. This method is applied in a manner somewhat different from that employed by Pauli and yields an asymptotic expansion which is simpler in form and of wider applicability than Pauli's original expression. This generalized form of Pauli's expansion can, for example, be applied to the computation of the fields diffracted by wedges which have exterior angles less than 180 degrees. It is shown that simply by rearranging the terms in this generalized Pauli expansion a generalized form of Oberhettinger's asymptotic expansion can be produced. This generalized expansion is applicable to problems involving wedges having exterior angles less than 180 degrees, and it is comparable with Oberhettinger's original series when the wedge angle is greater than this value.

Several examples of the scattering of a plane wave by a wedge are studied numerically. The superiority of the generalized Pauli asymptotic expression over previously derived asymptotic expressions is demonstrated in these numerical examples.

These asymptotic expressions are used to obtain scalar diffraction coefficients which are valid in the transition regions at the shadow and reflection boundaries.

DD FORM 1 JAN 64 1473

UNCLASSIFIED
Security Classification

UNCLASSIFIED

Security Classification

14. KEY WORDS	LINK A		LINK B		LINK C	
	ROLE	WT	ROLE	WT	ROLE	WT
Asymptotic series						
Diffraction						
Plane wave						
Two-dimensional						
Perfectly conducting						
Line source						
Complex integration						
Hard wedge						
Soft wedge						

INSTRUCTIONS

1. ORIGINATING ACTIVITY: Enter the name and address of the contractor, subcontractor, grantee, Department of Defense activity or other organization (*corporate author*) issuing the report.

2a. REPORT SECURITY CLASSIFICATION: Enter the overall security classification of the report. Indicate whether "Restricted Data" is included. Marking is to be in accordance with appropriate security regulations.

2b. GROUP: Automatic downgrading is specified in DoD Directive 5200.10 and Armed Forces Industrial Manual. Enter the group number. Also, when applicable, show that optional markings have been used for Group 3 and Group 4 as authorized.

3. REPORT TITLE: Enter the complete report title in all capital letters. Titles in all cases should be unclassified. If a meaningful title cannot be selected without classification, show title classification in all capitals in parenthesis immediately following the title.

4. DESCRIPTIVE NOTES: If appropriate, enter the type of report, e.g., interim, progress, summary, annual, or final. Give the inclusive dates when a specific reporting period is covered.

5. AUTHOR(S): Enter the name(s) of author(s) as shown on or in the report. Enter last name, first name, middle initial. If military, show rank and branch of service. The name of the principal author is an absolute minimum requirement.

6. REPORT DATE: Enter the date of the report as day, month, year, or month, year. If more than one date appears on the report, use date of publication.

7a. TOTAL NUMBER OF PAGES: The total page count should follow normal pagination procedures, i.e., enter the number of pages containing information.

7b. NUMBER OF REFERENCES: Enter the total number of references cited in the report.

8a. CONTRACT OR GRANT NUMBER: If appropriate, enter the applicable number of the contract or grant under which the report was written.

8b, 8c, & 8d. PROJECT NUMBER: Enter the appropriate military department identification, such as project number, subproject number, system numbers, task number, etc.

9a. ORIGINATOR'S REPORT NUMBER(S): Enter the official report number by which the document will be identified and controlled by the originating activity. This number must be unique to this report.

9b. OTHER REPORT NUMBER(S): If the report has been assigned any other report numbers (*either by the originator or by the sponsor*), also enter this number(s).

10. AVAILABILITY/LIMITATION NOTICES: Enter any limitations on further dissemination of the report, other than those imposed by security classification, using standard statements such as:

(1) "Qualified requesters may obtain copies of this report from DDC."

(2) "Foreign announcement and dissemination of this report by DDC is not authorized."

(3) "U. S. Government agencies may obtain copies of this report directly from DDC. Other qualified DDC users shall request through

_______________."

(4) "U. S. military agencies may obtain copies of this report directly from DDC. Other qualified users shall request through

_______________."

(5) "All distribution of this report is controlled. Qualified DDC users shall request through

_______________."

If the report has been furnished to the Office of Technical Services, Department of Commerce, for sale to the public, indicate this fact and enter the price, if known.

11. SUPPLEMENTARY NOTES: Use for additional explanatory notes.

12. SPONSORING MILITARY ACTIVITY: Enter the name of the departmental project office or laboratory sponsoring (*paying for*) the research and development. Include address.

13. ABSTRACT: Enter an abstract giving a brief and factual summary of the document indicative of the report, even though it may also appear elsewhere in the body of the technical report. If additional space is required, a continuation sheet shall be attached.

It is highly desirable that the abstract of classified reports be unclassified. Each paragraph of the abstract shall end with an indication of the military security classification of the information in the paragraph, represented as (*TS*), (*S*), (*C*), or (*U*).

There is no limitation on the length of the abstract. However, the suggested length is from 150 to 225 words.

14. KEY WORDS: Key words are technically meaningful terms or short phrases that characterize a report and may be used as index entries for cataloging the report. Key words must be selected so that no security classification is required. Identifiers, such as equipment model designation, trade name, military project code name, geographic location, may be used as key words but will be followed by an indication of technical context. The assignment of links, roles, and weights is optional.

UNCLASSIFIED

Security Classification